DOT/TSC-RA-3-8-4

Project Report
ATC-23

Improved Satellite Constellations for CONUS ATC Coverage

H. B. Lee
A. E. Wade

1 May 1974

Lincoln Laboratory
MASSACHUSETTS INSTITUTE OF TECHNOLOGY
LEXINGTON, MASSACHUSETTS

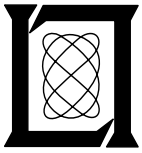

Prepared for the Federal Aviation Administration,
Washington, D.C. 20591

TECHNICAL REPORT STANDARD TITLE PAGE

1. Report No.	2. Government Accession No.	3. Recipient's Catalog No.
DOT/TSC-RA-3-8-4		

4. Title and Subtitle	5. Report Date
Improved Satellite Constellations for CONUS ATC Coverage	1 May 1974
	6. Performing Organization Code
7. Author(s)	8. Performing Organization Report No.
Harry B. Lee, Andrew E. Wade	ATC-23
9. Performing Organization Name and Address	10. Work Unit No.
Massachusetts Institute of Technology Lincoln Laboratory P. O. Box 73 Lexington, Massachusetts 02173	11. Contract or Grant No. DOT/TSC-RA-3-8 Task 1
	13. Type of Report and Period Covered
12. Sponsoring Agency Name and Address	Project Report
Transportation Systems Center Department of Transportation Cambridge, Massachusetts	14. Sponsoring Agency Code

15. Supplementary Notes

The work reported in this document was performed at Lincoln Laboratory, a center for research operated by Massachusetts Institute of Technology,

16. Abstract

This report examines the problem of designing a constellation of orbiting satellites capable of supporting an aircraft navigation/surveillance service over CONUS. It is assumed that the aircraft positions are determined by hyperbolic multilateration using all satellites visible at elevation angles exceeding a minimum angle.

Comprehensive analyses are presented of three "baseline" constellations. The constellations are representative of previous large, medium, and small constellations. The analyses include calculation of The Geometric Dilution of Precision (GDOP) during level flight, calculation of GDOP after a key satellite is deleted, and calculation of GDOP during aircraft banking. Comparison of the resulting GDOP's with the theoretical minimum values indicates that there is considerable room for improvement.

A new method of calculating GDOP is described. The method suggests that improved GDOP's can be obtained by placing satellites in retrograde orbits rather than the previous posigrade orbits. Accordingly, nine new constellations are designed that employ retrograde orbits. When subjected to the same analyses as the baseline constellations, the new constellations exhibit significantly improved GDOP's.

17. Key Words	18. Distribution Statement
Navigation Surveillance Geometric Dilution of Precision Satellite Constellation Multilateration Hyperbolic Multilateration	Document is available to the public through the National Technical Information Service, Springfield, Virginia 22151.

19. Security Classif. (of this report)	20. Security Classif. (of this page)	21. No. of Pages	22. Price
Unclassified	Unclassified	226	5.75 HC 1.45 MF

Form DOT F 1700.7 (8-69)

TABLE OF CONTENTS

TABLE OF CONTENTS (Contined)

TABLE OF CONTENTS (Contined)

LIST OF ILLUSTRATIONS

LIST OF ILLUSTRATIONS (Continued)

LIST OF ILLUSTRATIONS (Continued)

LIST OF ILLUSTRATIONS (Continued)

LIST OF ILLUSTRATIONS (Continued)

LIST OF TABLES

LIST OF TABLES (Continued)

LIST OF TABLES (Continued)

LIST OF TABLES (Continued)

LIST OF TABLES (Continued)

SECTION 1

INTRODUCTION AND SUMMARY

1.1 INTRODUCTION

A number of methods have been described for providing an aircraft surveillance/navigation service over the Continental United States (CONUS) using a constellation of orbiting satellites [1 - 9]. Basically, the methods treat the satellite positions as known, and determine the aircraft positions relative to the satellites by multilateration using signal time of arrival measurements.

This report examines the problem of designing the associated satellite constellations. It is assumed that the aircraft positions are determined by means of hyperbolic multilateration using all satellites visible at elevation angles exceeding a minimum angle.

The report approaches the problem of constellation design by asking the following questions:

1. What is the best performance that can be obtained given N satellites?
2. How closely can the theoretical optimum performance be achieved by real constellations?

While this approach is widely used in engineering design, it apparently has not been used previously in the design of constellations for navigation/surveillance applications.

It should be noted that the constellation design problem addressed here aims at providing multilateration service to a small portion of the earth's surface (i.e., CONUS). Thus, the problem differs from that of providing a global multilateration service. The problem also differs from that of providing either a local or global communication service.

1.2 MAIN RESULTS

The main results are as follows:

1. Comprehensive analyses of three "baseline" constellations are presented. The constellations are representative of previous small, medium, and large constellations. The analyses include:
    a. Calculation of the Geometric Dilution of Precision (GDOP) during level flight.*
    b. Calculation of GDOP after a key satellite has been deleted (to assess the impact of satellite failure).
    c. Calculation of GDOP for aircraft mading a 30^{o} bank on test headings of 0^{o}, 10^{o}, ... 350^{o} (to assess the impact of aircraft maneuvers).

    The calculations are performed at each point of a 119 point CONUS grid. In addition, the calculations are performed under the separate assumptions of "visibility down to aircraft wingtips," "visibility down to 15^{o} above the wingtips," and "visibility down to 30^{o} above the wingtips." The results are presented in the form of GDOP maps, and several statistical formats. Comparison of

*Basically, GDOP is an error magnification factor that indicates how much the basic ranging error is magnified by the constellation-aircraft geometry. See Section 2.4.

the resulting average GDOP's with the theoretical minimum GDOP's shows that the actual GDOP's vary between 2.2 and 4.5 times the minimum attainable GDOP.

2. A new procedure for calculating GDOP is described. The procedure "explains" the (comparatively high) GDOP's provided by the baseline constellations. The procedure also indicates that substantially improved GDOP's can be obtained by employing synchronous retrograde orbits in place of the previously used posigrade orbits.*

3. A variety of methods for utilizing retrograde orbits in constellations are examined. One method emerges as the best of those considered. The method involves using retrograde orbits to approximate an idealized constellation wherein the satellites are uniformly distributed within a "viewing cone."

4. New large, medium, and small constellations are designed by the foregoing method. The resulting constellations are subjected to the same analyses as the baseline constellations. In all cases, the new constellations exhibit smaller GDOP's. GDOP's for the new constellations vary between 1.6 and 2.3 times the optimum GDOP values.

5. The analyses of both the baseline constellations and the new small (seven satellite) constellations indicate that small constellations can produce useful values of GDOP (e.g., three) during level flight. However, the GDOP's are highly sensitive to satellite

*A retrograde orbit is one for which the rotational sense of the satellite is opposite to that of the earth. A posigrade orbit is one for which the rotational sense is the same as that of the earth. See Section 4.5.

failure or aircraft maneuvers. For example, during banking GDOP exceeds ten on more than 75% of the test headings if, "visibility down to 30^{o} above the wingtips" is assumed. Accordingly, use of more than seven satellites is indicated if high accuracy is to be maintained following a satellite failure, and during aircraft maneuvers. The analyses of medium-sized constellations suggest that ten satellites is a reasonable number.

1.3 SECTION BY SECTION SUMMARY

This report is organized as follows:

Section 2 - Reviews Hyperbolic Multilateration and conventional GDOP calculations.

Section 3 - Describes in detail the constellation design problem addressed by the report. Basically, GDOP is selected as a measure of constellation "goodness." Thus, a constellations is regarded as "good" if it provides reliably low values of GDOP across CONUS.

Section 4 - Reviews relevant properties of synchronous satellite orbits.

Section 5 - Presents analyses of the baseline constellations (RCA-8, Hybrid, and a constellation previously designed at Lincoln Laboratory).

Section 6 - Describes the alternate procedure for calculating GDOP. Basically, the procedure links GDOP to the moments and products of inertia of a simple configuration of unit masses.

It is shown that high GDOP's of previous constellations are due to the near planarity of the unit mass configuration.

Section 7 - Views the problem of reducing GDOP as being equivalent to that of disrupting the planarity of the unit mass configuration. It is shown that use of retrograde orbits in place of the previous posigrade orbits achieves this objective nicely.

Section 8 - Examines a variety of possible methods for employing retrograde orbits in a constellation intended for CONUS coverage. After analysis, one method emerges as the best of those considered.

Section 9 - Describes the best large (fifteen satellite) constellations designed by the foregoing method. The constellations are designed for viewing cone half angles of $\phi = 90^{\circ}$, 75°, and 60°. The GDOP's of all constellations are well below those of the baseline large constellation.

Section 10 - Describes the best medium-sized (ten satellite) constellations designed by the method of Section 8. The GDOP's of the resulting constellations are well below those of the baseline medium-sized constellation. In fact, the GDOP's generally are smaller than those of the baseline large constellation.

Section 11 - Describes the best small (seven satellite) constellations designed by the method of Section 8. The GDOP's of all

constellations are well below those of the baseline small constellation. The GDOP's, like those of the baseline small constellation, are highly sensitive to satellite failure and aircraft maneuvers.

Section 12 - Provides some perspective on the preceding results. Several tools are recommended for related work.

SECTION 2

HYPERBOLIC MULTILATERATION

This Section reviews the basic principles of hyperbolic multilateration systems. The positional errors inherent in such systems are discussed briefly. In addition, several accuracy measures are described including the geometric dilution of precision (GDOP).

Readers familiar with Eq. (2.11) and GDOP calculations can proceed directly to Section 3.

2.1 THE BASIC IDEA

Hyperbolic multilateration functions by utilizing measurements of range difference between a number of satellites and an aircraft. Each range difference serves to localize the aircraft to a hyperboloid of revolution having the corresponding pair of satellites as foci. Thus, the aircraft position is determined as the intersection of a number of hyperboloids.

At least three independent surfaces are required to locate a point in three-dimensional space. Thus, hyperbolic multilateration requires a minimum of three independent pairs of satellites, or four total satellites.

To reduce the effect of measurement errors it frequently is advantageous to utilize more than the minimum number of satellites. In principle, if N satellites are used, then the aircraft position is given by the common intersection of N-1 independent hyperboloids. Due to measurement errors,

however, the hyperboloids do not intersect at a common point. Instead, the surfaces intersect at several points in the vicinity of the aircraft. In such cases, an "average intersection" can be used to locate (approximately) the aircraft.

Figure 2.1 depicts an example of a system that could be utilized for aircraft surveillance. The system operates as follows. The aircraft transmits a timing signal which is received by a constellation of satellites. The signal time of arrival (TOA) at each stellite depends upon the distance between the aircraft and the satellite. Upon receipt of the signal, each satellite re-transmits the signal to a ground station. The ground station then utilizes differences in the TOA's (proportional to range differences) and the known positions of the satellites to calculate the position of the aircraft.

The accuracy of such a system is limited by the accuracy with which the satellite positions are known, by propagation disturbances in the atmosphere and by noise disturbances in the satellite receiver. More specifically, the atmospheric and receiver disturbances, and the satellite position errors are translated into TOA errors. The calculation performed at the ground station then translates the TOA errors into corresponding aircraft position errors.

2.2 ALGEBRAIC FORMULATION

From an algebraic point of view, the problem of determining the aircraft position amounts to that of solving the TOA equations.

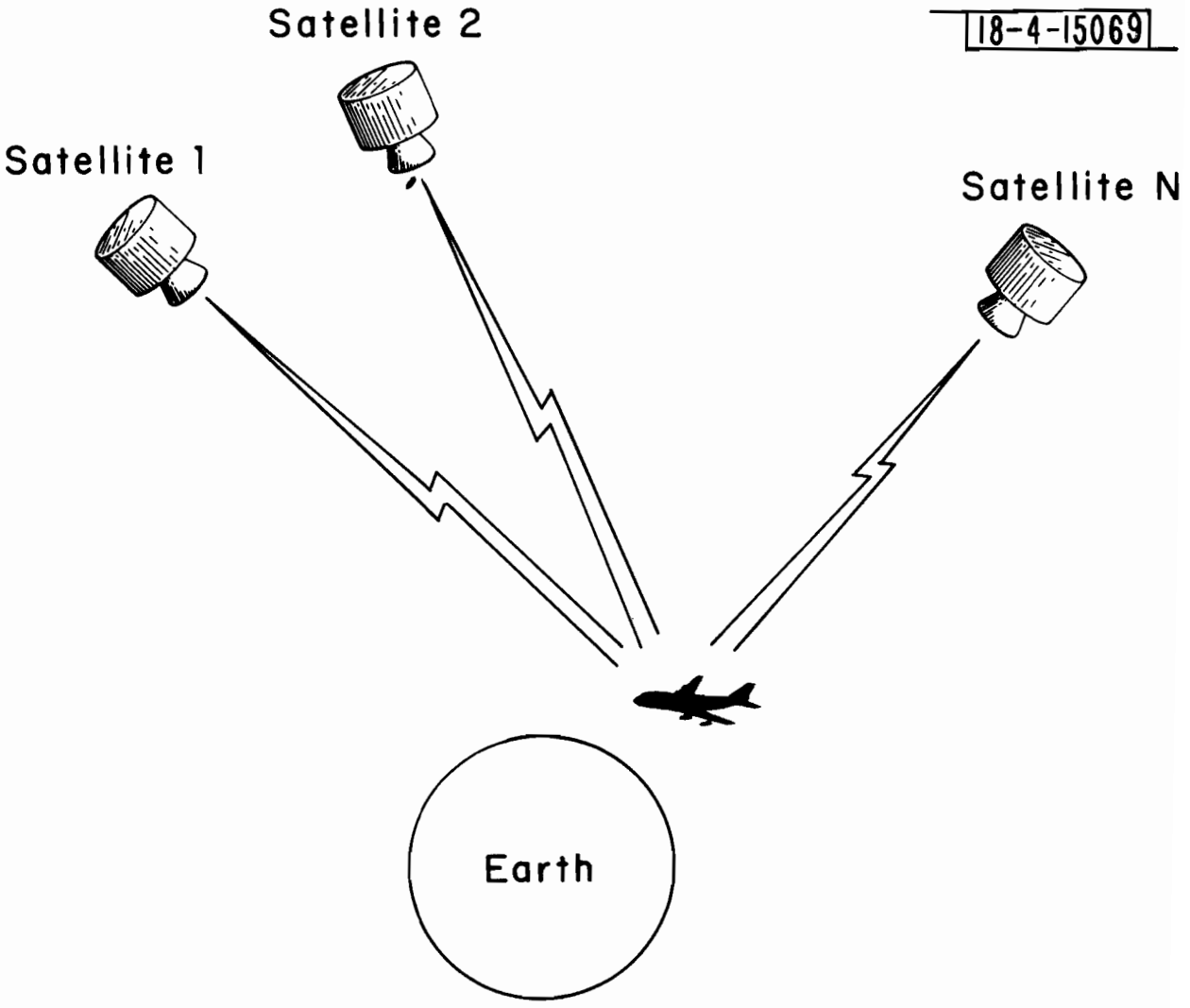

Fig. 2.1. Satellite-based surveillance system.

For the surveillance application illustrated in Fig. 2.1, the TOA equations take the following form.

$$\begin{aligned} t_1 &= T_o + d_1/c \\ t_2 &= T_o + d_2/c \\ &\vdots \\ t_N &= T_o + d_N/c \end{aligned} \qquad (2.1)$$

where

t_j = The TOA of the signal at the jth satellite.

T_o = The (unknown) time at which the signal was transmitted.

d_j = The distance from the actual position of the jth satellite to the (unknown) position of the aircraft.

c = The velocity of light.

In principle, the aircraft position can be determined by expressing the d_j in terms of the (known) satellite coordinates and the (unknown) aircraft coordinates and solving (2.1) for the aircraft coordinates and T_o.

In practice, however, the exact values of the quantities t_j and d_j in Eq. (2.1) are not available. Instead, approximations t_j^* and d_j^* of t_j and d_j are available as follows.

t_j^* = the measured TOA at the jth satellite

d_j^* = the distance from the assumed position of the jth satellite to the (unknown) position of the aircraft

The quantities t_j^*, T_o, and d_j^* are not related by Eq. (2.1). Instead, t_j^*, T_o, and d_j^* satisfy the following equations:

$$\begin{aligned} t_1^* &= T_o + d_1^*/c + \epsilon_1 \\ t_2^* &= T_o + d_2^*/c + \epsilon_2 \\ &\vdots \\ t_N^* &= T_o + d_N^*/c + \epsilon_N \end{aligned} \tag{2.2}$$

where

ϵ_j = An error term that accounts for TOA errors due to atmospheric disturbances and receiver noise, and also for errors in the assumed satellite position.

Several procedure (estimators) exist for calculating good approximations of the aircraft position from the values t_j^*, d_j^*, and Eq. (2.2). Some procedures are iterative in nature. Other procedures are explicit. The error in the calculated position depends upon the specific estimator used. It can be shown [10], however, that the mean-squared errors for most practical

estimators exceed those made by the generalized least squares procedure. Accordingly, throughout this report we assume that position is determined by the generalized least squares procedure.

2.3 ERRORS IN CALCULATED POSITION

The error made by the generalized least squares procedure is as follows:

$$\underline{\delta R} = c[\underline{F}' \underline{H}' (\underline{H} \underline{P}_{\epsilon} \underline{H}')^{-1} \underline{H} \underline{F}]^{-1} \underline{F}' \underline{H}' (\underline{H} \underline{P}_{\epsilon} \underline{H}')^{-1} \underline{H} \underline{\epsilon} \qquad (2.3)$$

where

$\underline{\delta R}$ = a (3 x 1) vector specifying the displacement of the calculated position from the actual aircraft position; see Fig. 2.2. It is assumed that $\underline{\delta R}$ is expressed in terms of a Cartesian coordinate system (X', Y', Z') centered at the aircraft.

$\underline{i}_j$ = a (1 x 3) unit vector pointing from the aircraft to the jth satellite; see Fig. 2.2.

$\underline{F}$ = an (n x 3) matrix, the rows of which are the unit vectors $\underline{i}_1, \underline{i}_2, \ldots, \underline{i}_N$; that is, the matrix

$$\underbrace{\begin{bmatrix} \underline{i}_1 \\ \underline{i}_2 \\ \vdots \\ \underline{i}_N \end{bmatrix}}_{\text{3 columns}} \Bigg\} \text{N rows} \qquad (2.4)$$

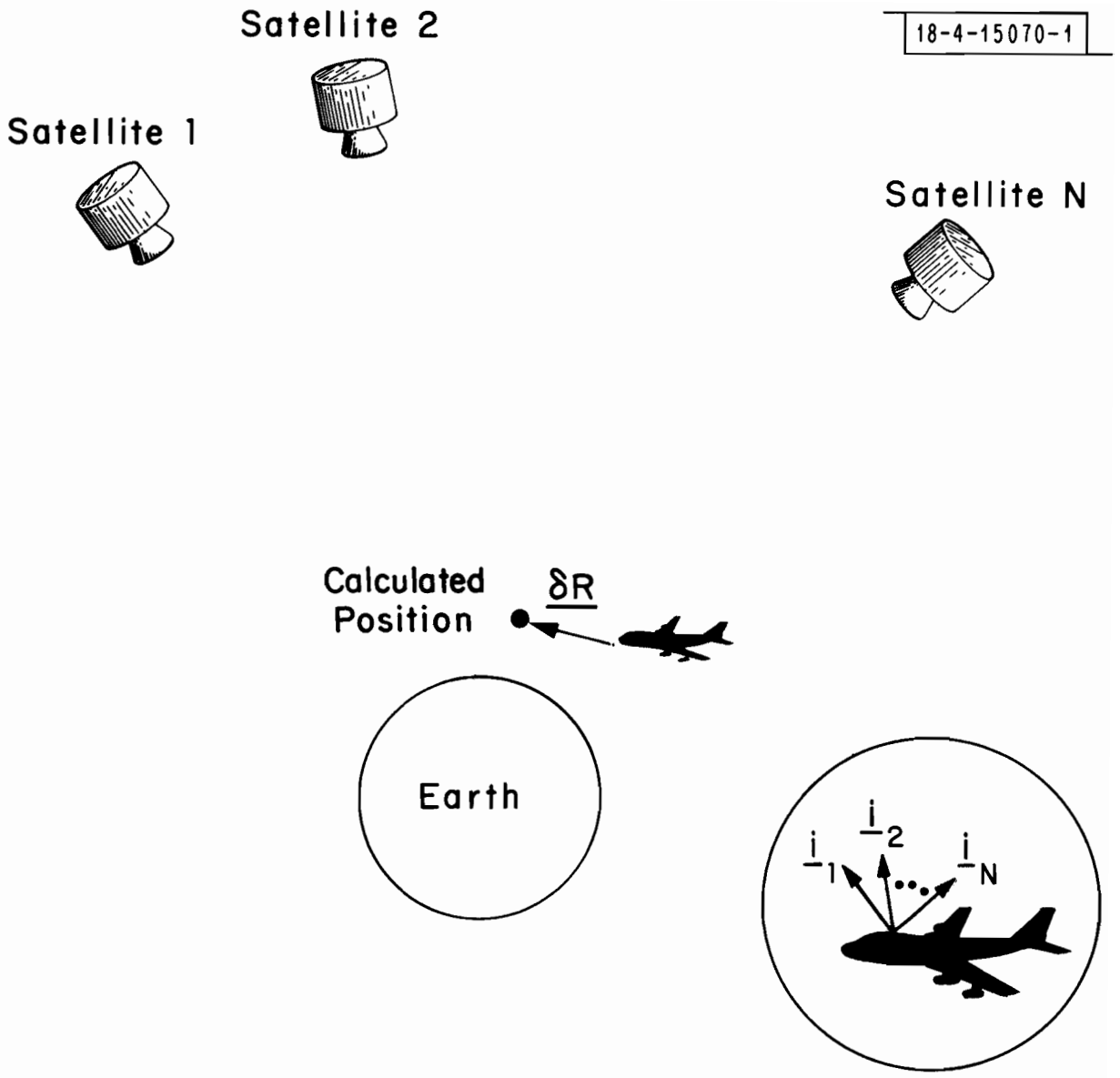

Fig. 2.2. Illustration of the vectors $\underline{\delta R}$ and $\underline{i}_1, \ldots, \underline{i}_N$.

$\underline{H}$ = a (N - 1) x N matrix of the form

$$\begin{bmatrix} 1 & -1 & & & \\ & 1 & -1 & & \\ & & \ddots & \ddots & \\ & & & 1 & -1 \end{bmatrix} \quad \text{N - 1 rows} \qquad (2.5)$$

N columns

$$\underline{\epsilon} = \begin{bmatrix} \epsilon_1 \\ \epsilon_2 \\ \vdots \\ \epsilon_N \end{bmatrix} \qquad (2.6)$$

$\underline{P}_{\epsilon}$ = The covariance matrix of the ϵ_j (2.7)

The statistical properties of the error vector $\underline{\delta R}$ depend on those of the ϵ_j. Following References [2, 3, 8], the ϵ_j are modelled as zero mean random variables having the common variance σ_τ^2. That is, it is assumed

$$E[\underline{\epsilon}] = \underline{0} \qquad (2.8)$$

$$E[\underline{\epsilon}\ \underline{\epsilon}'] = \sigma_\tau^2\ \underline{I} \qquad (2.9)$$

where E denotes expectation and $\underline{I}$ denotes the identity matrix.*

*Note that the zero mean assumption (2.8) presupposes that the t_j^* have been corrected for ionospheric delay.

With the assumptions (2.8) and (2.9), Eq. (2.3) reduces to

$$\underline{\delta R} = c[\underline{F}'\underline{H}'(\underline{H}\ \underline{H}')^{-1}\ \underline{H}\ \underline{F}]^{-1}\ \underline{F}'\ \underline{H}'(\underline{H}\ \underline{H}')^{-1}\ \underline{H}\ \underline{\epsilon} \quad . \tag{2.10}$$

The associated covariance matrix is as follows:

$$\underline{P}_{\Delta r} = E[\underline{\delta R}\ \underline{\delta R}']$$

$$= (c\sigma_\tau)^2\ [\underline{F}'\ \underline{H}'(\underline{H}\ \underline{H}')^{-1}\ \underline{H}\ \underline{F}]^{-1} \quad . \tag{2.11}$$

2.4 ACCURACY MEASURES

For the purpose of assessing accuracy, it is convenient to express the error covariance matirx (2.11) as follows:

$$\underline{P}_{\Delta R} = (\sigma_\tau c)^2\ \underline{\Gamma}$$

$$= (\sigma_\tau c)^2 \begin{bmatrix} \Gamma_{xx} & \Gamma_{xy} & \Gamma_{xz} \\ \Gamma_{xy} & \Gamma_{yy} & \Gamma_{yz} \\ \Gamma_{xz} & \Gamma_{yz} & \Gamma_{zz} \end{bmatrix} \tag{2.12}$$

where

$$\underline{\Gamma} = \underline{F}'\ \underline{H}'(\underline{H}\ \underline{H}')^{-1}\ \underline{H}\ \underline{F} \quad . \tag{2.13}$$

The quantity $(\sigma_\tau c)^2$ in (2.12) is the mean-squared ranging error.

All conventional accuracy measures can be expressed easily in terms of the elements of $\underline{\Gamma}$. For example, the ratios of the mean-squared errors in the x', y', z' directions to the mean-squared ranging error are given by expressions

$$\sigma_x^2/(\sigma_\tau c)^2 = \Gamma_{xx} \tag{2.14}$$

$$\sigma_y^2/(\sigma_\tau c)^2 = \Gamma_{yy} \tag{2.15}$$

$$\sigma_z^2/(\sigma_\tau c)^2 = \Gamma_{zz} \quad . \tag{2.16}$$

Similarly, the ratio of total mean-squared error $\left(\sigma_x^2 + \sigma_y^2 + \sigma_z^2\right)$ to the mean-squared ranging error is given by

$$\left(\sigma_x^2 + \sigma_y^2 + \sigma_z^2\right)/(\sigma_\tau c)^2 = \Gamma_{xx} + \Gamma_{yy} + \Gamma_{zz} \quad . \tag{2.17}$$

Finally, the gometric dilution of precision (GDOP), or the ratio of the rms position error to the rms ranging error is given by

$$\text{GDOP} = \sqrt{\sigma_x^2 + \sigma_y^2 + \sigma_z^2}/(\sigma_\tau c)$$

$$= (\Gamma_{xx} + \Gamma_{yy} + \Gamma_{zz})^{1/2} \tag{2.18}$$

Note that the functions of the Γ_{ij} that appear in the right hand sides of (2. 14 to 2. 18) can be interpreted as error magnification factors. For example, Eqs. (2. 14) and (2. 18) can be re-written as follows:

$$\sigma_x^2 = \Gamma_{xx} (\sigma_\tau c)^2 \tag{2. 19}$$

$$\sqrt{\sigma_x^2 + \sigma_y^2 + \sigma_z^2} = \sqrt{\Gamma_{xx} + \Gamma_{yy} + \Gamma_{zz}} \quad (\sigma_\tau c) \quad . \tag{2. 20}$$

Equation (2. 19) asserts that the mean-squared error in the X' direction equals the basic mean-squared ranging error $(\sigma_\tau c)^2$ magnified by Γ_{xx}. Similarly, Eq. (2. 20) asserts that the rms position error equals the rms ranging error magnified by $\sqrt{\Gamma_{xx} + \Gamma_{yy} + \Gamma_{zz}}$ (= GDOP).

Obviously, the smaller the measures (2. 14) to (2. 18) for a particular constellation, the better.

2.5 ILLUSTRATIVE GDOP CALCULATION

To illustrate a GDOP calculation using (2. I3) and (2. 18), consider the (idealized) constellation shown in Fig. 2. 3. The constellation has four visible satellites, S_1 - S_4. Three of the satellites (S_1 - S_3) are located at the corners of an equilateral triangle at elevation angles of 45^o, as shown. The fourth satellite S_4 is located at the center of the triangle.

For the coordinate system shown in Fig. 2. 3, the unit vectors $\underline{i}_1 \cdots \underline{i}_4$ are as follows:

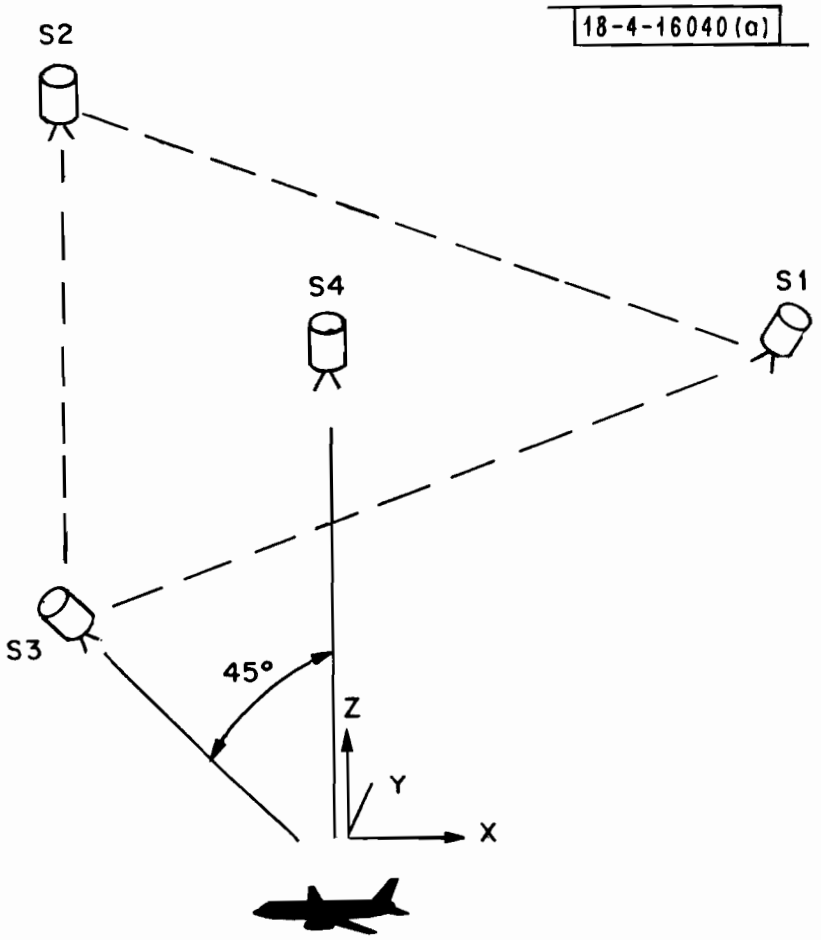

Fig. 2.3. Satellite-aircraft geometory for Section 2.5.

$$\underline{i}_1 = (1/\sqrt{2} \quad , \quad 0 \quad , \quad 1/\sqrt{2})$$

$$\underline{i}_2 = (-1/2\sqrt{2}, \sqrt{3}/2\sqrt{2} \ , \ 1/\sqrt{2})$$

$$\underline{i}_3 = (-1/2\sqrt{2}, -\sqrt{3}/2\sqrt{2}, \ 1/\sqrt{2})$$

$$\underline{i}_4 = (\ 0 \ , \ 0 \ , \ 1\ ) \tag{2.21}$$

Therefore, the $\underline{F}$ matrix (2.4) is given by

$$\underline{F} = \begin{bmatrix} 0.707 & 0 & 0.707 \\ -0.354 & 0.612 & 0.707 \\ -0.354 & -0.612 & 0.707 \\ 0 & 0 & 1.000 \end{bmatrix} . \tag{2.22}$$

The corresponding $\underline{H}$ matrix (2.5) is

$$\underline{H} = \begin{bmatrix} 1 & -1 & 0 & 0 \\ 0 & 1 & -1 & 0 \\ 0 & 0 & 1 & -1 \end{bmatrix} . \tag{2.23}$$

Straightforward matrix operations show that the $\underline{\Gamma}$ matrix (2.13) is

$$\underline{\Gamma} = \begin{bmatrix} 1.33 & 0 & 0 \\ 0 & 1.33 & 0 \\ 0 & 0 & 15.54 \end{bmatrix} . \tag{2.24}$$

Therefore, according to (2. 18)

$$\text{GDOP} = \sqrt{(1.33) + (1.33) + (15.54)}$$

$$= 4.27 \qquad (2.25)$$

SECTION 3

THE CONSTELLATION DESIGN PROBLEM

This section describes the constellation design problem addressed by the report. The section also indicates how the problem is approached.

Basically, GDOP (2.18) is selected as an index of constellation accuracy. Thus a constellation is regarded as "good" if it provides reliably low values of GDOP over CONUS.

The constellation design procedure used is an educated "cut and try" procedure. Although the procedure is basically similar to that used for previous constellations [2, 3, 8], the results (presented in Sections 9 to 11) are better due to a significantly improved initial "cut."

Two idealized constellations are described that provide useful guideposts for designing "good" constellations. These are an "optimum" constellation and the uniform constellation.

In addition, two performance measures are defined that are useful in assessing the "goodness" of candidate constellations.

3.1 STATEMENT OF THE PROBLEM

For the purposes of this report, GDOP, as given by (2.13) and (2.18), is used to assess contellation accuracy. Thus a constellation having a reliably "low GDOP" over CONUS is regarded as a desirable constellation.*

The constellation design problem is taken to be that of assigning satellites to physical orbits such that the following conditions are satisfied.

1. Low values of GDOP are obtained at all times throughout CONUS.
2. The GDOP's are relatively insensitive to satellite failure (dropout).
3. The GDOP's are relatively insensitive to typical aircraft maneuvers.

Note that the constellation design problem, as defined above, aims at providing multilateration service to a small portion of the earth's surface (i.e., CONUS). Thus the design problem differs significantly from that of providing a global multilateration service. The problem also differs from that of providing either a local or a global communications service.

3.2 THE BASIC DESIGN PROCEDURE

The approach taken to designing previous constellations [2, 3, 8] has been to use an educated "cut and try" procedure. The procedure can be summarized as follows:

Design Procedure

1. Select an initial constellation that provides a low value of GDOP in central CONUS.

*It should be noted that use of (2.13) and (2.18) to assess accuracy presupposes the idealizing assumptions (2.8) and (2.9). These assumptions appear to be reasonable ones provided the delay introduced by the ionosphere has been subtracted from the TOA's.

2. With the assistance of a computer program, determine the behavior of GDOP over the remainder of CONUS and the time dependence of GDOP (also, in some cases, * the impact on GDOP of satellite failure and aircraft banking).
3. If any significant problems are uncovered, modify the constellation, and repeat steps 2 and 3 until they are corrected.

The approach taken here is basically similar to that described above. The primary difference lies in the constellation selected as an initial "cut." Whereas, previous initial constellations have employed so-called posigrade satellite orbits almost exclusively, the initial constellations utilized here make extensive use of so-called retrograde orbits.

3.3 SATELLITE VISIBILITY CRITERIA

The accuracy of hyperbolic multilateration depends, of course, upon the number of measurements utilized, or, equivalently, upon the number of visible satellites.

Several criteria exist for deciding the question of satellite visibility. The simplest approach is to assume that any satellite is visible that is both above the local earth horizon, and also above the plane of the aircraft wingtips. An alternate approach is to regard as visible any satellite for which the received signal energy exceeds some threshold[8]. In the latter approach, specific account can be taken of the aircraft antenna pattern.

The approach taken here is to treat as visible any satellite which satisfies the following two conditions.

*Notably the Hybrid constellation. See Ref. [8].

Visibility Conditions

1. The satellite is above the local earth horizon, and
2. the satellite is within a "viewing cone" of half angle ϕ centered about the aircraft vertical as shown in Fig. 3.1.

This approach makes it possible to draw conclusions that are independent of any particular technology. For example, the results do not depend upon any assumption concerning "reasonable" transmitter power levels. At the same time the approach makes it possible to account for the cut-off characteristic of realistic antennas by varying the half angle ϕ of the viewing cone shown in Fig. 3.1.

3.4 USEFUL IDEALIZED CONSTELLATIONS

To facilitate selection of an initial constellation (Step 1, Section 3.2), and to assess the performance of the final constellation (Step 3, Section 3.2), we have made use of two idealized constellations. These are:

1. The "optimum" constellation.
2. The uniform constellation.

The optimum constellation evolves from answering the following question.

Question: Given N satellites confined to a viewing cone of half angle ϕ as shown in Fig. 3.2, what is the minimum GDOP that can be achieved? What is the corresponding optimum constellation of satellites?

The uniform constellation is one in which the satellites are distributed uniformly within a viewing cone of half angle ϕ.

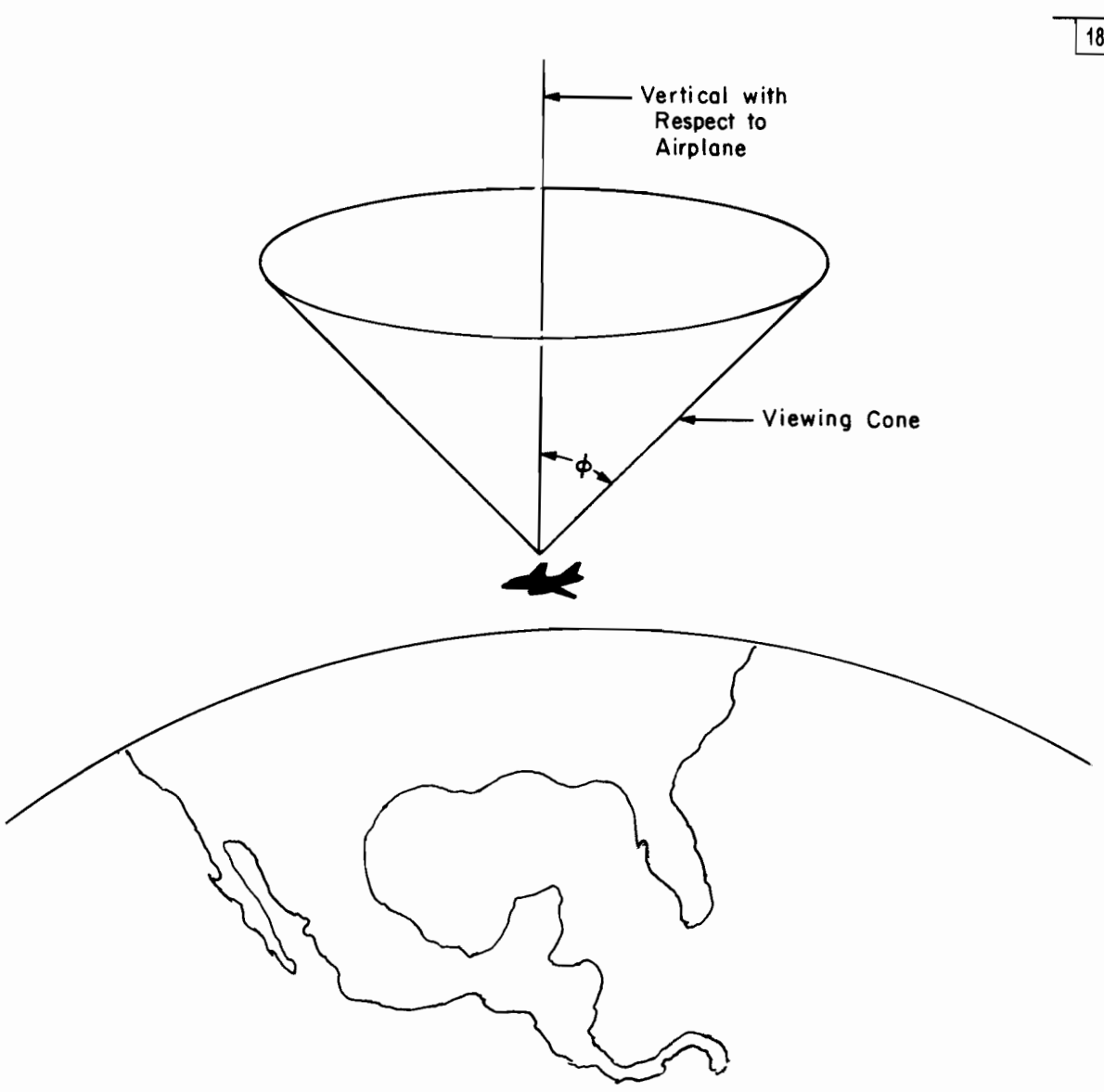

Fig. 3.1. The aircraft viewing cone.

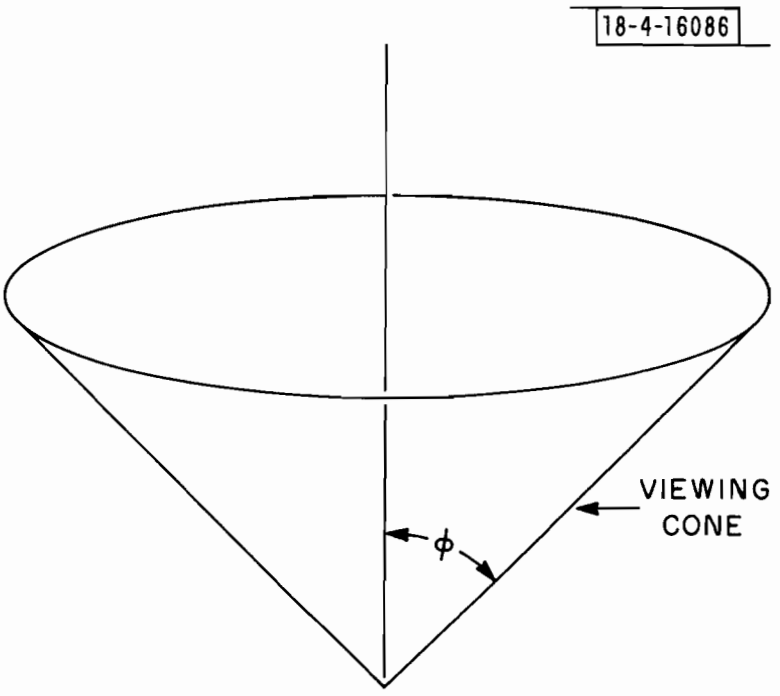

Fig. 3.2. Illustration of the optimization problem.

It has been shown [11] that the optimum constellation takes the form shown in Fig. 3.3. The constellation consists of N_1 satellites directly overhead and N_2 satellites uniformly distributed around the rim of the viewing cone. The values of the fractions N_1/N and N_2/N depend upon the angle ϕ as indicated in Table 3.1. The corresponding minimum GDOP is given by the expression

$$\text{GDOP} = \frac{1}{\sqrt{N}} \frac{4}{\sqrt{1 + \cos\phi}\ (\sqrt{5 - 3\cos\phi} - \sqrt{1 + \cos\phi})} \tag{3.1}$$

Table 3.1. Optimum allocation of satellites as a function of ϕ.

ϕ(deg)	N_1/N	N_2/N
1	0.500	0.500
20	0.485	0.515
40	0.447	0.553
60	0.395	0.605
90	0.309	0.691
100	0.279	0.721
109.5	0.250	0.750

A procedure for calculating GDOP for a uniform constellation of N satellites is given in Ref. [11]. Table 3.2 compares the GDOP for a uniform constellation with that for the optimum constellation for N = 15, and several values of ϕ. While the uniform constellation is sub-optimum, Table 3.2 shows that it is close to optimum.

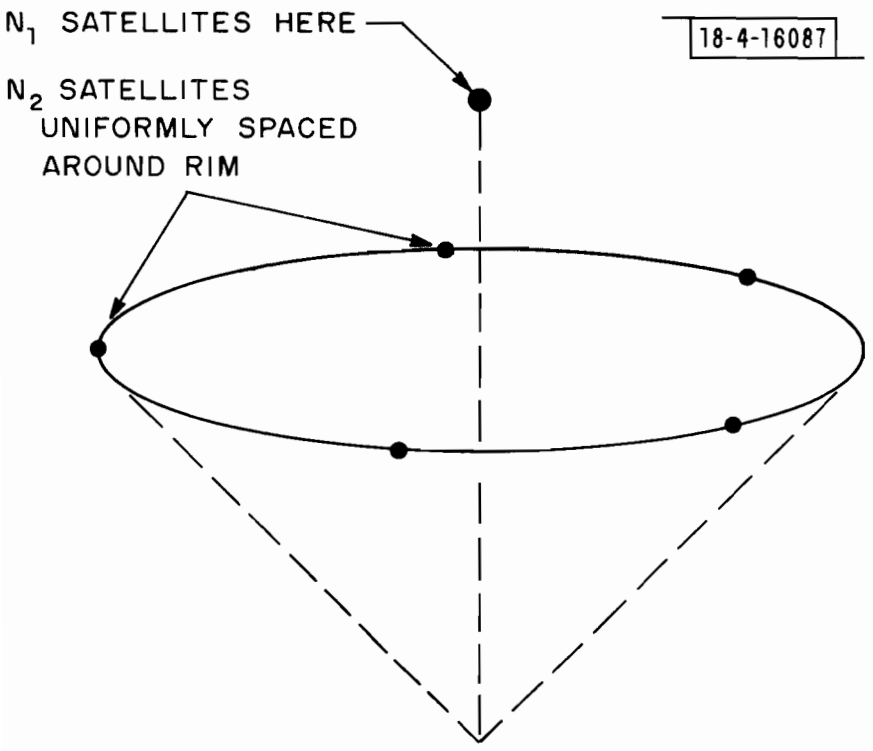

Fig. 3.3. The optimum satellite configuration.

Table 3.2. Comparison of GDOP for uniform and optimum constellations containing 15 satellites.

Cone half angle ϕ	GDOP (Uniform)	GDOP (Optimum)
20^{o}	9.86	8.82
40^{o}	2.71	2.46
60^{o}	1.40	1.30
90^{o}	0.89	0.84

3.5 PERFORMANCE MEASURES

Two performance measures have proven useful in assessing the extent to which candidate constellations satisfy conditions (1) and (2) of Section 3.1. These are the constellation Excess and the constellation Sensitivity.

Basically, the Excess compares the actual GDOP produced by a constellation with the minimum GDOP obtainable from the same number of satellites. The definition is as follows.

$$\text{Excess} = \frac{\text{Actual GDOP}}{\text{(Minimum GDOP for the same total number of satellites)}} \quad . \tag{3.2}$$

Thus, for example if a constellation exhibits a GDOP of 6 and (3.1) indicates that a GDOP of 2.5 is achievable with the same total number of satellites, then

$$\text{Excess} = \frac{6}{2.5} = 2.4 \quad . \tag{3.3}$$

The sensitivity measures the impact of a single satellite failure upon GDOP. The sensitivity is defined as follows:

$$\text{Sensitivity} = \frac{(\text{GDOP}^* - \text{GDOP})/\text{GDOP}}{(N - N^*)/N} \tag{3.4}$$

where

GDOP = Average GDOP with all satellites operational.

GDOP* = Average GDOP after a key satellite is removed.

N = The average number of visible satellites with all satellites operational.

N* = The average number of visible satellites after the satellite failure.

Thus, for example, if the failure of one out of ten visible satellites causes GDOP to increase from GDOP = 4 to GDOP* = 6, then

$$\text{Sensitivity} = \frac{(6 - 4)/4}{(10 - 9)/10} = 5. \tag{3.5}$$

SECTION 4

PROPERTIES OF SYNCHRONOUS SATELLITE ORBITS

This section reviews some relevant properties of satellite orbits.

Since the final satellite constellations are intended to provide coverage to a small portion of the northern hemisphere (i.e., CONUS), attention is restricted to synchronous orbits having an argument of perigee equal to 270°.

Readers familiar with synchronous satellite orbits can proceed directly to Section 5.

4.1 SYNCHRONOUS ORBITS

To a good approximation, a satellite in earth orbit traverses an ellipical trajectory having one focus at the mass center of the earth, as shown in Fig. 4.1. It can be shown that the orbital period T is given by the expression

$$T = 2\pi\sqrt{a^3/\gamma m} \tag{4.1}$$

where

a = The semimajor axis of the ellipse.

γ = The gravitational constant ($= 6.67 \times 10^{-11}$ newton - m^2/kgm^2).

m = The mass of the earth ($= 5.98 \times 10^{24}$ kgm).

Note that the period (4.1) is independent of the eccentricity e.

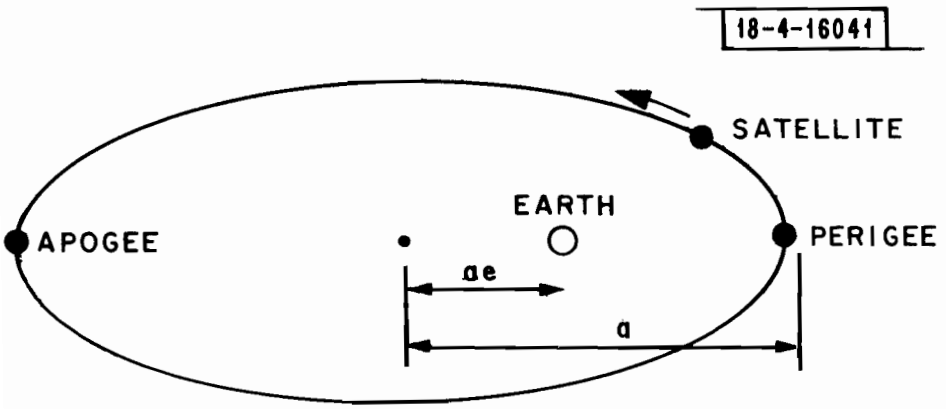

Fig. 4.1. A typical satellite orbit.

It is evident from (4.1) that the semi-major axis a can be selected so that the orbital period equals the time it takes the earth to make one revolution about its axis (i.e., one sidereal day). An orbit having such a period is called a synchronous orbit. The semi-major axis of a synchronous orbit equals 26, 200 statute miles.

4.2 WHY USE SYNCHRONOUS ORBITS

The sub-satellite point is defined as the intersection between a line connecting the center of earth and the satellite with the earth's surface. At this point on earth the satellite appears directly overhead, or at zenith. The succession of sub-satellite points traced out by a satellite constitutes a locus of points on the surface of the earth called its ground track.

The ground tracks of synchronous orbits have the desirable property of being repetitive. That is, the sub-satellite point retraces the same earth path every (sidereal) day. Thus, synchronous orbits can be configured to give preferential coverage to a specific geographic area (e.g., CONUS).

By contrast, the ground tracks of non-synchronous orbits generally are not repetitive. Instead, the ground tracks gradually migrate around the earth, showing preference for no particular longitudes.

Since the present objective is to provide CONUS coverage rather than global coverage, we restrict consideration to synchronous orbits.*

4.3 PERIGEE LOCATION

The point at which a satellite is farthest from the earth is called the apogee; the point at which it is closest is called the perigee (see Fig. 4.1).

*This decision parallels that made in Ref. [2, 3, 8].

According to Kepler's Second Law, satellites sweep out "equal areas in equal times." Thus a satellite moves slowest at apogee and fastest at perigee.

Since the present objective is to provide CONUS coverage, it is advantageous to configure all inclined orbits so as to maximize the time of satellite visibility from CONUS. Accordingly, we further require that the apogee of any inclined orbit be the northernmost point of the orbit or, equivalently, that the perigee be the southernmost point.*

4.4 ORBITAL PARAMETERS

Normally, six orbital parameters are required to describe the trajectory of a satellite. For the synchronous orbits described in Section 4.3, however, the following four parameters suffice:

e = The orbit eccentricity.

i = The inclination of the orbital plane with respect to the equatorial plane (see Fig. 4.2).

γ_p = The longitude of the sub-perigee point.

T_p = The time of passage through perigee.

The remaining two parameters are the semi-major axis of the ellipse, and the "argument of perigee" (which specifies the angular offset in the orbital plane of the perigee with respect to the equatorial plane). The restriction that orbits are synchronous requires that the semi-major axis equal 26, 200 miles for all orbits. The restriction (of Section 4.3) on the perigee location requires that the argument of perigee equal 270° for all orbits.

*Again, this decision follows that of Ref. [2, 3, 8,].

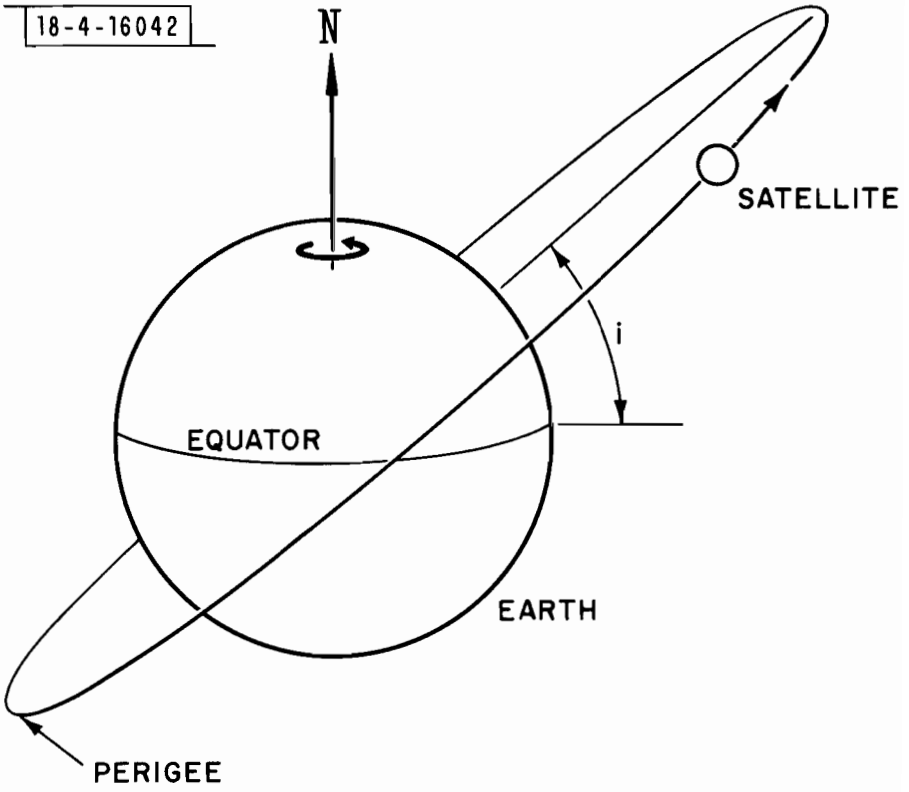

Fig. 4.2. A typical posigrade orbit.

4.5 GROUND TRACKS OF POSIGRADE ORBITS

Satellite orbits for which the inclination satisfies the condition

$$0 \leq i \leq 90^{\circ} \tag{4.2}$$

are called posigrade orbits. Satellites in posigrade orbits have the same sense of rotation about the earth's axis as the earth itself (see Fig. 4.2). Satellite orbits for which

$$90^{\circ} \leq i < 180^{\circ} \tag{4.3}$$

are called retrograde orbits. Satellites in retrograde orbits have a rotational sense opposite to that of the earth.

The ground tracks of synchronous posigrade orbits can take several different forms as shown in Fig. 4.3 (a) to (d). The ground track of a circular equatorial orbit ($e = 0$, $i = 0$), consists of a single point as shown in Fig. 4.3 (a). The ground track of an inclined circular orbit ($e = 0$) takes the form of a "figure eight" (Fig. 4.3 (b)). As the orbit becomes modestly eccentric, the upper loop of the figure eight becomes smaller, the lower loop becomes larger, and the "cross point" moves up into the northern hemisphere (Fig. 4.3 (c)). As the orbit becomes highly eccentric so that the condition

$$\sqrt{\frac{1 - e}{(1 + e)^3}} \leq \cos i \tag{4.4}$$

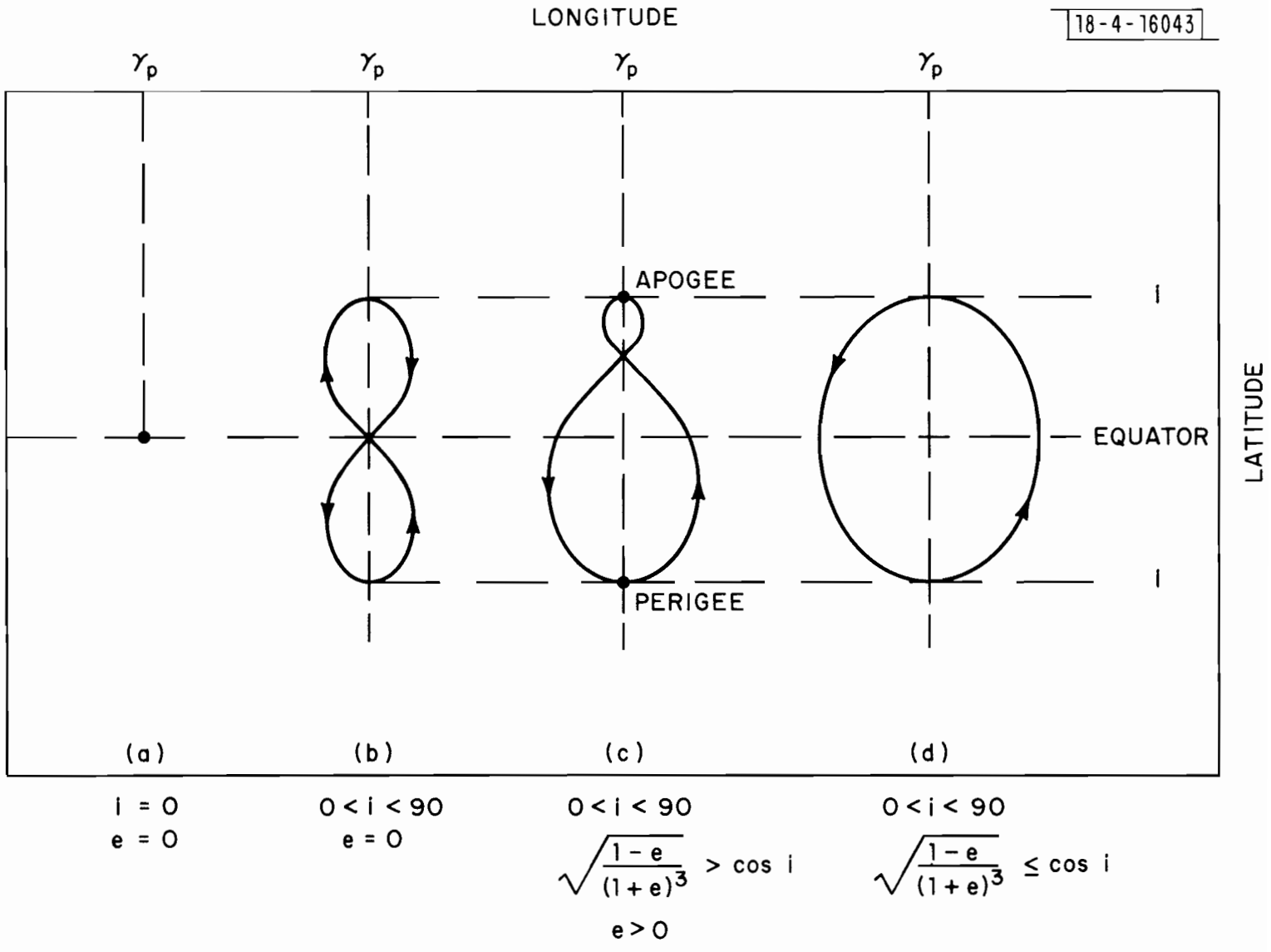

Fig. 4.3. Representative Ground Tracks.

is satisfied, the upper loop disappears altogether and the ground track becomes a simple loop (Fig. 4.3 (d)). In all cases, the latitudes of the northernmost and southernmost points of the ground track equal the inclination i of the orbital plane.

Discussion of the ground tracks of retrograde orbits is deferred to Section 7.

4.6 COMMON GROUND TRACKS

The period of a constellation is the shortest interval of time in which the pattern of sub-satellite points repeats itself. Constellations of synchronous satellites in which all satellites traverse different ground tracks have periods of twenty four hours. Shorter periods can be achieved by placing the satellites in orbits such that

1. The satellites traverse a common ground track.
2. The sub-satellite points are equally spaced "in time" along the ground track.

Thus, for example, if a constellation consists of six satellites in orbits described by the parameters in Table 4.1, then the pattern of sub-satellite points repeats itself every four hours.

Most previous constellations, as well as the constellations described in Sections 5, 9, 10, and 11, employ common ground tracks. The reason for this is to reduce the time variations in GDOP.

Table 4.1. Typical orbital parameters for satellites having a common ground track.

	e	i	γ_p	T_p
Satellite 1	e_o	i_o	γ_{po}	0
Satellite 2				4
Satellite 3				8
Satellite 4				12
Satellite 5				16
Satellite 6				20

4.7 ORBITAL STABILITY

Actual satellite orbits depart from ideal elliptical orbits due to the gravitational fields of the sun and moon, and anomalies in the earth's gravitational field. The perturbatory effects of the sun and moon are extremely small. The effect of anomalies in the earth's gravitational field also is small, but more significant.

Anomalies in the earth's gravitational field result primarily from the earth's equatorial bulge. The anomalies affect an orbiting satellite in two ways. First, the orbital plane slowly precesses about the earth's polar axis. Second, the orbit's perigee slowly rotates within the orbital plane. The former effect can be cancelled by shortening the semi-major axis of the orbit (see Eq. (4.1)). The latter effect (perigee rotation) does not affect circular orbits, but can bring the perigee of an eccentric orbit into northern latitudes. It can be shown that the perigee rotates at the rate

$$0.67 \times 10^{-2} \frac{(5 \cos^2 i - 1)}{(1 - e^2)^2} \text{ degrees/day} \quad . \qquad (4.5)$$

Clearly, (4.5) vanishes for $\cos^2 i = 1/5$, or

$$i = \begin{cases} 63.4^\circ \\ 116.6^\circ \end{cases} \qquad (4.6)$$

Thus, from the viewpoint of orbital stability, the best synchronous orbits are either circular orbits (at any inclination), or elliptical orbits inclined at the angles (4.6).

SECTION 5

ANALYSES OF THREE PREVIOUS CONSTELLATIONS

To provide a baseline for assessing the constellations of Sections 9 to 11, this section presents analyses of several previous constellations. In particular, the section treats the RCA-8 and Hybrid constellations [3, 8] and a constellation designed at Lincoln Laboratory [2]. These constellations are representative of small, medium-sized, and large constellations.

The constellations were analyzed to determine GDOP for level flight, and also to determine the impact upon GDOP of satellite failure and aircraft maneuvers.

5.1 NATURE OF THE ANALYSES

The three constellations were examined over a grid extending from 60 to 140° west longitude and from 25 to 55° north latitude. The grid encompasses the Continental Unites States (CONUS) and its oceanic approaches as shown in Fig. 5.1. Adjacent grid points are separated by five degrees in longitude and/or latitude. Thus the grid conssits of 119 points.

The following analyses were performed for each constellation.

1. To assess accuracy during level flight, GDOP was calculated at each grid point.

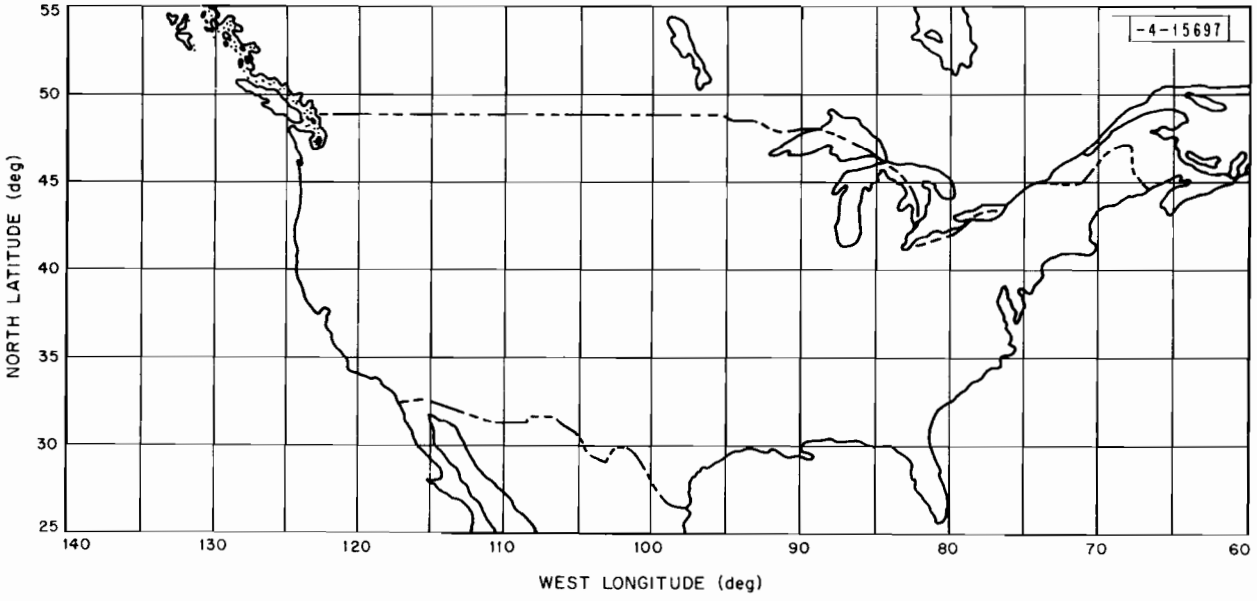

Fig. 5.1. The grid used for calculations.

2. To assess the impact of satellite failure, GDOP was recalculated at each grid point after a key satellite was deleted.

3. To assess the impact of aircraft maneuvers on accuracy, GDOP was calculated for aircraft in a 30° bank at test headings of 0°, 10°, 20°, ..., 350° at each grid point.

The analyses were performed for cone half angles of $\phi = 90^{\circ}$, 75° and 60°. Note that a half angle of $\phi = 90^{\circ}$ corresponds to visibility "down to the horizon."

The results for level flight are presented in the form of GDOP maps which depict contours of constant GDOP, and also in several tabular formats. Tables supporting the GDOP maps are given in Appendix B. The tables contain GDOP values as well as lists of visible satellites at alternate grid points.

The results for satellite failure are presented in a tabular format. The results include the ID of the failed satellite, the average GDOP over CONUS after failure, and a parameter summarizing the sensitivity of GDOP to the failure. The key satellite deleted in each case was selected with a view toward maximally impacting GDOP.*

The results for aircraft banking are presented in tabular format. The tables include the percentages of banking aircraft with GDOP's in excess of five, and in excess of ten, as well as the average of the GDOP's smaller than ten.

All results were generated using three computer programs described in Appendix A.

*Section 6.6 explains how the key satellite was selected.

5.2 THE RCA-8 CONSTELLATION

The RCA-8 constellation as modified by Autonetics* is an early constellation designed for possible ATC service over CONUS. The constellation utilizes eight satellites. Two of the satellites are in circular equatorial orbits; the remaining six satellites are in elliptical orbits of eccentricity 0.25 inclined at 80°. The constellation parameters are given in Table 5.1. Figure 5.2 depicts deployment of the satellites at time t = 0 hrs. The six satellites in elliptical orbits have a common ground track which is indicated by the dotted curve in Fig. 5.2.

The dashed lines in Fig. 5.2 indicate the approximate limits of visibility from a grid point in Kansas when the viewing cone has half angles of 90°, 75° and 60°, respectively.† Thus, at time t = 0, satellites are visible at the grid point as follows:

Half Angle of Cone	Visible Satellites
90°	2, 3, 4, 5, 6, 7, 8
75°	2, 3, 4, 5, 6, 7, 8
60°	3, 4, 5, 7, 8

While the orientation of the viewing cone varies somewhat from grid point to grid point, the dashed curves in Fig. 5.2 are indicative of the masking effect produced by the viewing cones over most of CONUS.

*See Page B-32, Appendix B. Vol. III, Ref. [3].
†Based on circular synchronous orbits.

Table 5.1. The RCA-8 constellation.

SATELLITE DEPLOYMENT

SATELLITE NO.	INC. (DEG)	ECC.	T(P) (HOURS)	LONG.(P) (DEG)
POSIGRADE				
1	80.00	0.25	0.0	-100.0
2	80.00	0.25	4.000	-100.0
3	80.00	0.25	8.000	-100.0
4	80.00	0.25	12.000	-100.0
5	80.00	0.25	16.000	-100.0
6	80.00	0.25	20.000	-100.0
EQUATORIAL				
7	0.0	0.0	0.0	-85.0
8	0.0	0.0	0.0	-115.0

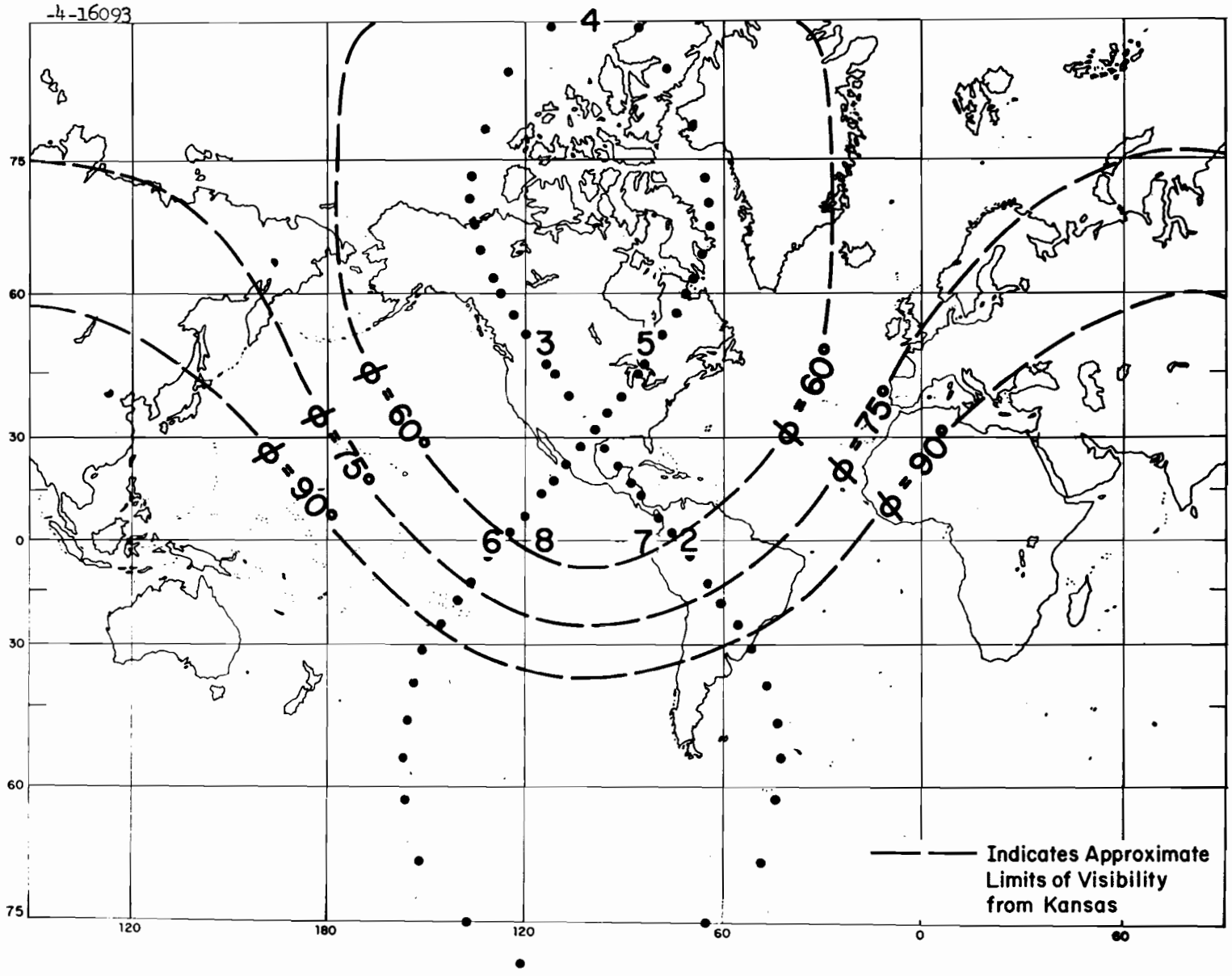

Fig. 5.2. The ground track for RCA-8.

Maps showing contours of constant GDOP for the three cone angles are given in Fig. 5.3, 5.4, and 5.5 for time t = 0 hr. Figure 5.3 shows that for $\phi = 90^{\circ}$ GDOP is highly uniform over all of CONUS. Figure 5.4 shows that as ϕ is reduced to 75°, GDOP becomes somewhat larger and more variable. It is evident from Fig. 5.5 that as ϕ is reduced to 60°, GDOP's increase further and become even more variable, particularly over extreme northern and southern CONUS. Shading indicates regions in which GDOP's are larger than ten. The high GDOP's over northern CONUS are due to the fact that the equatorial satellites no longer fall within the viewing cone and, therefore, are invisible (see Fig. 5.2). The high GDOP's in southern CONUS are due to the fact that the northernmost satellite no longer is visible.

The GDOP maps shown in Fig. 5.3 to 5.5 vary somewhat with time, but repeat every four hours.

GDOP statistics for the three viewing cones are shown in Table 5.2 for time t = 0 hr. The entries in the second column are the average numbers of satellites visible at time t = 0 over all of CONUS. As expected, the average number of visible satellites decreases as the cone half angle is made smaller. The sizable decrease between the second and third entries reflects the masking of the equatorial and northernmost satellites. The entries in the third column are the percentages of grid points in Figs. 5.2 to 5.4 at which GDOP exceeds ten. The entry of 26% again reflects the non-availability of satellites over extreme northern and southern CONUS. The entries in the fourth column are the averages of the GDOP's smaller than ten. The entries in the fifth column are the rms deviations of the GDOP's smaller than ten. Note that even when GDOP's larger than ten are discounted, the GDOP's for $\phi = 60^{\circ}$ are larger and more variable than those for $\phi = 75^{\circ}$ and $\phi = 90^{\circ}$.

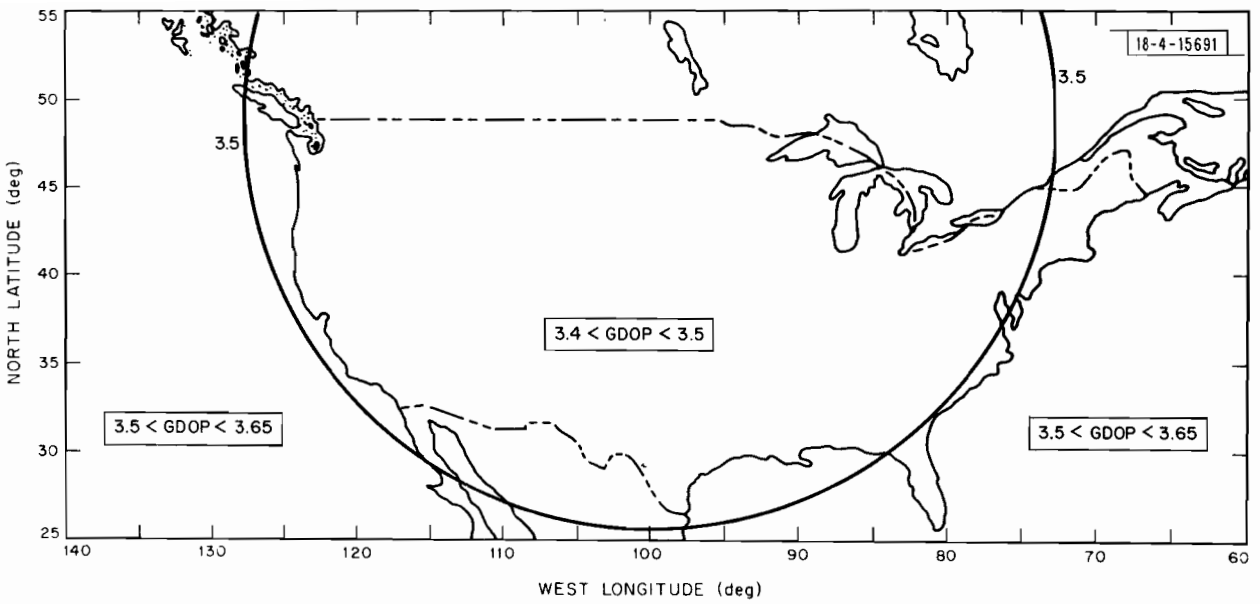

Fig. 5.3. RCA-8 constellation ($\phi = 90^{o}$). Time 0.0 minutes

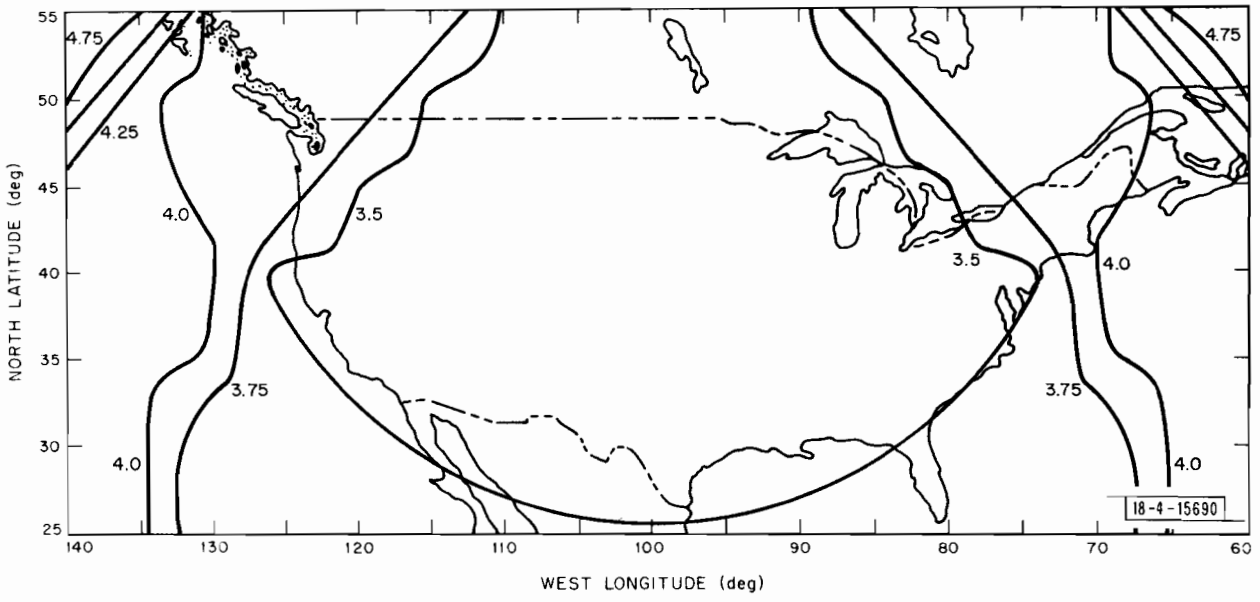

Fig. 5.4. RCA-8 constellation ($\phi = 75^{o}$). Time 0.0 minutes.

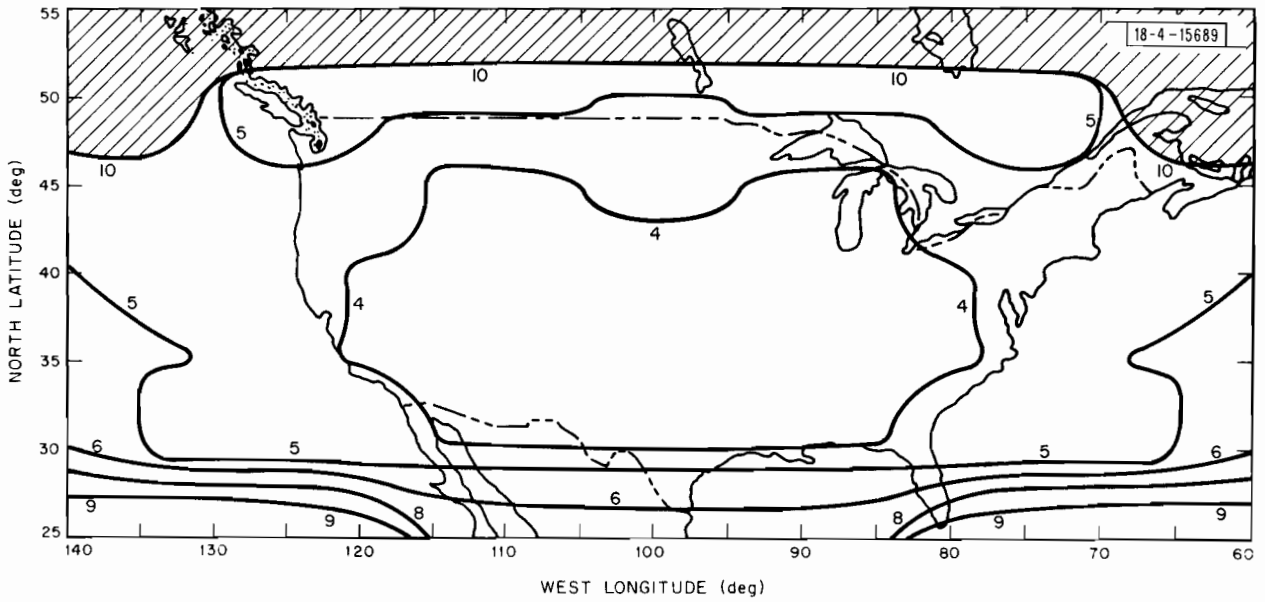

Fig. 5.5. RCA-8 constellation ($\phi = 60^{o}$). Time 0.0 minutes.

RCA-8 CONSTELLATION

Table 5.2. Nominal results.

Cone Half Angle	Average Number Visible	Percent GDOP > 10	Average GDOP < 10	rms Deviation	Excess
90°	7.00	0%	3.509	0.044	3.06
75°	6.53	0%	3.761	0.378	2.78
60°	4.99	26%	4.70	0.983	2.64

Table 5.3. Dropout results.

Cone Half Angle	Average Number Visible	Percent GDOP > 10	Average GDOP < 10	S (Sensitivity)	Failed Satellite
90°	6.00	0%	7.776	8.51	4
75°	5.53	42%	7.621	6.70*	4
60°	4.13	86%	7.417	3.35*	4

*Larger if GDOP's exceeding ten are included.

Table 5.4. 30° bank results.

Cone Half Angle	Average Number Visible	Percent GDOP > 5	Percent GDOP > 10	Average GDOP < 10
90°	6.48	7.2%	2 %	3.846
75°	5.59	37.8%	17.2%	4.554
60°	4.35	78.6%	53.7%	5.534

The entries in the E or "Excess" column compare the actual GDOP's with the minimum attainable GDOP's as explained in Section 3.5. Thus the entry of 3.06 in the first row of the E column indicates that the average actual GDOP is 3.06 times the smallest GDOP possible from 8 satellites in a viewing cone of half angle $\phi = 90^{\circ}$. Similarly, the entry 4.15 in the second row shows that the average GDOP of 4.57 is 4.15 times the smallest GDOP possible from 8 satellites in a viewing cone of half angle $\phi = 75^{\circ}$.

Dropout results are summarized in Table 5.3 for failure of the northernmost satellite. It is evident from the first row of the table that the failure significantly impacts accuracy even for a cone half angle of 90°. GDOP more than doubles as the average number of visible satellites decreases by one. The second row shows that the impact is more substantial for a cone half angle of 75°. Specifically, GDOP at 42% of the grid points exceeds ten, with GDOP at the remainder averaging 7.621. The third row shows that the impact is severe for a cone half angle of 60°. GDOP at 86% of the grid points exceeds 10, with GDOP at the remainder averaging 7.417. The "Sensitivity" column of Table 5.3 indicates the sensitivity of GDOP to the specific satellite failure. Thus, for example, with $\phi = 90^{\circ}$, failure of satellite No. 4 increases the average GDOP by 121%, while decreasing the average number of satellites by 14%, so that Sensitivity = 8.51 (=121/14).

The bank analysis results are summarized in Table 5.4. The results cover aircraft making 30° banks at headings of 0°, $10^{\circ}, \ldots, 350^{\circ}$ at each grid point within CONUS. The first row of that table shows that in the case of a viewing cone half angle of $\phi = 90^{\circ}$, the impact upon accuracy is modest. The banking aircraft "see" 6.48 satellites on the average. Moreover, only 7.2%

of the banking aircraft have GDOP's in excess of five, and only 2% have GDOP's in excess of ten. The average GDOP is 3.846 for aircraft with GDOP < 10. The second and third rows of the table show that banking impacts accuracy substantially in the case of smaller viewing cones. For $\phi = 75^{o}$, the banking aircraft see 5.59 satellites on the average. Approximately 37.8% of the aircraft have GDOP's in excess of five and 17.2% have GDOP's in excess of ten. For $\phi = 60^{o}$, the average number of visible satellites falls to 4.35, or just 0.35 above the minimum number required. Approximately 78.6% of the banking aircraft have GDOP's in excess of five and 53.7% have GDOP's in excess of ten.

To summarize, the RCA-8 constellation produces a highly uniform GDOP over all of CONUS. Accuracy is highly sensitive to failure of a single satellite, however. Moreover accuracy degrades substantially during aircraft maneuvers (e.g., banking), particularly for the smaller viewing cones.

5.3 THE LL-I CONSTELLATION

The LL-I constellation* is another early constellation for possible ATC service over CONUS. The constellation is larger than RCA-8 in that it contains twelve satellites rather than eight.

The parameters of the LL-I constellation are given in Table 5.5. The satellite deployment at time t = 0 hr is shown in Fig. 5.6. Note that the orbits are arranged so that satellites 1, 3, 5, 7, 9, and 11 share one ground track, while satellites 2, 4, 6, 8, 10, and 12 share another. The ground tracks are offset so as to provide improved east-west geometry. The choice of eccentricity e = 0.4 causes the ground tracks to be highly degenerate figure eights.

*See pp. 131 and 134, Ref. [2].

Table 5.5. The LL-I constellation.

SATELLITE NO.	INC. (DEG)	ECC.	T(p) (HOURS)	LONG.(P) (DEG)
		SATELLITE DEPLOYMENT		
POSIGRADE				
1	63.40	0.40	0.0	-115.0
2	63.40	0.40	2.000	-80.0
3	63.40	0.40	4.000	-115.0
4	63.40	0.40	6.000	-80.0
5	63.40	0.40	8.000	-115.0
6	63.40	0.40	10.000	-80.0
7	63.40	0.40	12.000	-115.0
8	63.40	0.40	14.000	-80.0
9	63.40	0.40	16.000	-115.0
10	63.40	0.40	18.000	-80.0
11	63.40	0.40	20.000	-115.0
12	63.40	0.40	22.000	-80.0

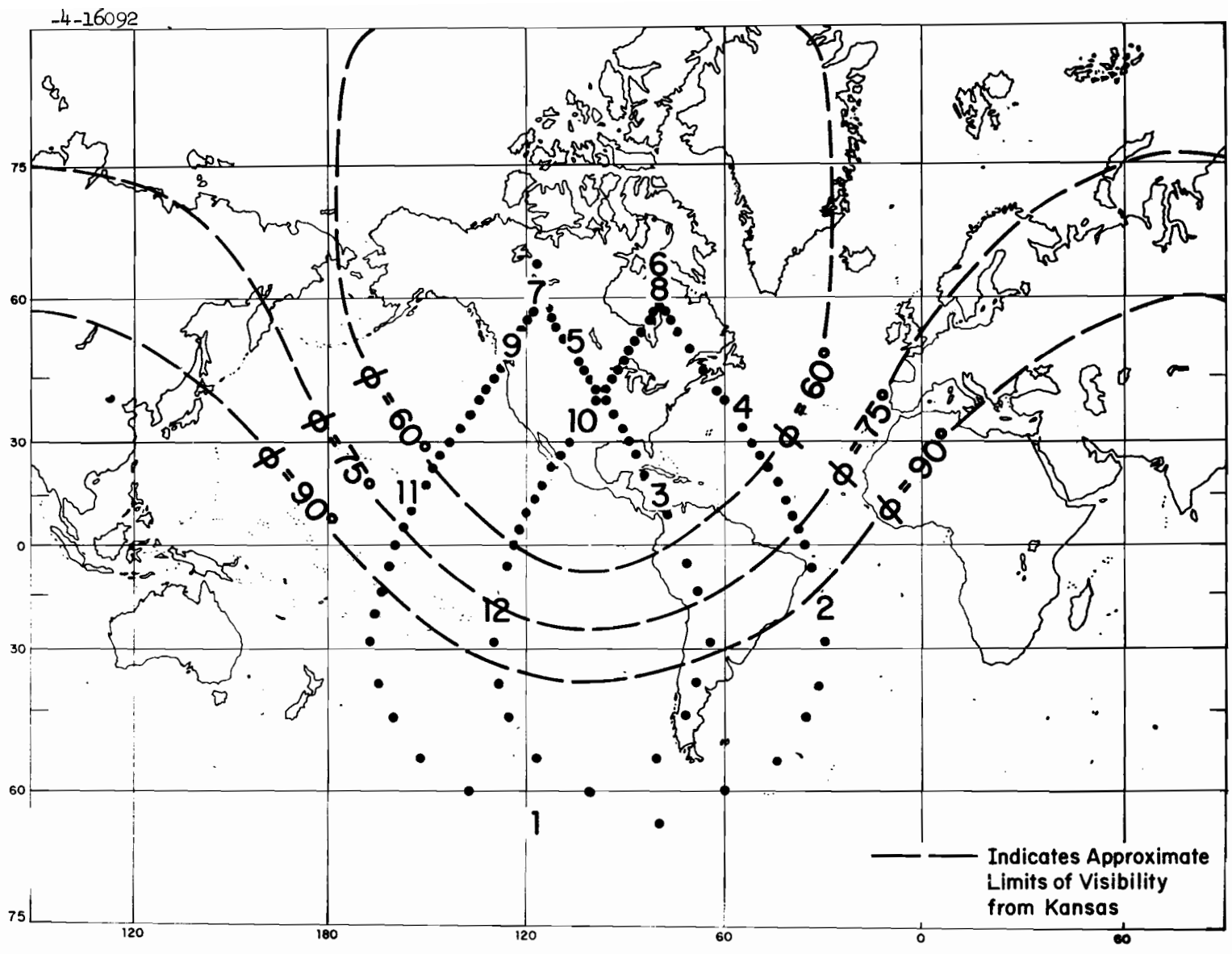

Fig. 5.6. The ground track for LL-I.

Once again the dashed lines show the approximate limits of visibility from a grid point within Kansas for viewing cone angles of 90^{o}, 75^{o}, and 60^{o}.

GDOP maps for the constellation at time t = 0 hr are shown in Figs. 5.7 to 5.9. Figure 5.7 shows that for $\phi = 90^{o}$ the GDOPs are in the range 3.0 to 3.25 over western CONUS and are somewhat lower over eastern CONUS. The favorable GDOP's over southeastern CONUS are due to the availability of Satellite No. 2 in an extreme southeastern position (see Fig. 5.6). Figure 5.8 shows that for $\phi = 75^{o}$ the GDOP's over western CONUS are substantially unchanged while the previously low GDOP's over eastern CONUS now are larger. The degradation over eastern CONUS is due to the disappearance of Satellites Nos. 11 and 12 in southwesterly positions. Figure 5.9 shows that for $\phi = 60^{o}$ the GDOP's are high and much more variable. The large values over eastern CONUS are not due to the number of satellites visible, but rather their deployment. For example, the grid points (long. = 70^{o} lat = 35^{o}) and (long. = 130^{o} lat. = 35^{o}) both have eight satellites in view, but GDOP at the former equals 9.11 while GDOP at the latter equals 4.15.

The GDOP patterns shown in Figs. 5.7 to 5.9 repeat every four hours. Due to the symmetrical disposition of the two ground tracks, the patterns "mirror image" every two hours. For example, the patterns at time t = 2 hrs are identical to those of figures rotated about the 100^{o} longitude line.

GDOP statistics for the constellation are given in Table 5.6. Again, the average number of visible satellites decreases as the cone half angle is reduced from 90^{o} to 60^{o}. The "Excess" column indicates that the GDOP's achieved by the constellation are 3 to 4.5 times larger than those which result from optimal placement of the 12 satellites in the viewing cones considered.

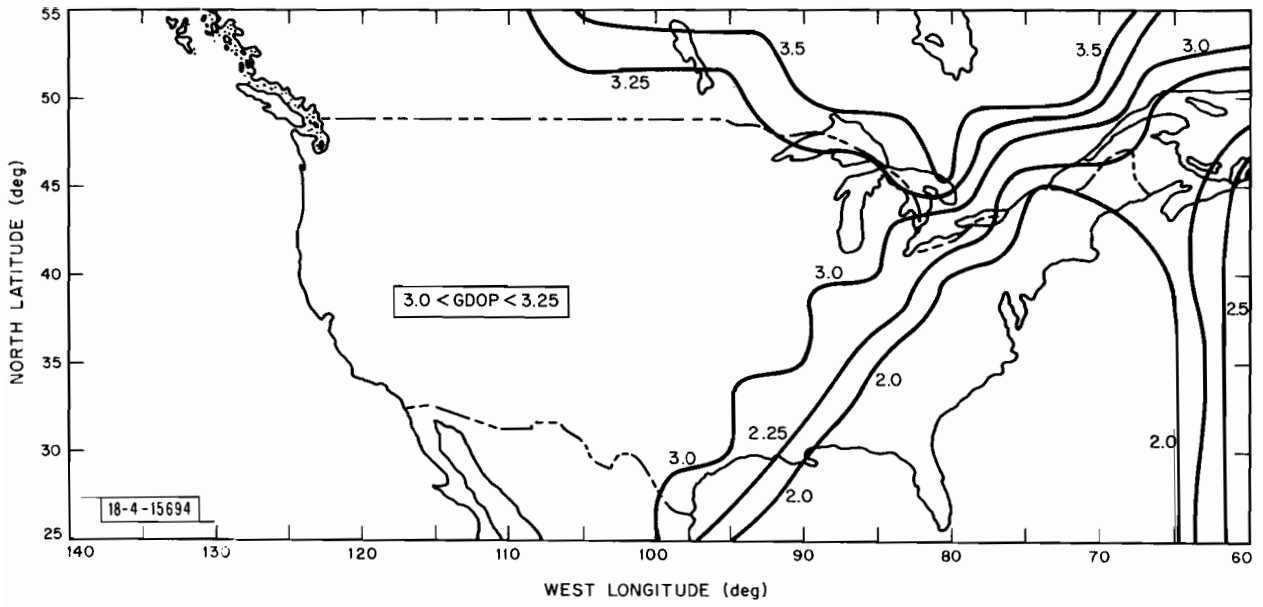

Fig. 5.7. LL-I constellation ($\phi = 90^{o}$). Time 0.0 minutes.

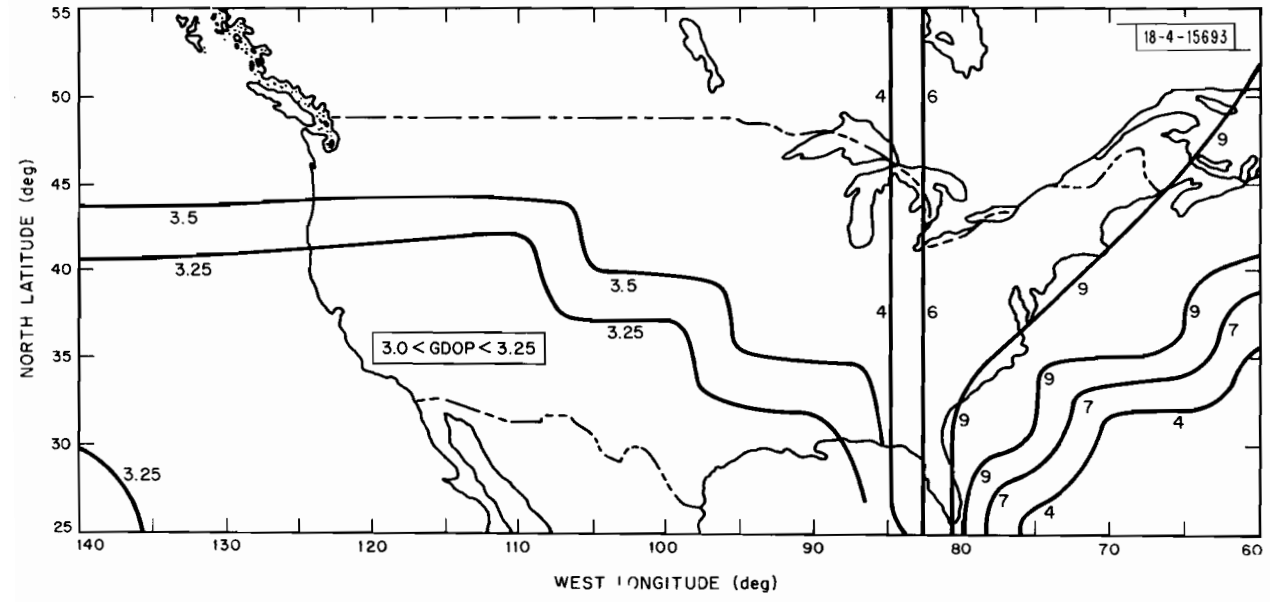

Fig. 5.8. LL-I constellation ($\phi = 75^{o}$). Time 0.0 minutes.

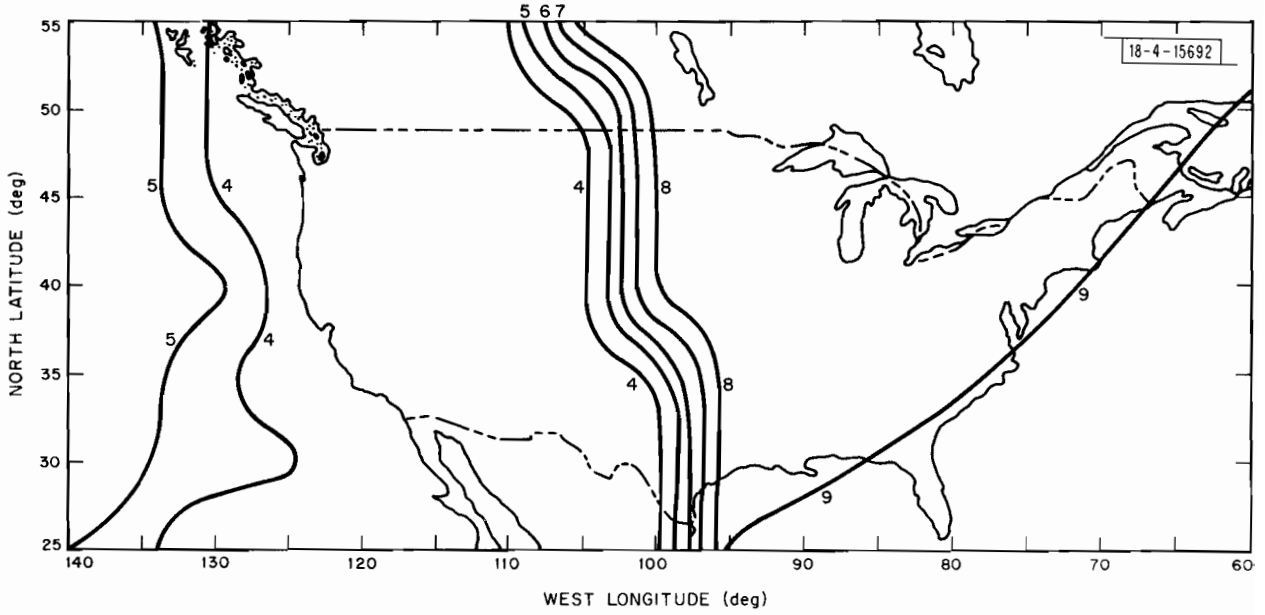

Fig. 5.9. LL-I constellation ($\phi = 60^{o}$). Time 0.0 minutes.

LL-I CONSTELLATION

Table 5.6. Nominal results.

Cone Half Angle	Average Number Visible	Percent GDOP > 10	Average GDOP < 10	rms Deviation	Excess
90°	9.95	0%	2.87	0.56	3.08
75°	9.09	0%	4.57	2.40	4.15
60°	8.21	0%	6.55	2.53	4.48

Table 5.7. Dropout results.

Cone Half Angle	Average Number Visible	Percent GDOP > 10	Average GDOP < 10	S (Sensitivity)	Failed Satellite
90°	9.00	0 %	3.70	3.02	11
75°	8.39	0 %	6.55	5.63	11
60°	7.72	14.3%	8.52*	5.04*	11

*Larger if GDOP's exceeding ten are included.

Table 5.8. 30° Bank results.

Cone Half Angle	Average Number Visible	Percent GDOP > 5	Percent GDOP > 10	Average GDOP < 10
90°	9.37	8.7%	0%	3.636
75°	8.72	29.4%	1.1%	4.696
60°	7.34	68.4%	22.1%	6.210

Dropout results are summarized in Table 5.7 for failure of Satellite No. 11 which occupies an extreme southwesterly position in the viewing cone. The average number of visible satellites decreases by almost unity for $\phi = 90^{\circ}$, 75° since Satellite No. 11 is visible over most of CONUS for these cone half angles. The decrease is smaller (0.51) for $\phi = 60^{\circ}$, in which case Satellite No. 11 is visible over approximately half of CONUS.

The bank analysis results are given in Table 5.8. The first row shows that for a viewing cone half angle $\phi = 90^{\circ}$, banking does not degrade accuracy significantly. Specifically, the average GDOP increases by 25% compared to level flight. The second and third rows show that banking degrades accuracy more substantially for smaller viewing cones. For example, for $\phi = 75^{\circ}$, 29.4% of the banking aircraft have GDOP's in excess of five, and 1.1% have GDOP's in excess of ten. For $\phi = 60^{\circ}$, 68.4% of the aircraft have GDOP's in excess of five and 22.1% have GDOP's in excess of ten.

In summary, the LL-I constellation provides reasonably uniform GDOP over CONUS for a viewing cone half angle of $\phi = 90^{\circ}$. As the size of the viewing cone is reduced, GDOP increases significantly and loses its uniformity. Again, accuracy is sensitive to failure of a single satellite and also to aircraft maneuvers.

5.4 THE HYBRID CONSTELLATION

A more recent constellation for providing CONUS coverage is the Hybrid constellation proposed by Autonetics [3, 8].* The Hybrid constellation derives from the earlier RCA-8 constellation. The changes consist of placing three

*Note: The constellation is called the "System-A Constellation" in Ref. [8]. See pp. 2-57 to 2-75, Vol. 2, Book 1.

additional satellites in inclined orbits, and four additional satellites in equatorial orbits.

The parameters defining the constellation are given in Table 5.9. The deployment of the satellites at time t = 0 is shown in Fig. 5.10. Note that the figure eight ground track is identical to that in Fig. 5.2.

GDOP maps for the three cone angles are shown in Fig. 5.11 to 5.13. Figure 5.11 shows that for $\phi = 90^{\circ}$, the constellation produces a relatively uniform GDOP of approximately two. The ridge of "high" GDOP in central CONUS is due to masking of two equatorial satellites (numbers 10 and 15), by the rim of the viewing cone. To the left of the ridge, Satellite 10 is available; to the right, Satellite 15 is available.* Figure 5.12 shows that for $\phi = 75^{\circ}$ GDOP's continue to be relatively uniform but are somewhat higher. The valleys of low GDOP (2.0) in southern CONUS are due to the fact that five equatorial satellites are visible there rather than the more normal four. Figure 5.13 shows that as ϕ is reduced to 60°, GDOP becomes higher and more variable. The high GDOP's in northern CONUS are due to non-availability of equatorial satellites.

The GDOP maps for the Hybrid constellation repeat every 2 hrs 40 min.

GDOP statistics for the Hybrid constellation at time t = 0 hrs are given in Table 5.10. Again, the average number of visible satellites decreases as the cone half angle is reduced. The unit reduction from 10.82 to 9.83 is due to masking of one or another of the equatorial satellites by the 75° viewing cone. The reduction from 9.83 to 8.00 is due to further masking of one or

*Note that the GDOP's indicated in Fig. 5.11 are smaller than those given in Ref. [8]. This is a consequence of using a visibility criteria based on cone angle, rather than on the signal-to-noise ratio at the receiver. See Section 3.3.

Table 5.9. The HYBRID constellation.

SATELLITE NO.	INC. (DEG)	ECC.	T(P) (HOURS)	LONG.(P) (DEG)
		SATELLITE DEPLOYMENT		
TYPE 1				
1	80.	0.25	0.0	-100.0
2	80.	0.25	2.667	-100.0
3	80.	0.25	5.333	-100.0
4	80.	0.25	8.000	-100.0
5	80.	0.25	10.667	-100.0
6	80.	0.25	13.333	-100.0
7	80.	0.25	16.000	-100.0
8	80.	0.25	18.667	-100.0
9	80.	0.25	21.333	-100.0
TYPE 3				
10	-	-	-	180.0
11	-	-	-	-140.0
12	-	-	-	-115.0
13	-	-	-	-85.0
14	-	-	-	-60.0
15	-	-	-	-20.0

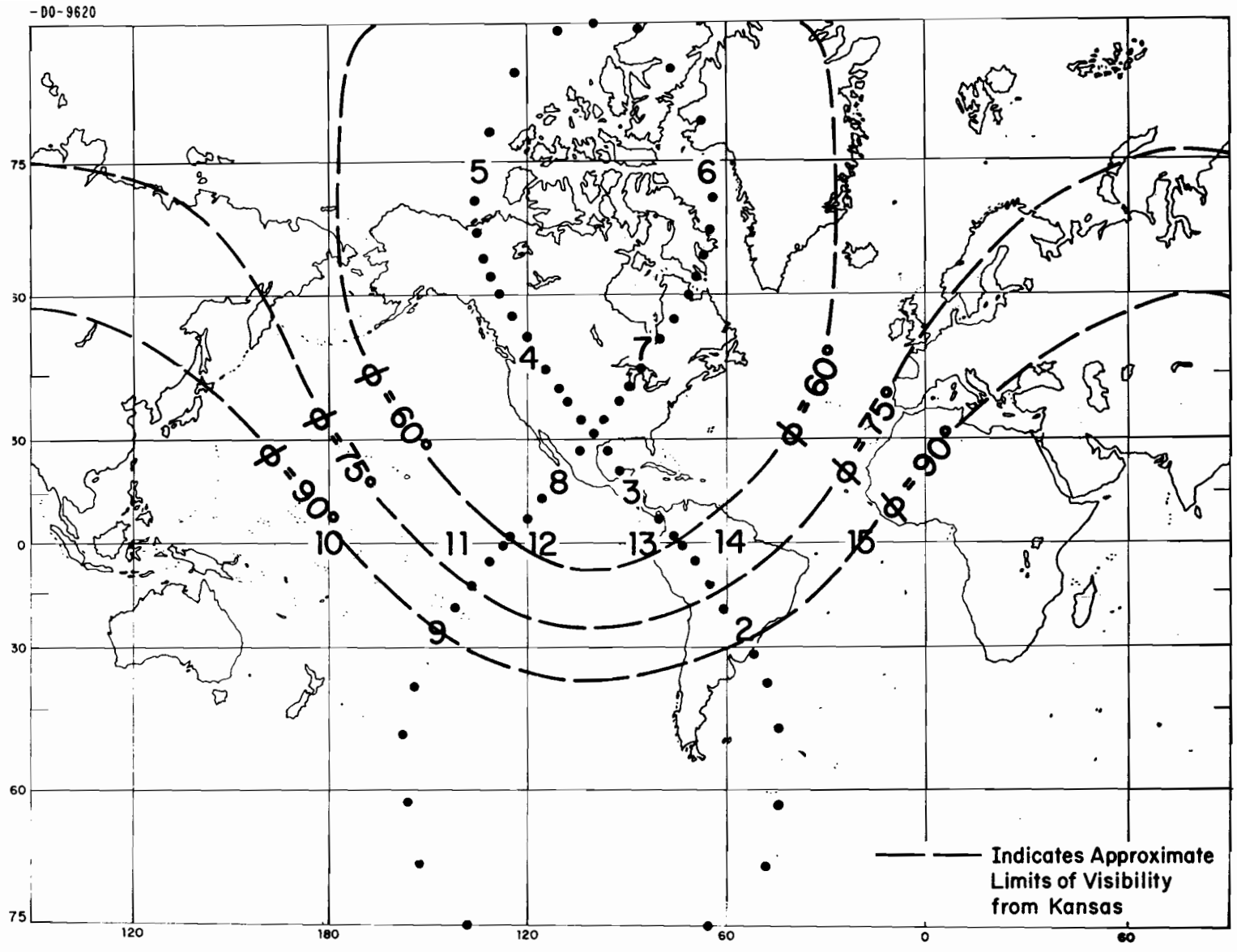

Fig. 5.10. The ground track for Hybrid.

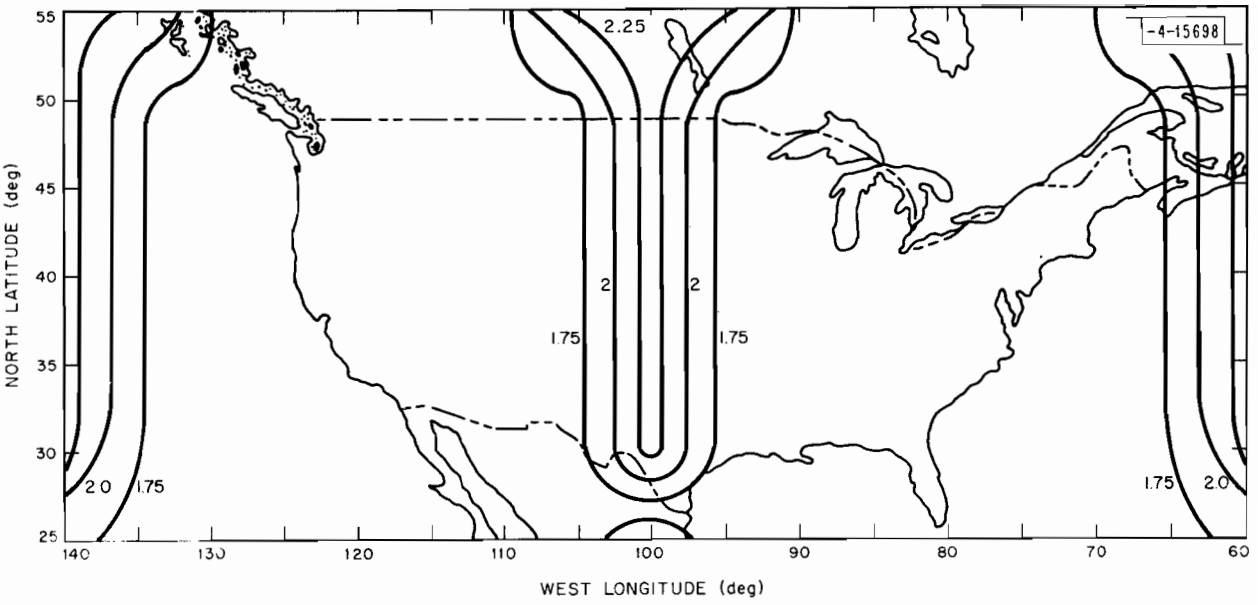

Fig. 5.11. Hybrid constellation ($\phi = 90^{o}$). Time 0.0 minutes.

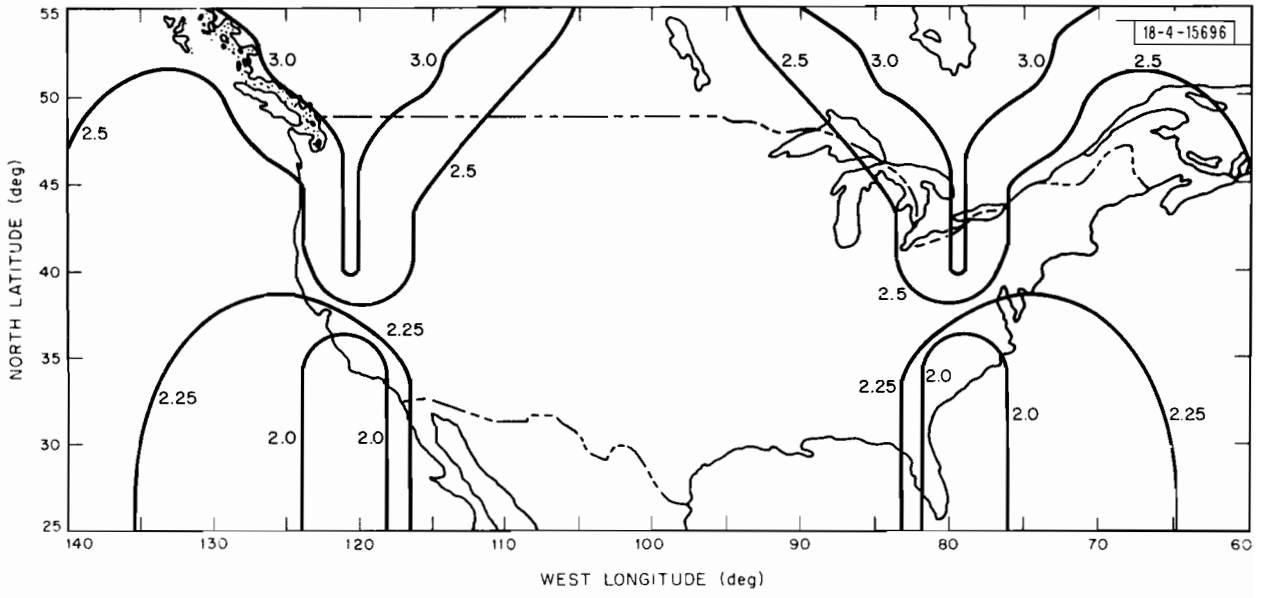

Fig. 5.12. Hybrid constellation ($\phi = 75^{o}$). Time 0.0 minutes.

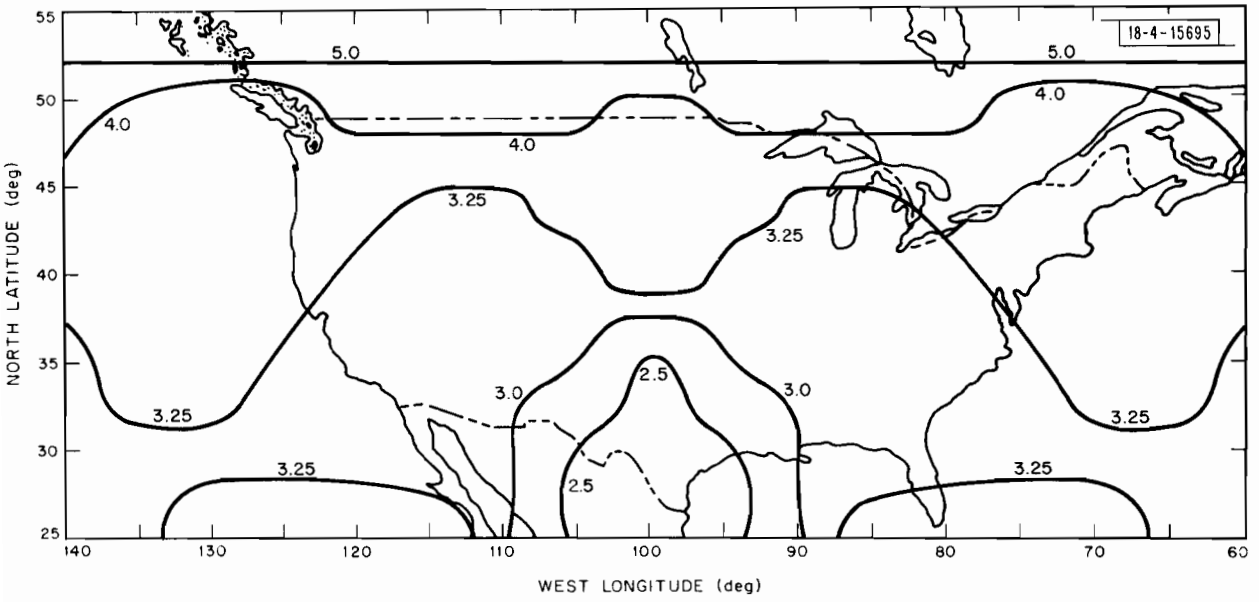

Fig. 5.13. Hybrid constellation ($\phi = 60^{o}$). Time 0.0 minutes.

HYBRID CONSTELLATION

Table 5.10. Nominal results.

Cone Half Angle	Average Number Visible	Percent GDOP > 10	Average GDOP < 10	rms Deviation	Excess
90°	10.82	0%	1.801	0.254	2.16
75°	9.83	0%	2.448	0.352	2.48
60°	8.00	0%	3.793	1.108	2.91

Table 5.11. Dropout results.

Cone Half Angle	Average Number Visible	Percent GDOP > 10	Average GDOP < 10	S (Sensitivity)	Failed Satellite
90°	10.35	0%	2.151	4.47	10
75°	9.13	0%	2.784	1.92	11
60°	7.60	0%	4.061	1.41	11

Table 5.12. 30° Bank results.

Cone Half Angle	Average Number Visible	Percent GDOP > 5	Percent GDOP > 10	Average GDOP < 10
90°	9.99	1.2%	0 %	2.329
75°	8.71	11.0%	0.3 %	3.151
60°	6.75	39.9%	11.74%	4.554

more equatorial satellites, and one or more non-equatorial satellites. It is evident that Hybrid provides uniform and comparatively low GDOPs over all of CONUS. For example, for $\phi = 90^{o}$ the average GDOP is 1.801. The entries in the "Excess" column show that GDOPs for Hybrid are 2.16 to 2.91 times larger than those which can be obtained by optimally positioning the satellites within the viewing cones considered.

Dropout results for the Hybrid constellation are summarized in Table 5.11 for failure of an equatorial satellite near the southwestern cone horizon. Clearly, the constellation is relatively insensitive to single satellite failure.

The results of the bank analysis are given in Table 5.12. The table shows that degradation is not significant for the viewing cone half angles $\phi = 90^{o}$ and $\phi = 75^{o}$. For $\phi = 60^{o}$, degradation becomes more noticable. Here, 39.9% of banking aircraft have GDOP's in excess of five and 11.7% have GDOP's in excess of ten.

To summarize, the Hybrid constellation provides low and relatively uniform GDOP's over CONUS. Accuracy is not seriously degraded either by failure of a single satellite, or by aircraft maneuvers.

5.5 COMPARISON

The following conclusions can be drawn on basis of Sections 5.2 to 5.4.

Level Flight:

Table 5.13 summarizes the average GDOP's for the three constellations. It is evident from the table that the Hybrid constellation produces the lowest GDOP in all cases.

Table 5.13. Comparison of average GDOP.

	$\phi = 90^{\circ}$	$\phi = 75^{\circ}$	$\phi = 60^{\circ}$
RCA-8	3.509	3.761	4.70*
LL-I	2.87	4.57	6.55
Hybrid	1.801	2.448	3.793

It is not surprising that Hybrid produces the smallest GDOP's since it contains the most satellites. To properly compare the qualities of the constellations a "normalized" GDOP should be used. It is shown in Section 6.7 that the product $\sqrt{N}$ x GDOP is a suitable normalized GDOP.

Table 5.14 contains the values of normalized GDOP for the three constellations. For the half angles $\phi = 90^{\circ}$ and $\phi = 75^{\circ}$, the Hybrid constellation again exhibits the smallest values. Thus, for $\phi = 90^{\circ}$ and $\phi = 75^{\circ}$, Hybrid is the "best" constellation. For $\phi = 60^{\circ}$ the RCA-8 constellation exhibits the smallest normalized GDOP. Since the primary difference between Hybrid and RCA-8, apart from scale, is the presence of Satellites Nos. 10 and 15, this result indicates that Satellites 10 and 15 are not efficiently placed for $\phi = 60^{\circ}$.

Table 5.14. Comparison of normalized GDOP.

	$\phi = 90^{\circ}$	$\phi = 75^{\circ}$	$\phi = 60^{\circ}$
RCA-8	9.92	10.64	13.29*
LL-I	9.94	15.8	22.70
Hybrid	6.98	9.48	14.69

Satellite Failure:

Table 5.15 summarizes the sensitivities of the constellations to single satellite failure.

Table 5.15. Comparison of sensitivity to single satellite failure.

	$\phi = 90^{o}$	$\phi = 75^{o}$	$\phi = 60^{o}$
RCA-8	8.51	6.70*	3.35*
LL-I	3.02	5.63	5.04*
Hybrid	4.47	1.92	1.41

*Larger, if GDOP's exceeding ten are included.

Reference to Table 5.15 shows that on the whole, RCA-8 is most sensitive to a single satellite failure, LL-I is next most sensitive, and Hybrid is least sensitive.

It is quite reasonable that Hybrid is the least sensitive to satellite failure. Hybrid is the most redundant constellation in that it contains the largest number of satellites, and has the smallest mean spacing between satellites.

Maneuvers:

Tables 5.16 and 5.17 summarize the banking results for the three constellations.

Table 5.16. Percentage of GDOP's larger than five.

	$\phi = 90^{o}$	$\phi = 75^{o}$	$\phi = 60^{o}$
RCA-8	7.2%	37.8%	78.6%
LL-I	8.7%	29.4%	68.4%
Hybrid	1.2%	11 %	39.9%

Table 5.17. Percentage of GDOP's larger than ten.

	$\phi = 90^{o}$	$\phi = 75^{o}$	$\phi = 60^{o}$
RCA-8	2%	17.2%	53.7%
LL-I	0%	1.1%	22.1%
Hybrid	0%	0.3%	11.7%

The tables indicate an inverse correlation between constellation size and the percentages of excessive GDOP's. Specifically, the smallest constellation (RCA-8) exhibits the largest percentages of excessive GDOP's. The next smallest constellation (LL-I) exhibits the next largest percentage of excessive GDOP's. The largest constellation (Hybrid) exhibits fewest excessive GDOP's.

The inverse correlation is due to the following factors.

1. GDOP's for the small constellations are large to begin with.

2. As a banking aircraft is stepped through headings of 0^{o}, 10^{o}, ..., 350^{o} the fractional number of satellites visible fluctuates most for small constellations.
3. GDOP's for small constellations are the most sensitive to fractional changes in the number of visible satellites.

5.6 IMPROVING GDOP

A review of the GDOP maps of Sections 5.2 through 5.4 leads to the following observations.

1. Trenches in the GDOP maps occur where a relatively large number of satellites are visible at low elevation angles (e.g., equatorial satellites, satellites at apogee).
2. Ridges in the GDOP maps occur where a relatively small number of satellites is visible at low elevation angles.

These observations suggest that a good strategy for obtaining low values of GDOP consists of placing as many satellites as possible at low elevation angles. It is shown in Section 7 that retrograde orbits achieve this objective nicely.

SECTION 6

ANALYTICAL BASIS FOR IMPROVING GDOP

While the formulas (2. 13) and (2. 18) produce accurate values for GDOP, they provide little insight into possible ways of reducing GDOP. Accordingly, the present section describes an alternate procedure for calculating GDOP, one that does provide such insight. The alternate procedure links GDOP to the moments of inertia of a configuration of masses that is easily derivable from the constellation-aircraft geometry. This connection makes it possible to apply intuition about moments of inertia to the problem of reducing GDOP.

The insight provided by the alternate calculation procedure also makes it possible to resolve two related issues. First, the procedure suggests a method for deleting a satellite from a constellation so as to maximally impact GDOP. (This information is important for assessing the sensitivity of a constellation to satellite failure). Second, the procedure leads to a suitable definition of "normalized GDOP."

6.1 AN ALTERNATE PROCEDURE FOR CALCULATING GDOP

The alternate calculation procedure* consists of three basic steps. First, a simple configuration of masses is constructed from the satellite-aircraft geometry. Next, the moments and products of inertia of the mass

*A derivation of the procedure can be found in Ref. [11].

configuration about its center of mass are calculated. Finally, GDOP is calculated from the inverse of the moment of inertia matrix.

The procedure for constructing the configuration of masses is illustrated in Fig. 6.1. The details of the construction are as follows:

1. Draw a sphere of unit radius centered at the aircraft.
2. Draw unit vectors $\underline{i}_1, \underline{i}_2, \ldots, \underline{i}_N$ from the center 0 of the unit sphere pointing to each of the satellites.
3. Place unit masses $m_1, m_2, \ldots, m_N$ at the tips of the unit vectors as shown in Fig. 6.1.

The next step consists of calculating the moment of inertia matrix of the mass configuration about its center of mass (CM). To perform this step it is necessary to locate the center of mass, and set up a Cartesian coordinate system (X, Y, Z) there. Then, the moment of inertia matrix $\underline{L}$ is calculated from the expression

$$\underline{L} = \begin{bmatrix} \sum_{j=1}^{N} X_j^2 & \sum_{j=1}^{N} Y_j X_j & \sum_{j=1}^{N} Z_j X_j \\ \sum_{j=1}^{N} X_j Y_j & \sum_{j=1}^{N} Y_j^2 & \sum_{j=1}^{N} Z_j Y_j \\ \sum_{j=1}^{N} X_j Z_j & \sum_{j=1}^{N} Y_j Z_j & \sum_{j=1}^{N} Z_j^2 \end{bmatrix}$$

(equation continued on next page)

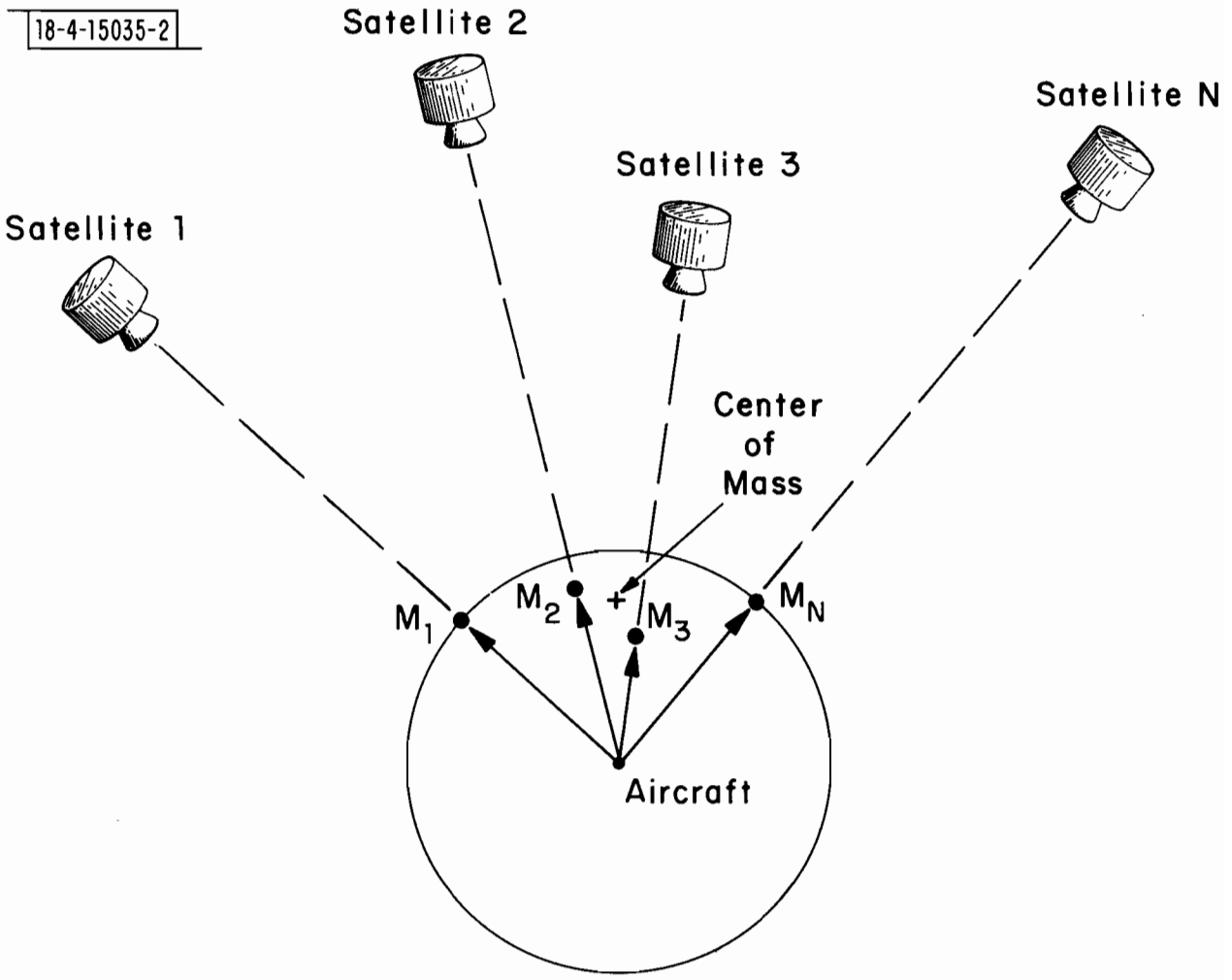

Fig. 6.1. Construction of the unit mass configuration.

$$= \begin{bmatrix} L_{xx} & L_{xy} & L_{xz} \\ L_{xy} & L_{yy} & L_{yz} \\ L_{xz} & L_{yz} & L_{zz} \end{bmatrix} \tag{6.1}$$

where X_j, Y_j, Z_j denote the coordinates of the jth mass.

The final step consists of inverting the $\underline{L}$ matrix (6.1) to obtain the $\underline{\Gamma}$ matrix (2.13). The matrix takes the form

$$\underline{\Gamma} = \underline{L}^{-1} = \begin{bmatrix} \Gamma_{xx} & \Gamma_{xy} & \Gamma_{xz} \\ \Gamma_{xy} & \Gamma_{yy} & \Gamma_{yz} \\ \Gamma_{xz} & \Gamma_{yz} & \Gamma_{zz} \end{bmatrix} \tag{6.2}$$

GDOP then is calculated from the expression

$$\text{GDOP} = (\Gamma_{xx} + \Gamma_{yy} + \Gamma_{zz})^{1/2} \tag{6.3}$$

6.2 ILLUSTRATIVE EXAMPLE

As an illustration of the procedure, consider the constellation-aircraft geometry shown in Fig. 6.2. Figure 6.3 depicts the appropriate set of unit vectors, $\underline{i}_1, \ldots, \underline{i}_4$ and unit masses $m_1, \ldots, m_4$.

A simple calculation shows that the center of mass (CM) of $m_1, \ldots, m_4$ is located a distance

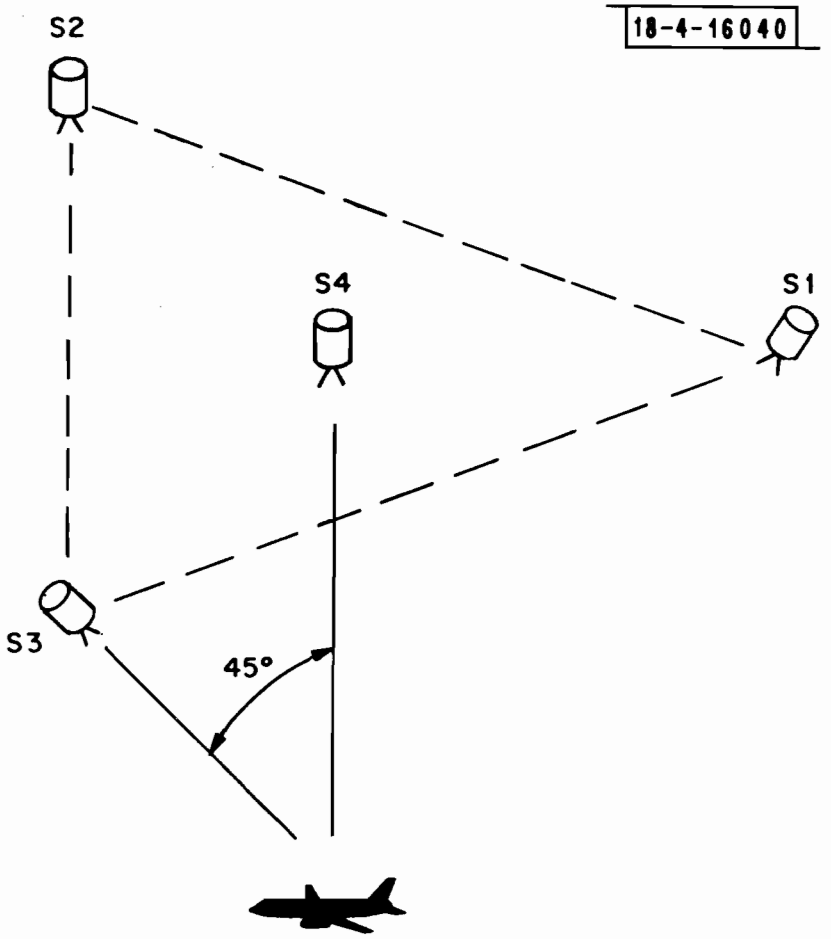

Fig. 6.2. The satellite-aircraft geometry for Section 6.2.

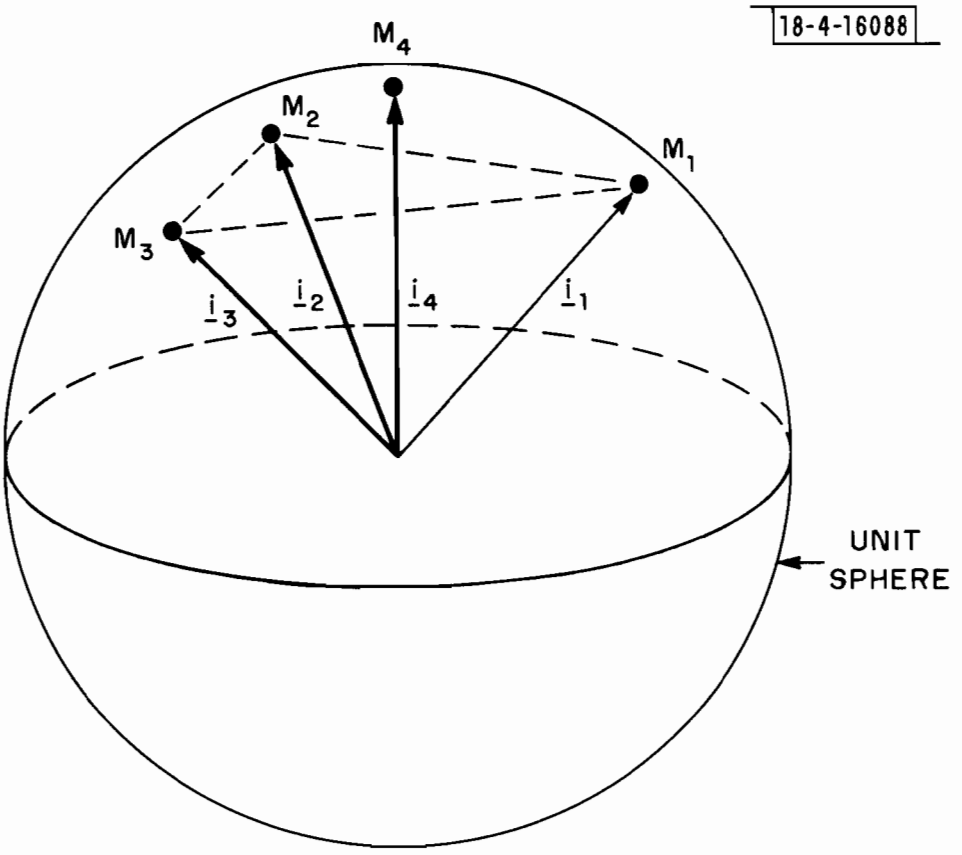

Fig. 6.3. The unit mass configuration.

$$d = \frac{1}{4}\,(3/\sqrt{2} + 1) = 0.780 \tag{6.4}$$

directely above the sphere center 0.

The moments and products of inertia of $m_1, \ldots, m_4$ about CM can be calculated straightforwardly. For the coordinate system indicated in Fig. 6.4 the relevant quantities are as follows:

$$L_{xx} = m_1\,(1/\sqrt{2})^2 + (m_2 + m_3)\,(1/2\sqrt{2})^2 = 3/4 \tag{6.5}$$

$$L_{yy} = (m_2 + m_3)\left(\frac{1}{\sqrt{2}} - \frac{\sqrt{3}}{2}\right)^2 = 3/4 \tag{6.6}$$

$$L_{zz} = (m_1 + m_2 + m_3)\,(0.780 - 1/\sqrt{2})^2 + m_4\,(1 - 0.780)^2$$

$$= 0.0643 \tag{6.7}$$

$$L_{xy} = L_{xz} = L_{yz} = 0 \quad . \tag{6.8}$$

Consequently, the moment of inertia matrix $\underline{L}$ is as follows:

$$\underline{L} = \begin{bmatrix} 0.75 & 0 & 0 \\ 0 & 0.75 & 0 \\ 0 & 0 & 0.0643 \end{bmatrix} \quad . \tag{6.9}$$

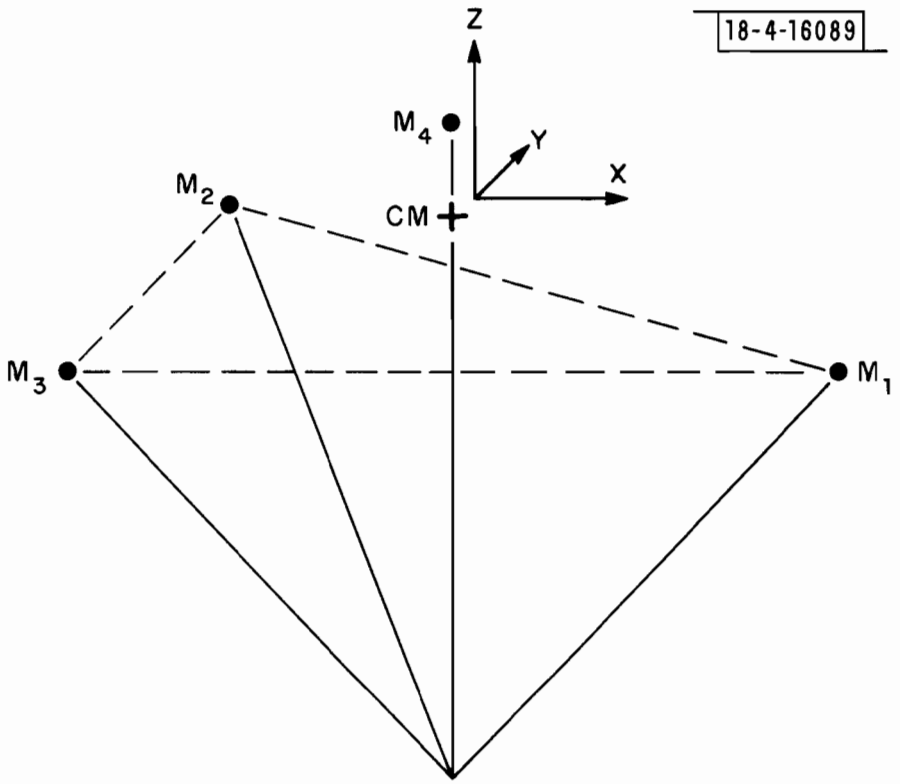

Fig. 6.4. The coordinate system for calculating the $\underline{L}$ Matrix.

The corresponding $\underline{\Gamma}$ matrix is given by:

$$\underline{\Gamma} = \underline{L}^{-1} = \begin{bmatrix} 1.33 & 0 & 0 \\ 0 & 1.33 & 0 \\ 0 & 0 & 15.54 \end{bmatrix} . \qquad (6.10)$$

The value of GDOP now can be calculated from (2.18). Specifically;

$$\text{GDOP} = \sqrt{(1.33) + (1.33) + (15.54)}$$

$$= 4.27 \qquad (6.11)$$

which agrees with the previous result (2.25).

6.3 CONSTELLATION DESIGN STRATEGY

By working backward through the steps in Section 6.1, it is possible to deduce attributes of a constellation exhibiting low values of GDOP.

Specifically, GDOP as given by (6.3), can small only if the trace of $\underline{\Gamma}$ is small. But, the trace of $\underline{\Gamma}$ is small only if that of $\underline{L}$ ($=\underline{\Gamma}^{-1}$) is large.* The diagonal elements of $\underline{L}$ correspond to the moments of inertia of the mass constellation shown in Fig. 6.1. Accordingly, to obtain a (comparatively) small value of GDOP **it** is necessary that the moments of inertia L_{xx}, L_{yy}, and L_{zz} be large.

*It is easy to show that $Tr[\underline{\Gamma}] > 9/TR[\underline{L}]$ with equality possible iff $L_{xx} = L_{yy} = L_{zz}$. Thus, a small value of $Tr[\underline{\Gamma}]$ implies a large value of $Tr[\underline{L}]$.

This conclusion suggests that the following is a good strategy for obtaining low GDOPs.

Strategy: Select the satellite orbits so that masses $m_1, m_2, \ldots, m_N$ exhibit large moments of inertia in all three directions.

The strategy obviously produces large values of L_{xx}, L_{yy} and L_{zz}. It also tends to produce small values of Γ_{xx}, Γ_{yy}, and Γ_{zz} so that GDOP, as calculated from (6.3), is small.

6.4 THE HYBRID CONSTELLATION

It is instructive to calculate GDOP via the method of Section 6.1 for the Hybrid Constellation considered in Section 5.4.

The unit vectors pointing from the grid point at

longitude = 100° W

latitude = 35° N

to the satellites at time t = 0 hours are given in Table 6.1. The vectors are expressed in terms of an North-East-Vertical coordinate system as shown in Fig. 6.5. Projections of the unit masses at the tips of the vectors onto the three coordinate planes are shown in Figs. 6.6 to 6.8. Each integer denotes the location of the unit mass for the correspondingly numbered satellite. An asterisk denotes multiple masses immediately to the left of the asterisk.

Straightforward calculation shows that the $\underline{L}$ matrix is as follows:

$$\underline{L} = \begin{bmatrix} 2.607 & -4.4 \times 10^{-8} & 0.158 \\ -4.4 \times 10^{-8} & 1.444 & -3.0 \times 10^{-9} \\ 0.158 & -3.0 \times 10^{-9} & 0.229 \end{bmatrix}. \qquad (6.12)$$

Table 6.1. Unit vectors for Hybrid at t = 0.

NSAT	U(N)	U(E)	U(V)
3	-0.31581	0.25416	0.91415
4	0.31369	-0.22524	0.92242
5	0.71647	-0.15842	0.67939
6	0.71647	0.15842	0.67939
7	0.31369	0.22524	0.92242
8	-0.31581	-0.25416	0.91415
11	-0.48099	-0.70444	0.52194
12	-0.62557	-0.29250	0.72327
13	-0.62557	0.29250	0.72327
14	-0.48099	0.70444	0.52194
CM	-0.78440D-01	0.90306D-08	0.75223

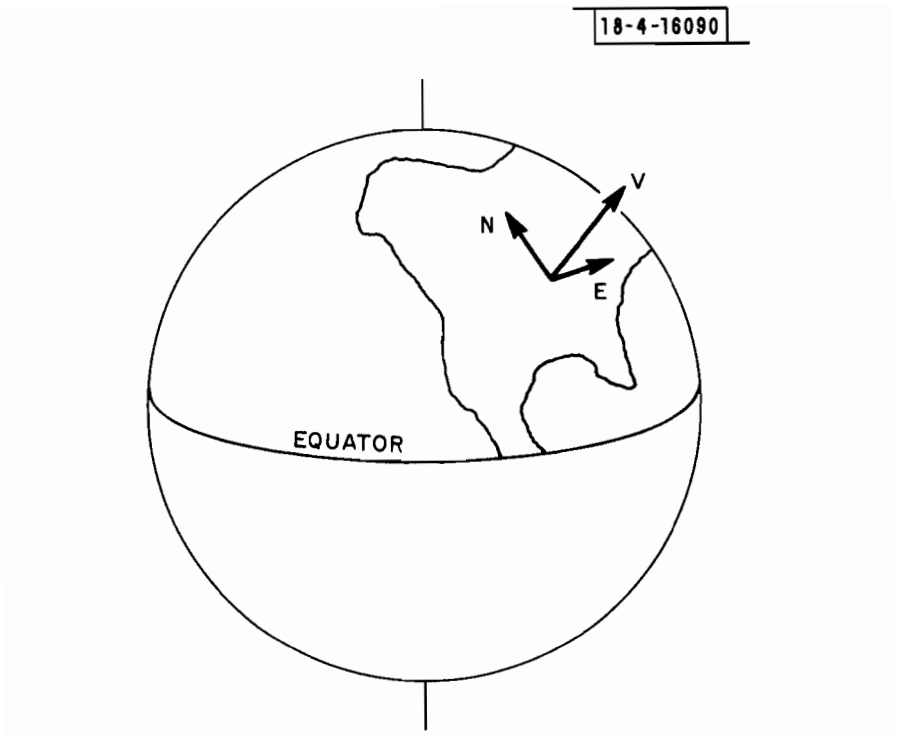

Fig. 6.5. The north-east-vertical coordinate system.

Projections of the Unit Masses for
the HYBRID Constellation

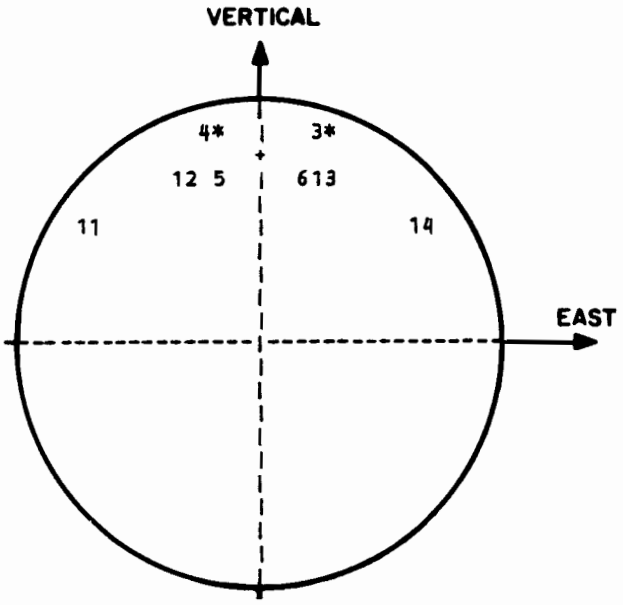

Fig. 6.6. Vertical-East projection.

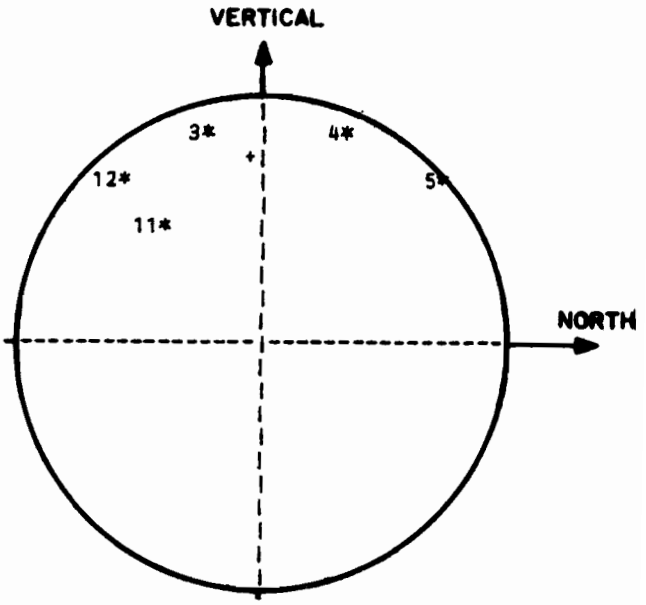

Fig. 6.7. Vertical-North projection.

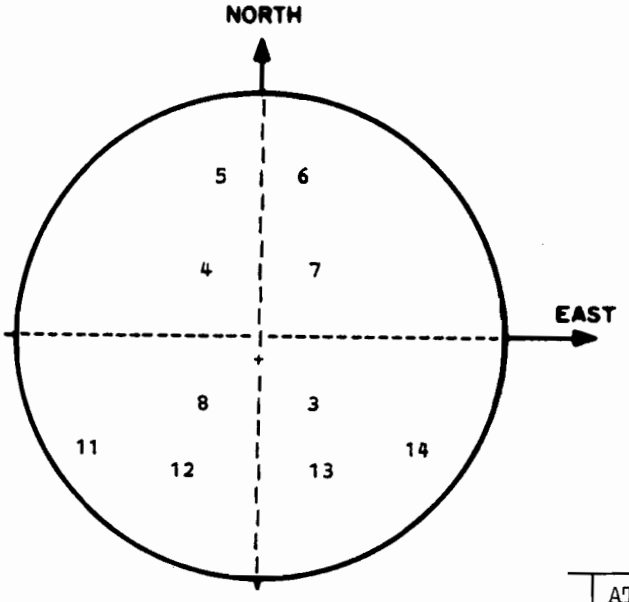

Fig. 6.8. North-East projection.

ATC-23(6.6-8)

THE VISIBLE SATELLITES ARE NUMBERS
3 4 5 6 7 8 11 12 13 14

The reason for the smallness of the 3-3 element compared to the 2-2 and the 1-1 elements is the near planarity of the unit masses as indicated in the V-N projection of the masses (see Fig. 6.7).

The corresponding $\underline{\Gamma}$ matrix is given by

$$\underline{\Gamma} = \begin{bmatrix} 0.400 & 0.117 & -0.276 \\ 0.117 & 0.692 & 9.5 \times 10^{-10} \\ -0.276 & 9.5 \times 10^{-10} & 4.56 \end{bmatrix} . \qquad (6.13)$$

The relative largness of the 3-3 element is a direct consequence of the smallness of the 3-3 element in (6.12).

GDOP can be calculated directly from (6.13). Specifically,

$$\text{GDOP} = \sqrt{(0.400) + (0.692) + (4.56)} \quad .$$

$$= 2.38 \qquad (6.14)$$

Note that (6.14) is identical to the entry in Table B-9 of Appendix B for the grid point at 100° W longitude and 35° N latitude.

The minimum value of GDOP that is obtainable by optimally placing 15 satellites in a cone of half angle $\phi = 90^{\circ}$ is as follows:

$$\text{GDOP} = \left[\frac{1}{\sqrt{N}} \quad \frac{4}{\sqrt{1 + \cos\phi}\,(\sqrt{5 - 3\cos\phi} - \sqrt{1 + \cos\phi})} \right]_{\substack{\phi = 90^{\circ} \\ N = 15}} .$$

$$= 0.8355 \qquad (6.15)$$

Thus, the GDOP value (6.14) is 2.38/0.8355 = 2.85 times larger than the minimum GDOP attainable with 15 satellites.

If the development (6.12) to (6.14) is reviewed, the following conclusions stand out.

1. The GDOP calculation (6.14) is dominated by the quantity $\Gamma_{zz} = 4.56$
2. The large value of Γ_{zz} is due to the near planarity of the unit masses as indicated in Fig. 6.7.

Thus, the high value of GDOP for the Hybrid Constellation compared to (6.15) is a direct consequence of the near planarity of the unit masses as indicated in Fig. 6.7.

6.5 THE ROLE OF HYBRID'S EQUATORIAL SATELLITES

The importance of equatorial satellites to the Hybrid Constellation was stressed in the report that proposed the constellation [8]. The importance of the equatorial satellites also has been noted in Section 5.4. Thus, it is relevant to inquire into the significance of equatorial satellites in terms of the results of Sections 6.1 and 6.4.

Thus, assume for the moment, that the six equatorial satellites (Satellite Nos. 10 to 15) are removed from the Hybrid Constellation. The projections of the remaining unit masses into the three coordinate planes are shown in Fig. 6.9 to 6.11. The moment of inertia matrix is as follows:

Projections of the Unit Masses for the HYBRID Constellation with the Equatorial Satellites Removed

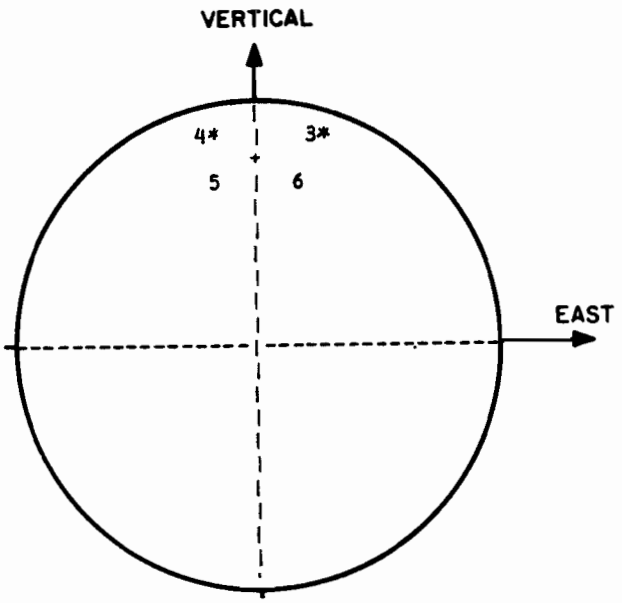

Fig. 6.9. Vertical-East projection.

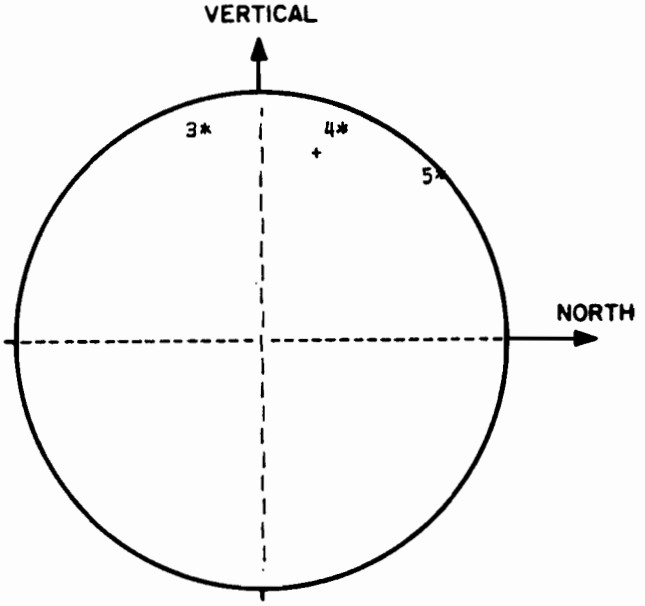

Fig. 6.10. Vertical-North projection.

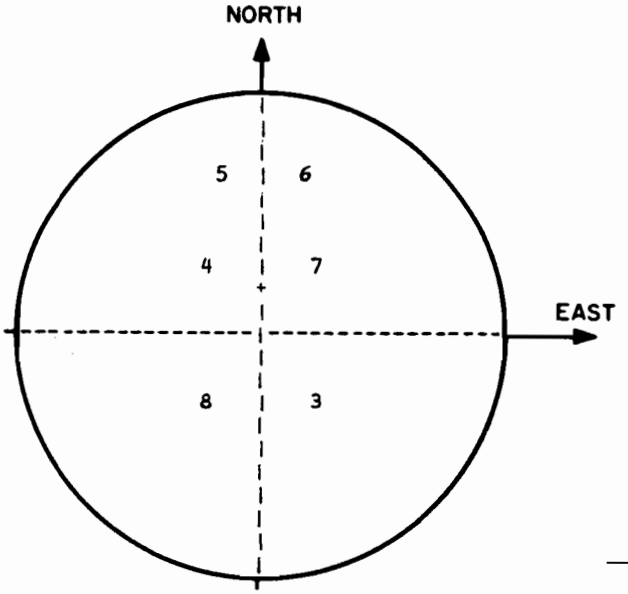

Fig. 6.11. North-East projection.

ATC-23(6.9-11)

THE VISIBLE SATELLITES ARE NUMBERS
3 4 5 6 7 8

$$\underline{L}^{-} = \begin{bmatrix} 1.082 & -7.2 \times 10^{-8} & -0.223 \\ -7.2 \times 10^{-8} & 0.281 & -1.1 \times 10^{-8} \\ -0.223 & -1.1 \times 10^{-8} & 0.076 \end{bmatrix} . \quad (6.16)$$

The z-z element of $\underline{L}^{-}$ is a factor of three smaller than the corresponding element of (6.12) due to the increased planarity of the unit masses as indicated in Fig. 6.10. The corresponding $\underline{\Gamma}$-matrix is given by

$$\underline{\Gamma}^{-} = \begin{bmatrix} 2.337 & 0.871 & 6.854 \\ 0.871 & 3.561 & 3.1 \times 10^{-6} \\ 6.854 & 3.1 \times 10^{-6} & 33.23 \end{bmatrix} . \quad (6.17)$$

The largeness of the z-z element of (6.17) is due to the smallness of the z-z element in (6.16). The associated GDOP can be claculated from (6.3) as follows:

$$\text{GDOP} = \sqrt{(2.337) + (3.561) + (33.23)}$$

$$= 6.255 \quad (6.18)$$

Comparison of (6.18) with (6.14) shows that removal of the equatorial satellites greatly increases GDOP.

A parallel review of the development (6.16) to (6.18) and (6.12) to (6.14) indicates that:

1. The decrease in GDOP from (6.18) to (6.14) is due to the decrease in Γ_{zz}.
2. The decrease in Γ_{zz} is due to the reduced planarity of the unit masses from Fig. 6.10 to Fig. 6.7.

Thus, the mechanism whereby the equatorial satellites reduce GDOP is quite clear. These satellites add new masses that disrupt the almost perfect planarity of the unit masses for Satellites Nos. 1-9.

6.6 ASSESSING SATELLITE FAILURE

A reasonable method for assessing the sensitivity of any constellation to satellite failure is to delete a key satellite and recalculate GDOP. To apply the method, however, one must be able to identify a "key satellite." The results of Sections 6.4 and 6.5 suggest the following simple procedure for doing this.

Procedure

1. Find the plane that best "fits" the unit mass configuration.
2. Take as the "key satellite" the satellite whose unit mass is farthest from the plane.

Indeed, this is the procedure that has been used in most cases to select the "failed satellite" for the dropout studies.

The procedure was applied by working with the Vertical-North, Vertical-East, and North-East projections of the unit mass configuration for a grid point in central CONUS. Figures 6.12 to 6.14 are a representative set of projections. The problem of finding the "best plane" was solved by visually finding the "best straight line" in the projections. Thus, for example, the dashed line in Fig. 6.13 was selected as the best straight line for the

Projections of the Unit Masses for
the HYBRID Constellation

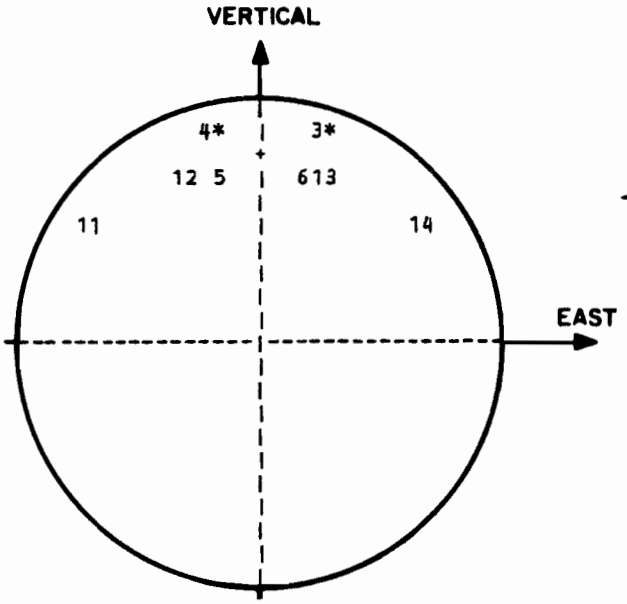

Fig. 6.12. Vertical-East projection.

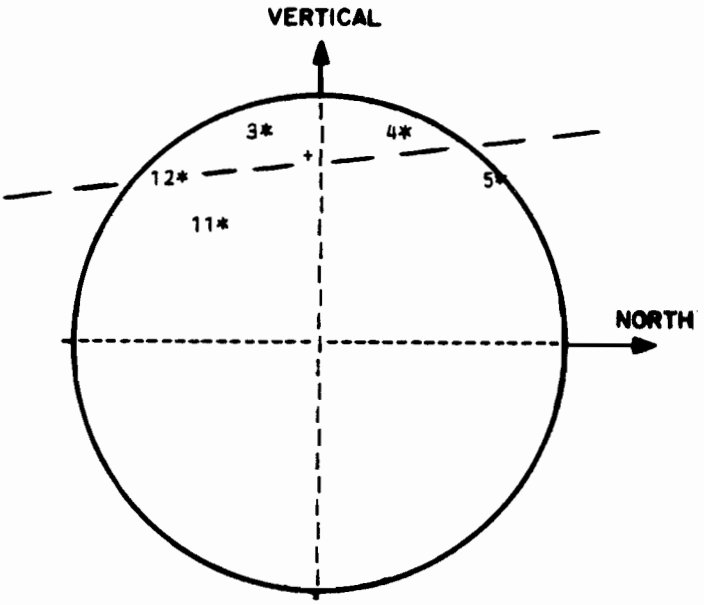

Fig. 6.13. Vertical-North projection.

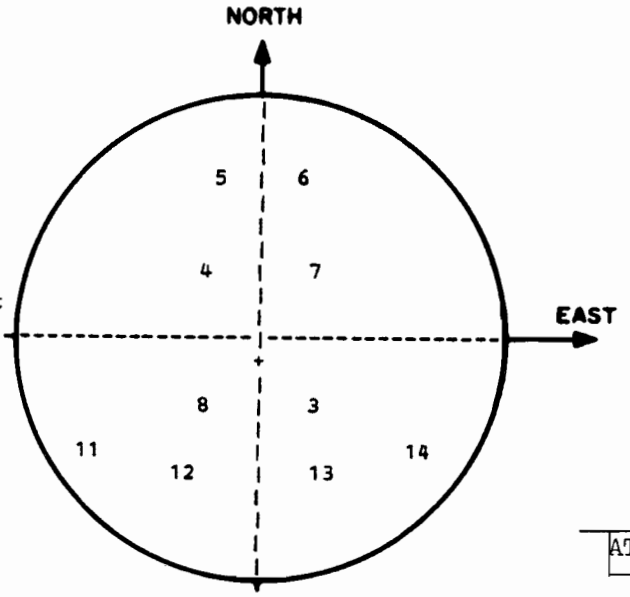

Fig. 6.14. North-East projection.

ATC-23(6.12-14)

THE VISIBLE SATELLITES ARE NUMBERS
3 4 5 6 7 8 11 12 13 14

projections of Fig. 6.12 to 6.14. Once this was done, it was apparent that the Hybrid constellation is sensitive to failure of Satellite 11 at time t = 0. Accordingly, Satellite 11 was used as the "failed satellite" in the Hybrid dropout study (see the second and third rows of Table 5.11).

6.7 NORMALIZED GDOP

Often it is desirable to have a "normalized GDOP" to compare the "efficiencies" of constellations that have different numbers of satellites. A virtue of the GDOP formulation of Section 6.1 is that it suggests a suitable "normalized GDOP."

Thus, let C be any constellation. If C is scaled by a factor of k in the sense that each satellite is replaced by k satellites, then the following changes occur.

1. Each unit mass in Fig. 6.1 is replaced by k unit masses.
2. All moments and products of inertia increase by a factor of k, so that the $\underline{L}$ matrix (6.1) increases by a factor of k.
3. The $\underline{\Gamma}$ matrix (6.2) decreases by a factor of k.
4. The right hand member of (6.3) decreases by $\sqrt{k}$.

It follows that GDOP for C and all scaled versions of C satisfy the relationship

$$\text{GDOP} = \frac{A_1(C)}{\sqrt{k}} \tag{6.19}$$

or equivalently

$$\text{GDOP} = \frac{A_o(C)}{\sqrt{N}} \tag{6.20}$$

where $A_1(C)$ and $A_o(C)$ are constants independent of the total number N of satellites. The result (6.20) suggests that GDOP's of constellations having different numbers of satellites can be compared independent of N by comparing their values of A_o, or equivalently by comparing their products $\sqrt{N}$ x GDOP. Accordingly, we define the normalized GDOP as follows:

$$\text{Normalized GDOP} \triangleq \sqrt{N} \times \text{GDOP} \quad . \tag{6.21}$$

SECTION 7

PROPERTIES OF RETROGRADE ORBITS

All posigrade orbits produce results similar to those described in Section 6.4. That is, the unit masses tend to lie in a plane as shown in Fig. 7.1. As a result, the second moment along the local vertical (z) axis is small so that the z-z entry in (6.1) is small, and the z-z entry in (6.2) is correspondingly large. The quantity Γ_{zz} then substantially exceeds Γ_{xx} and Γ_{yy}, and dominates the GDOP calculation (6.3).

Thus, the problem of obtaining improved GDOPs is a very simple one. The problem amounts to removing the planarity of the unit mass configuration.

One method of eliminating planarity is to add equatorial satellites as done in the Hybrid Constellation (see Section 6.5).

A more effective method of removing planarity is to place satellites in synchronous retrograde orbits. Basically, a retrograde orbit is one with an inclination exceeding 90^{o} as shown in Fig. 7.2. The rotational motion of the satellites then is counter to that of the earth as shown. The orbit is "synchrounous" if its period equals one sidereal day.

This section describes certain basic properties of retrograde orbits, as these orbits play a central role in the constellations of Sections 9 to 11.

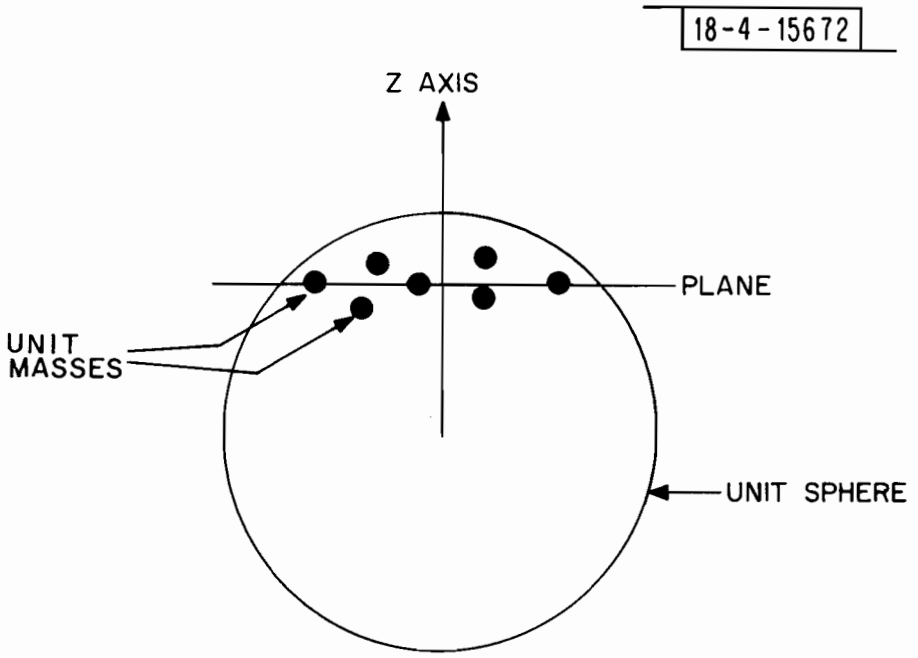

Fig. 7.1. Typical distribution of the unit masses for a posigrade orbit.

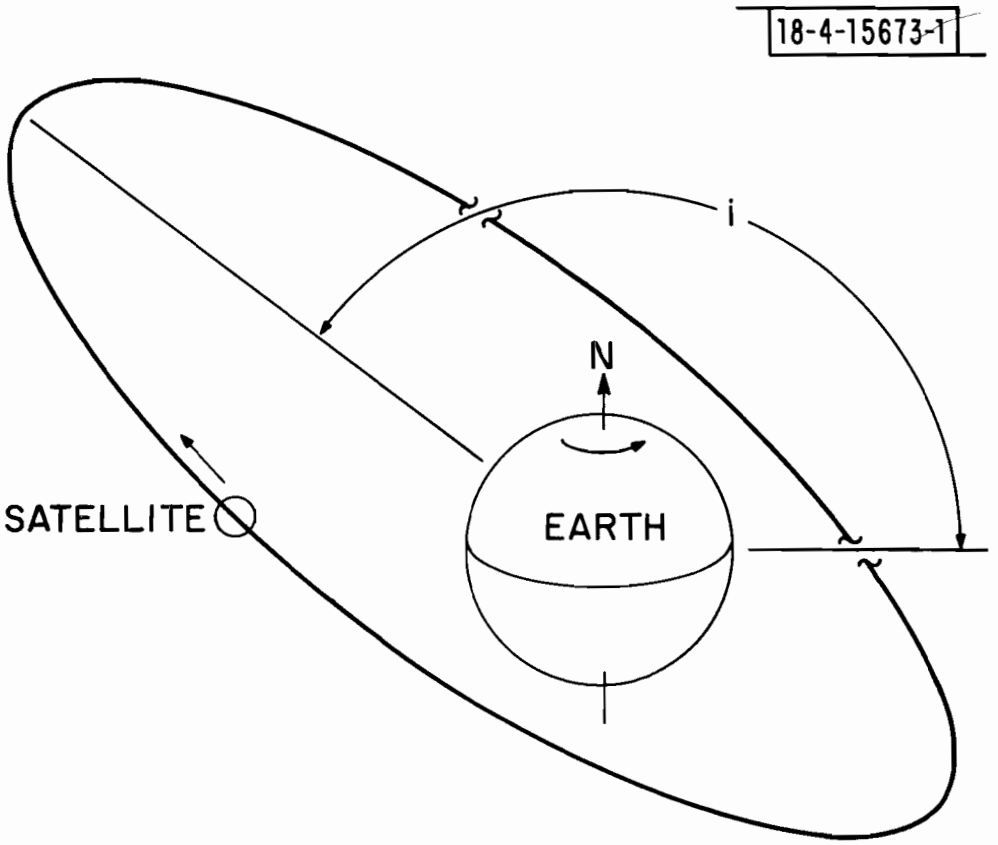

Fig. 7.2. A typical retrograde orbit.

7.1 GROUND TRACKS

Because a satellite in retrograde orbit moves counter to the rotation of the earth, it does not hover over one area of the earth. Rather, its sub-satellite point moves rapidly accross the earth's surface traversing all longitudes.

Figure 7.3 depicts the gound track of a satellite in a circular retrograde orbit. Figure 7.4 depicts the ground track of a satellite in an elliptical retrograde orbit. The ground tracks of Figs. 7.3 and 7.4 are basically similar to those for posigrade orbits except that the tops and bottoms of the figure eights are moved over the north and south poles.

Like a satellite in synchronous posigrade orbit, a satellite in synchronous retrograde orbit retraces its ground track every (sideral) day. At apogee, the ground track has a latitude of $(180^{\circ} - i)$ north, where i denotes the inclination of the orbital plane. At perigee the ground track has a latitude of $(180^{\circ} - i)$ south. The point at which the figure eight crosses itself lies on the equator for for a circular orbit ($e = 0$). As the ecentricity is increased, the crossing point moves northward, approaching the latitude $180^{\circ} - i$ as $e \to 1$. For highly eccentric orbits, the upper loop of the figure eight approximates the circle of constant $180^{\circ} - i$ latitude.

7.2 VISIBILITY

The ground track shown in Fig. 7.4 is one that might be used by a satellite constellation to provide ATC services over CONUS.

In spite of the fact that the sub-satellite point spends much of its time on the backside of the earth, the satellite is continually visible from the

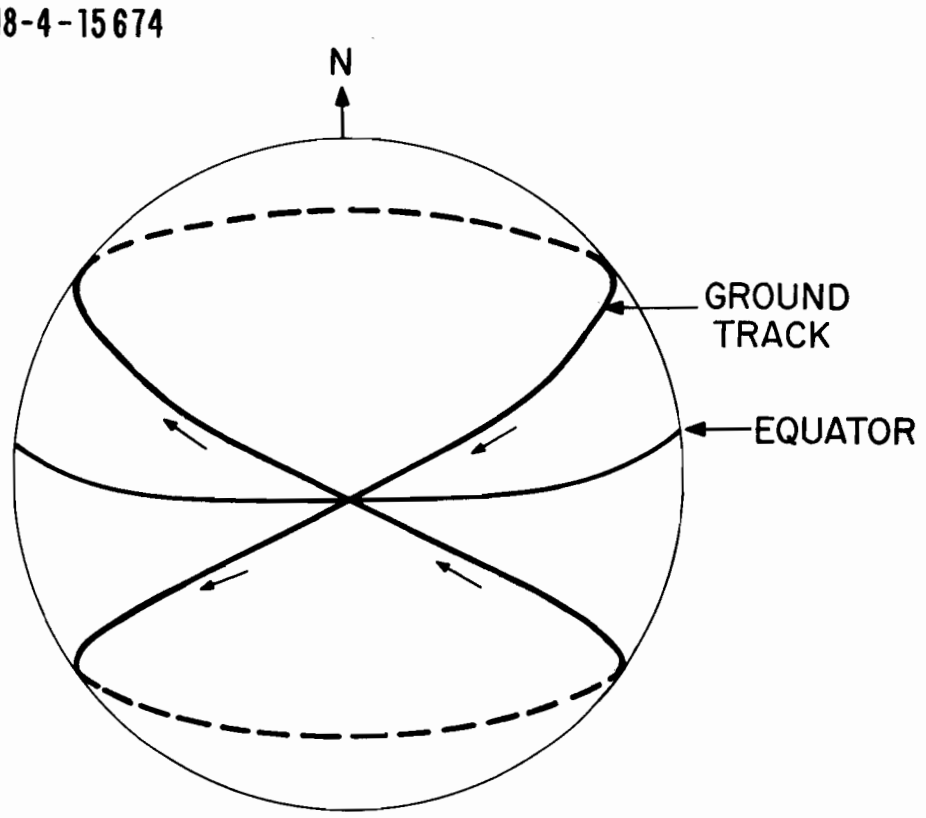

Fig. 7.3. Typical ground track for a circular retrograde orbit.

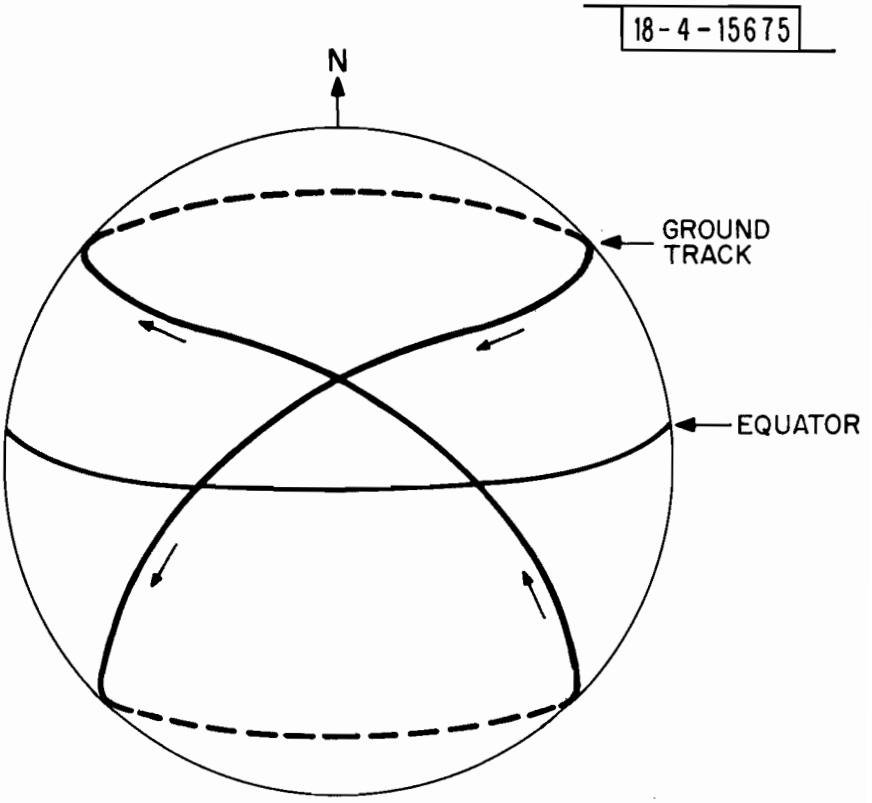

Fig. 7.4. Typical ground track for an elliptical retrograde orbit.

center of CONUS throughout its northern passage provided the orbital inclination is not excessive. Figure 7.5 depicts the satellite trajectory as it would appear looking upward from a point in Kansas. The cross in the center corresponds to the point directly overhead. Radial distance measured inward from the bounding circle corresponds to elevation angle. The polar angle corresponds to azimuth. The data points indicate the positions of a single satellite at the times indicated. The satellite "rises" shortly before t = 2 hrs and is continuously visible through apogee at time t = 10 hrs until shortly after t = 18 hrs when it "sets." The solid triangles indicate equatorial crossings. Thus, the satellite is visible throughout its northern passage.

It is clear that the trajectory of Fig. 6.5 exhibits its worst case elevation at apogee. Thus, it is natural to conjecture that, "if a satellite in retrograde orbit is visible at apogee, then it is visible throughout its northern passage." A computer analysis was performed to explore this question for orbits having $\gamma_p = 100^\circ$ W longitude, and a viewing point located within central CONUS (100 W longitude, 40° N latitude). The results confirmed the conjecture. Accordingly, it is quite easy to ensure that the trajectory of a retrograde orbit as seen from central CONUS remains above a specific viewing cone. To do so, it is only necessary to ensure that the trajectory at apogee is above the cone.

It is interesting to compare Fig. 7.5 with a similiar figure for a posigrade orbit. Figure 7.6 dipicts the trojectory of a posigrade orbit of eccentricity e = 0.25 inclined at an angle of $i = 63.4^\circ$. Comparison of the two figure shows that while both satellites are visible for approximately the same time, the

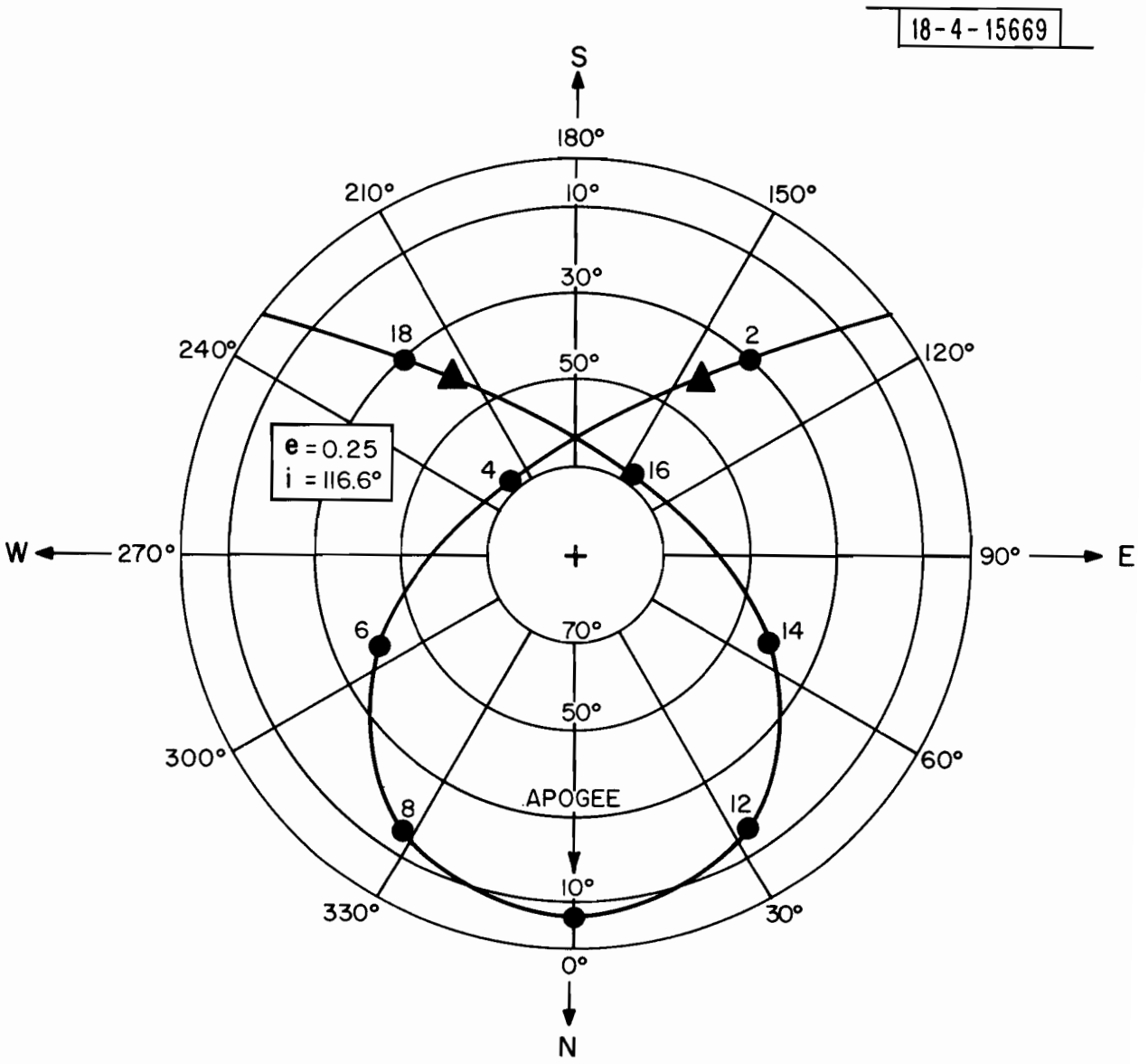

Fig. 7.5. A "planetarium view" of the trajectory for a typical retrograde orbit.

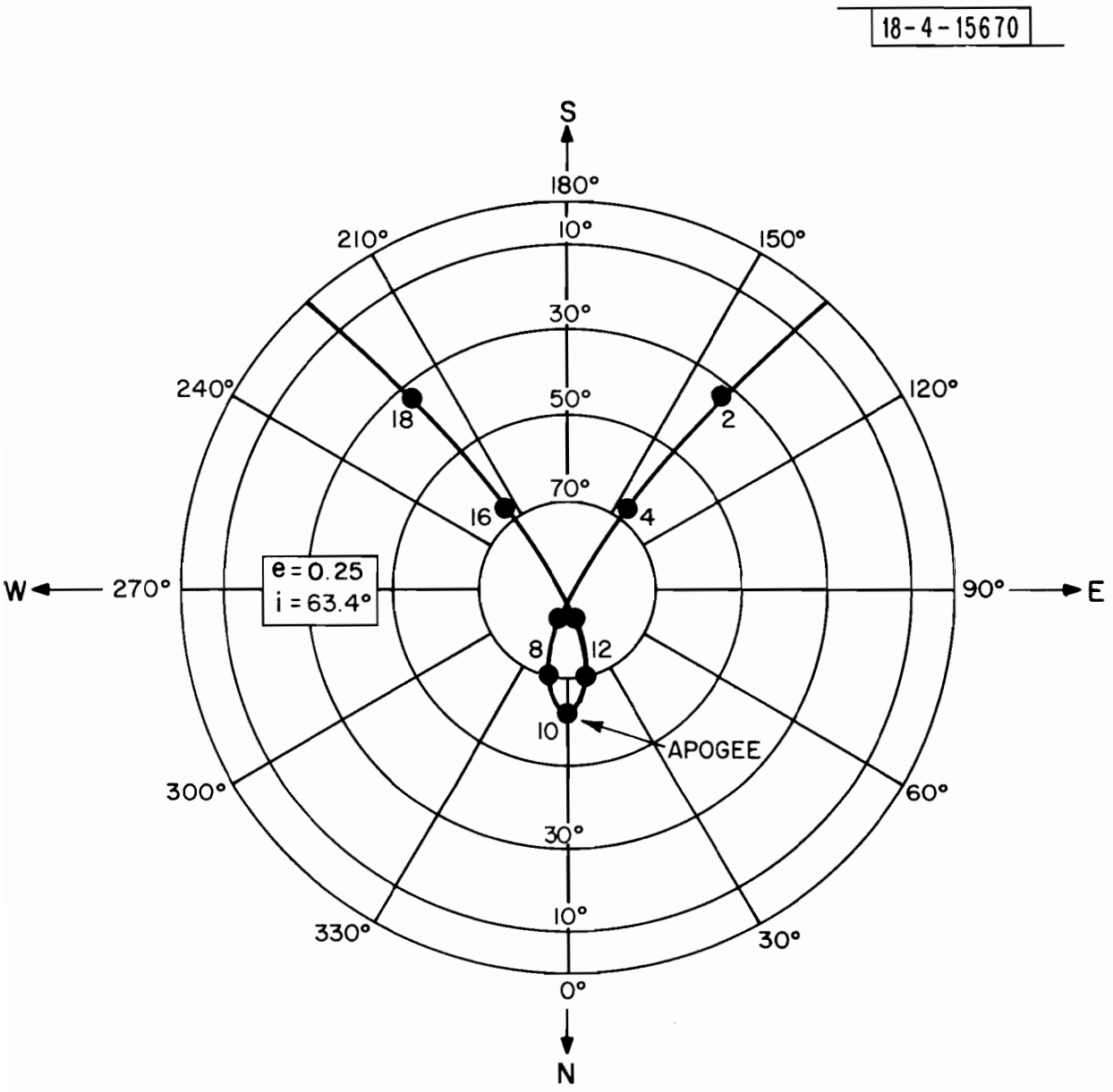

Fig. 7.6. A "planetarium view" of the trajectory for a typical posigrade orbit.

satellite in retrograde orbit is visible at low elevation angles for a much longer time. This difference is a significant one in view of the discussion of Section 5.6.

Figure 7.7 illustrates how the trajectories of retrograde orbits depend upon eccentricity. The figure depicts trajectories of orbits having eccentricities of 0, 0.2,...,0.8 inclined at 116.6°*. Note that the elevation angle at apogee increases slightly as eccentricity is increased. Also, note how the loop of the trajectory approaches a circle as $e \rightarrow 1$.

7.3 DISRUPTING PLANARITY

It is instructive to compare a constellation having all satellites in retrograde orbits with one having all satellites in posigrade orbits. Thus, consider the following constellations:

Posigrade Constellation

Twelve satellites deployed in elliptical orbits of eccentricty 0.25 and inclination 63.4° as specified in Table 7.1.

Retrograde Constellation

Twelve satellites deployed in elliptical orbits of eccentricity 0.25 and inclination 116.6° as specified in Table 7.2.

Figure 7.8 to 7.10 and 7.11 to 7.13 depict unit mass plots at time t = 0 for the two constellations as viewed from a point in central CONUS.** Figure 7.9 illustrates the near planarity of the unit masses for the posigrade constellation. Comparison of Fig. 7.9 with Fig. 7.12 shows how the retrograde constellation

*Viewed from the grid point at 100 W longitude and 40 N latitude.
**Specifically, the grid point at 100° W longitude and 40° N latitude.

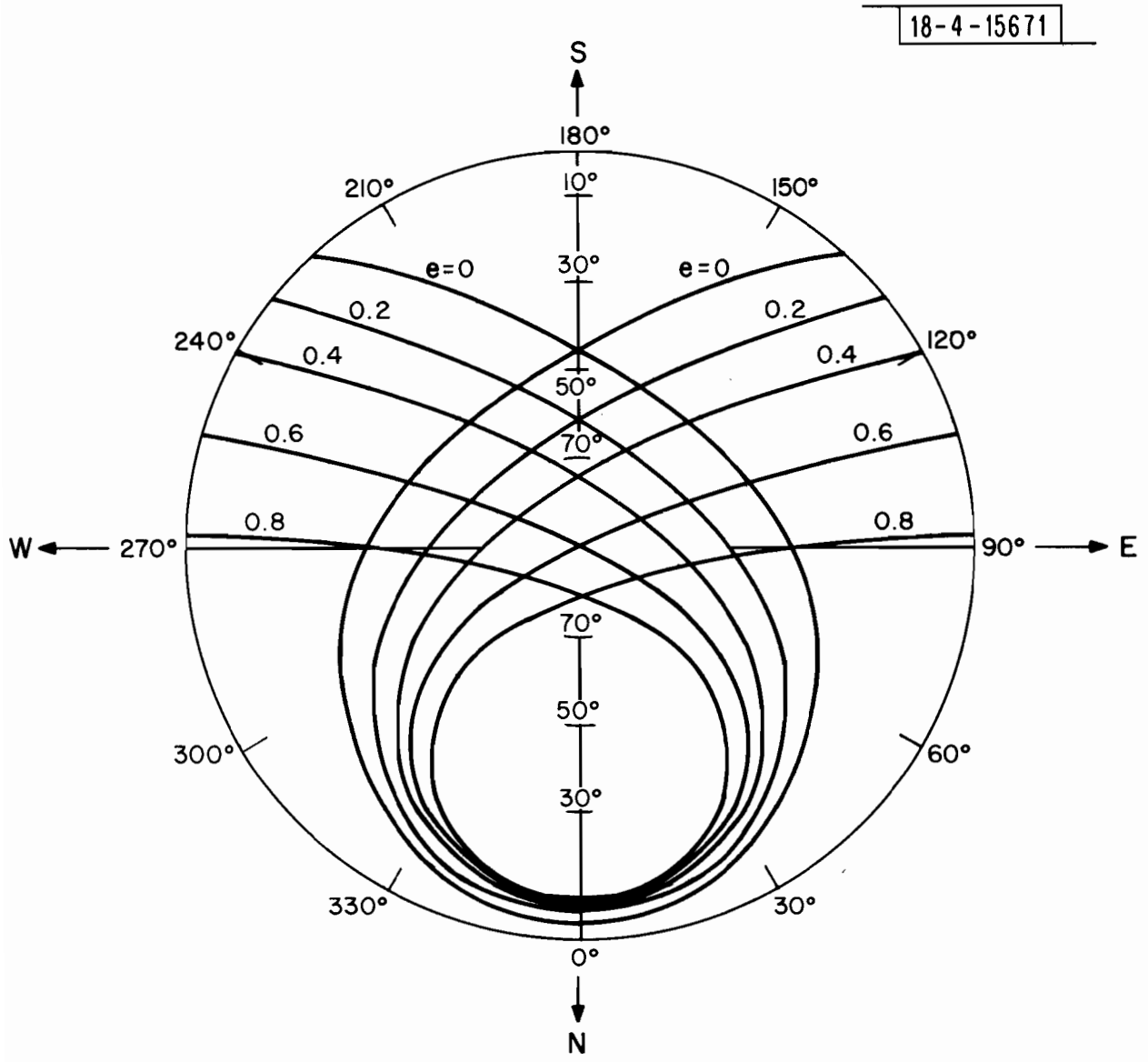

Fig. 7.7. A "planetarium view" of the trajectories for representative orbits inclined at 116.6°.

Table 7.1. The Retrograde constellation.

SATELLITE DEPLOYMENT

SATELLITE NO.	INC. (DEG)	ECC.	T(P) (HOURS)	LONG.(P) (DEG)
RETROGRADE				
1	116.6	0.25	0.0	-100.0
2	116.6	0.25	2.000	-100.0
3	116.6	0.25	4.000	-100.0
4	116.6	0.25	6.000	-100.0
5	116.6	0.25	8.000	-100.0
6	116.6	0.25	10.000	-100.0
7	116.6	0.25	12.000	-100.0
8	116.6	0.25	14.000	-100.0
9	116.6	0.25	16.000	-100.0
10	116.6	0.25	18.000	-100.0
11	116.6	0.25	20.000	-100.0
12	116.6	0.25	22.000	-100.0

Table 7.2. The Posigrade constellation.

SATELLITE DEPLOYMENT

SATELLITE NO.	INC. (DEG)	ECC.	T(P) (HOURS)	LONG.(P) (DEG)
POSIGRADE				
1	63.40	0.25	0.0	-100.0
2	63.40	0.25	2.000	-100.0
3	63.40	0.25	4.000	-100.0
4	63.40	0.25	6.000	-100.0
5	63.40	0.25	8.000	100.0
6	63.40	0.25	10.000	-100.0
7	63.40	0.25	12.000	-100.0
8	63.40	0.25	14.000	-100.0
9	63.40	0.25	16.000	-100.0
10	63.40	0.25	18.000	-100.0
11	63.40	0.25	20.000	-100.0
12	63.40	0.25	22.000	-100.0

Projections of the Unit Masses for
the Posigrade Constellation

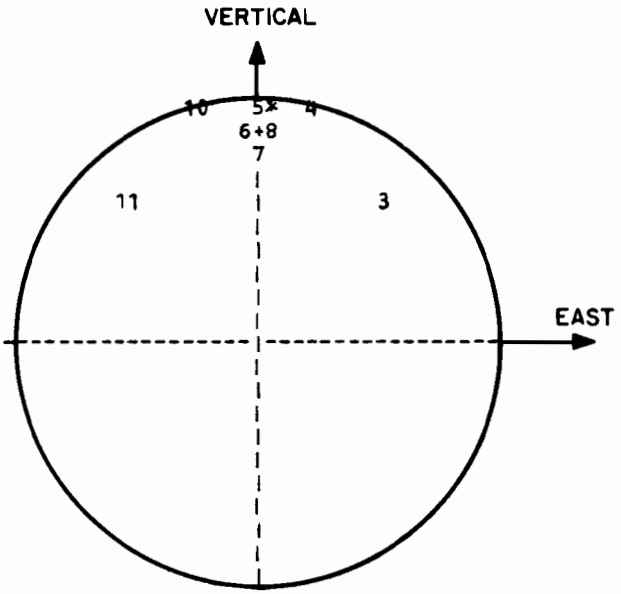

Fig. 7.8. Vertical-East projection.

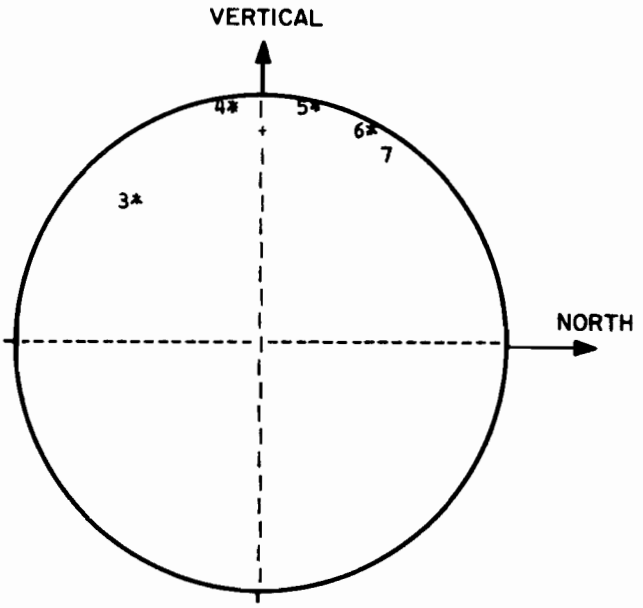

Fig. 7.9. Vertical-North projection.

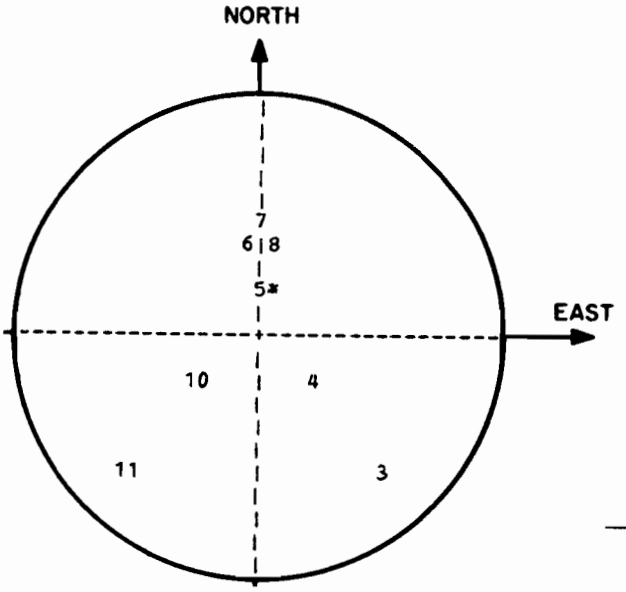

Fig. 7.10. North-East projection.

ATC-23(7.8-10)

THE VISIBLE SATELLITES ARE NUMBERS
3 4 5 6 7 8 9 10 11

Projections of the Unit Masses for
the Retrograde Constellation

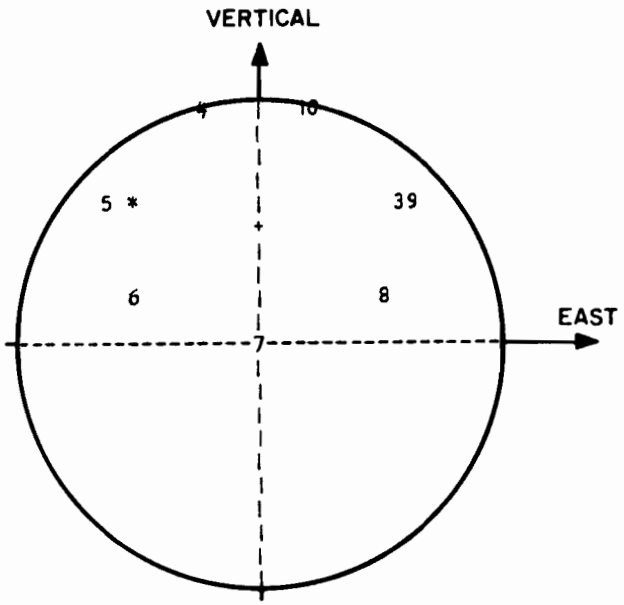

Fig. 7.11. Vertical-East projections.

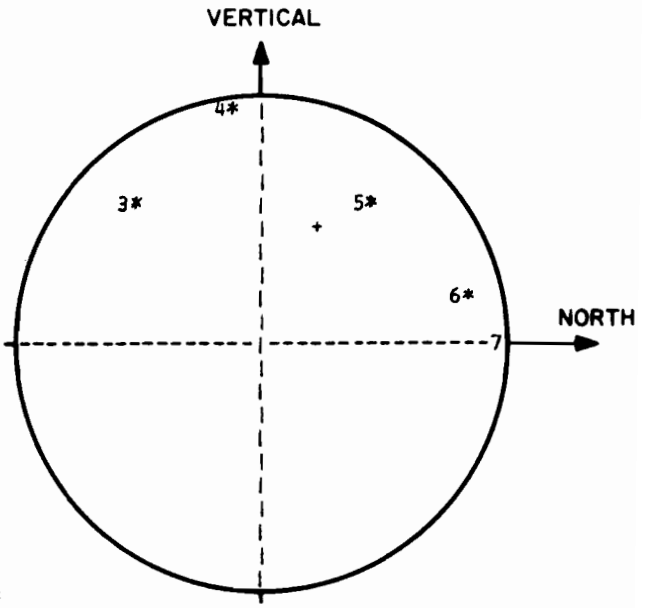

Fig. 7.12. Vertical-North projection.

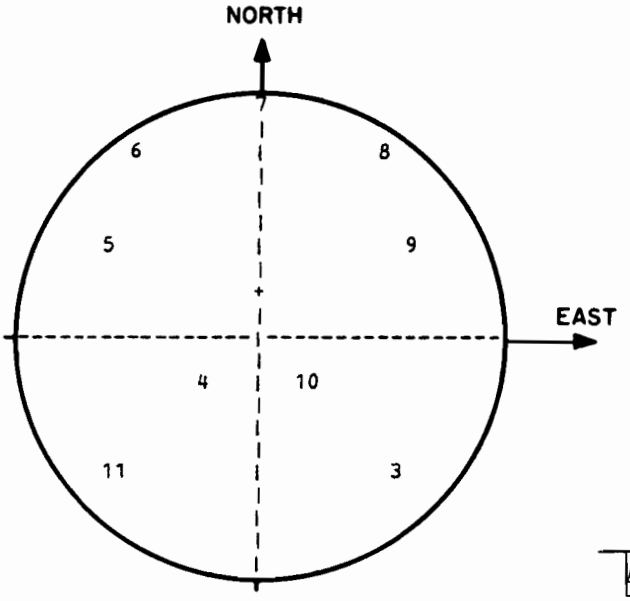

Fig. 7.13. North-East projection.

ATC-23(7.11-13)

THE VISIBLE SATELLITES ARE NUMBERS
3 4 5 6 7 8 9 10 11

disrupts the planarity. Comparison of Figs. 7.8 and 7.10 with Figs. 7.11 and 7.13 shows that the retrograde orbits also spread the unit masses out more in the Vertical-East and the North-East projections.

The $\underline{L}$ matrices for the two sets of masses in a North-East-Vertical coordinate system are as follows:

$$\underline{L}_p = \begin{bmatrix} 1.424 & -9.0 \times 10^{-8} & 0.460 \\ -9.0 \times 10^{-8} & 0.710 & -7.8 \times 10^{-8} \\ 0.460 & -7.8 \times 10^{-8} & 0.262 \end{bmatrix} \qquad (7.1)$$

$$\underline{L}_R = \begin{bmatrix} 3.272 & -1.4 \times 10^{-7} & -0.991 \\ -1.4 \times 10^{-7} & 2.197 & -7.9 \times 10^{-8} \\ -0.991 & -7.9 \times 10^{-8} & 0.651 \end{bmatrix} . \qquad (7.2)$$

The increase in the 3-3 element between (7.1) and (7.2) is directly due to the elimination of planarity.* The increases in the 1-1 and 2-2 elements are due to the fact that the unit masses are more spread out in Figs. 7.11 and 7.13 than in Figs. 7.8 and 7.10 and therefore, have longer moment arms.

The corresponding $\underline{\Gamma}$ matrices are as follows:

$$\underline{\Gamma}_p = \begin{bmatrix} 1.619 & -1.0 \times 10^{-7} & -2.839 \\ -1.0 \times 10^{-7} & 1.409 & 6.0 \times 10^{-7} \\ -2.839 & 6.0 \times 10^{-7} & 8.790 \end{bmatrix} \qquad (7.3)$$

*A similar increase occurs when the two $\underline{L}$ matrices are transformed normal coordinates.

$$\underline{\Gamma}_R = \begin{bmatrix} 0.568 & 6.6 \times 10^{-7} & 0.865 \\ 6.6 \times 10^{-7} & 0.455 & 1.5 \times 10^{-7} \\ 0.865 & 1.5 \times 10^{-7} & 2.854 \end{bmatrix} . \qquad (7.4)$$

The GDOP's for the two constellations can be calculated directly from (7.3) and (7.4). The results are:

$$GDOP_p = \sqrt{(1.619) + (1.409) + (8.790)} \qquad (7.5)$$

$$= 3.437$$

$$GDOP_R = \sqrt{(0.568) + (0.455) + (2.854)} \qquad (7.6)$$

$$= 1.969 \quad .$$

7.4 FURTHER DISRUPTION OF PLANARITY

Even more impressive reductions in GDOP can be obtained by using both retrograde and equatorial satellites to disrupt the planarity of the unit masses.

For example, addition of equatorial satellites as follows to the retrograde constellation of Section 7.3 produces the unit mass deployment shown in Fig. 7.14 to 7.16.

Projections of the Unit Masses for
the Augmented Retrograde Constellation

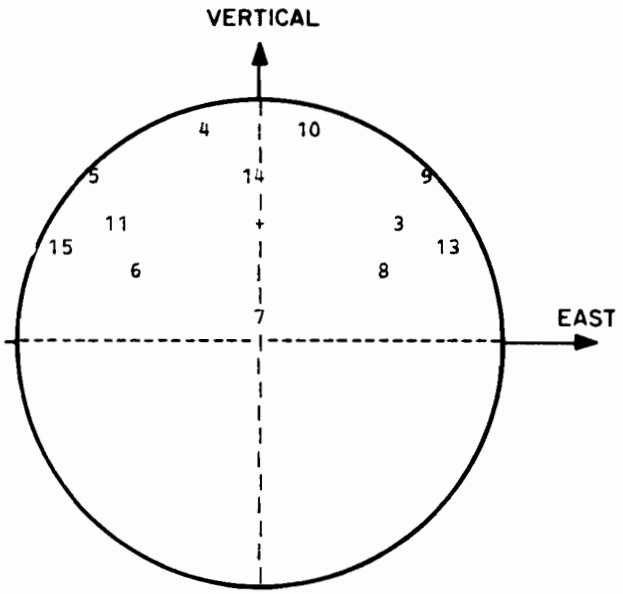

Fig. 7.14. Vertical-East projection.

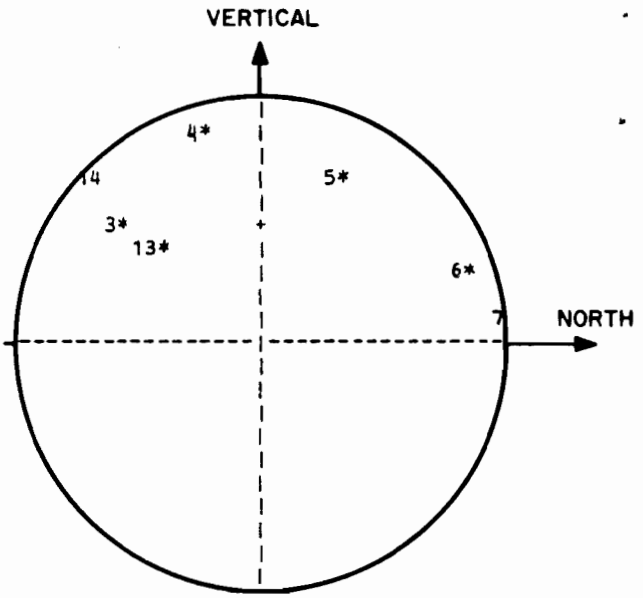

Fig. 7.15. Vertical-North projection.

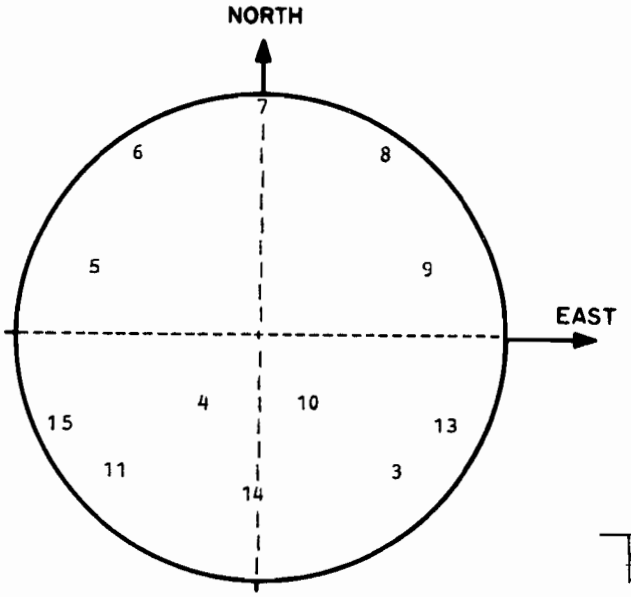

Fig. 7.16. North-East projection.

ATC-23(7.14-16)

THE VISIBLE SATELLITES ARE NUMBERS
3 4 5 6 7 8 9 10 11 13 14 15

Satellite No.	W Longitude
13	50^{o}
14	100^{o}
15	150^{o}

The $\underline{L}$ matrix for the augmented constellation in a North-East-Vertical reference frame is as follows:

$$\underline{L}_{RE} = \begin{bmatrix} 4.404 & -1.06 \times 10^{-7} & -0.945 \\ -1.06 \times 10^{-7} & 3.541 & -7.56 \times 10^{-8} \\ -0.945 & -7.56 \times 10^{-8} & 0.733 \end{bmatrix} . \quad (7.7)$$

The corresponding $\underline{\Gamma}$ matrix is:

$$\underline{L}_{RE} = \begin{bmatrix} 0.314 & 1.80 \times 10^{-8} & 0.405 \\ 1.80 \times 10^{-8} & 0.282 & 5.24 \times 10^{-8} \\ 0.405 & 5.24 \times 10^{-8} & 1.886 \end{bmatrix} . \quad (7.8)$$

The resulting GDOP is:

$$GDOP = \sqrt{(0.314) + (0.282) + (1.886)}$$

$$= 1.575$$

The efficiency of the fifteen satellite augmented constellation can be compared to that of the twelve satellite posigrade and retrograde constellations by comparing normalized GDOPs. The results are summarized in Table 7.3. Clearly, the augmented retrograde constellation is most efficient. The retrograde constellation is next most efficient. The posigrade constellation is least efficient.

Table 7.3. Normalized GDOP's.

Constellation	$\sqrt{N}$ x GDOP
Posigrade	11.906
Retrograde	6.821
Augmented Retrograde	6.101

SECTION 8

CONSTELLATION DESIGN USING RETROGRADE ORBITS

It is evident from the results of Section 7.3 that significantly reduced GDOP's over CONUS can be obtained by constructing constellations that employ retrograde orbits in place of (or in addition to) the posigrade orbits previously used. However, no one way of utilizing retrograde orbits is immediately and obviously the best. Accordingly, we have examined a variety of possible methods. This section describes several alternatives.

Of the procedures considered, one emerges as the best. The procedure consists of placing a majority of the satellites in retrograde orbits so as to traverse a single ground track, and placing the remaining satellites in circular equatorial orbits.

8.1 APPROXIMATING THE OPTIMUM CONSTELLATION

One design method that initially suggests itself is that of utilizing retrograde orbits to approximate the optimum constellation described in Section 3.4. Several satellites could be placed in retrograde orbits to approximate the rim of the viewing cone. The remaining satellites could be placed in posigrade orbits to approximate the overhead satellites.

A preliminary consideration that argues against such an approach is the fact that a constellation which is optimum in New York City is not optimum

in San Francisco, or even in Kansas. For example, a simple calculation shows that a satellite in circular synchronous orbit which is directly overhead in New York City is at an elevation angle of 55° in San Francisco.

A more basic problem is that the satellites on the rim of the viewing cone require a large circular ground track as shown in Fig. 8.1. Such a ground track can be approximated by the large loop of a figure eight having its crossing point in the southern hemisphere. However, the orbits associated with such ground tracks have apogees in the southern hemisphere. Thus, although the satellites occupy favorable positions when over the northern hemisphere, they spend most of the time over the southern hemisphere. Consequently, additional satellites are required to offset the reduced visibility.

Several attempts were made to approximate the optimum constellation. The results were the worst of all design methods considered, however. Accordingly, they are not presented here.

8.2 APPROXIMATING THE UNIFORM CONSTELLATION

Another design approach that suggests itself is that of using retrograde orbits to approximate a uniform constellation (see Section 3.4). This approach potentially has the advantages of:

1. Providing near optimum GDOP's (see Section 3.4).
2. Minimizing the GDOP degradation due to satellite failure, and aircraft maneuvers.

This approach proved to be a much more viable one. Indeed, three different methods for approximating uniform constellations were developed. These methods are summarized in Table 8.1.

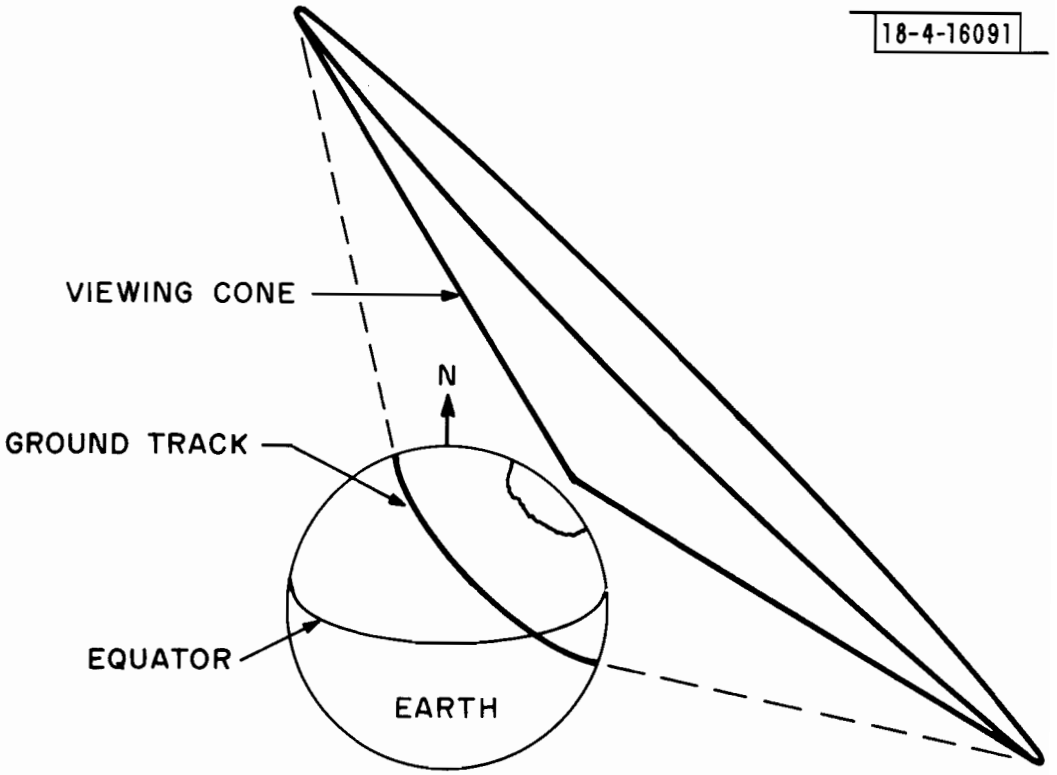

Fig. 8.1. Ground track required by the optimum constellation.

Table 8.1. Methods for approximating uniform constellations.

Method	Form of Constellation
I.	Some Satellites in Retrograde Orbits + Some Satellites in Posigrade Orbits + Some Satellites in Equatorial Orbits
II.	Most Satellites in Retrograde Orbits (one ground track) + Some Satellites in Equatorial Orbits (or near-equatorial orbits)
III.	Most Satellites in Retrograde Orbits (two ground tracks) + Some Satellites in Equatorial Orbits (or near-equatorial orbits)

The first method involves placing satellites in all three types of orbits: retrograde, posigrade, and equatorial. The satellites in retrograde orbits provide coverage near the rim of the viewing cone, particularly toward the north. The satellites in posigrade orbits provide coverage overhead, while those in equatorial orbits provide coverage to the south.

The second method utilizes satellites in retrograde and equatorial orbits only. The retrograde orbits are configured so that the satellites traverse a single ground track. The retrograde satellites are used to provide coverage overhead, along the northern, northeastern and northwestern horizons, and also in the southeast and southwest. The equatorial satellites provide additional coverage near the southern horizon.

The third method also utilizes satellites in retrograde and equatorial orbit only. Here, however, the retrograde orbits are configured so that the satellites traverse two identical ground tracks offset in the east-west direction.

Again, the retrograde satellites provide coverage overhead, and along the northern horizon. The reason for offsetting the ground tracks is to obtain improved coverage near the eastern and western horizons. Once again, the equatorial satellites provide coverage near the southern horizon.

8.3 COMPARISON OF THE METHODS

To determine the relative merits of the three methods, one or more constellations was constructed using each. Fifteen satellites were used for this purpose, and visibility "down to the horizon" (i.e., $\phi = 90^{\circ}$) was assumed.

Each constellations was designed in two steps. First, a "ballpark" set of parameters was selected. Then the constellation was "tuned" by repeatedly analyzing it and varying the constellation parameters. The parameter values that produced the smallest average GDOP for level flight were selected as the final values.

The retrograde orbits for each initial constellation were selected to have their apogees on the northern rim of a viewing cone located in Kansas. The parameter γ_p initially was taken to be 100° W longitude (except for Method III). The tuning step involved varying γ_p and the orbital inclinations in increments of 5° (or smaller) and varing the orbital eccentricities in increments of 0.05.

The GDOP results for level flight are summarized in Table 8.2. It is evident from the table that the second method is the best of those considered.

A comparison of Table 8.2 with Table 5.10 shows that all of the resulting constellations have GDOP's well below that of the Hybrid constellation. Furthermore, a comparison of Table 8.2 with Table 5.14 shows the resulting

constellations also have normalized GDOP's well below those for the constellations analyzed in Section 5.

The following five sections discuss the constellations in more detail. For easy reference, the constellations are designated U1, U2, . . . , U7 as indicated in Table 8.2.

Table 8.2. "Uniform" constellations constructed by Methods I, II, and III.

Method	Constellation	Retrograde	Posigrade	Equatorial	Average GDOP	Normal. GDOP
I	U1	6	6	3	1.465	5.674
II	U2	12	0	3	1.354	5.244
	U3	13	0	2	1.356	5.252
	U4	5	0	10	1.356	5.252
	U5	12	0	3	1.356	5.252
	U6	6	0	9	1.376	5.329
III	U7	6+6	0	3	1.383	5.386

8.4 APPROXIMATION METHOD I (Constellation U1)

Table 8.3 contains the orbital parameters for the constellation U1. The constellation consists of six satellites in circular retrograde orbits of inclination 116.6°, six satellites in posigrade orbits of eccentricity 0.32 and inclination 80°, and three satellites in equatorial orbits. *

*In cases where the optimum incination was within a few degrees of 116.6°, the latter inclination was selected with a view toward orbital stability. (See Section 4.7.)

Table 8.3. The U1 constellation.

SATELLITE DEPLOYMENT

SATELLITE NO.	INC. (DEG)	ECC.	T(P) (HOURS)	LONG.(P) (DEG)
RETROGRADE				
1	116.6	0.0	0.0	-100.0
2	116.6	0.0	4.000	-100.0
3	116.6	0.0	8.000	-100.0
4	116.6	0.0	12.000	-100.0
5	116.6	0.0	16.000	-100.0
6	116.6	0.0	20.000	-100.0
POSIGRADE				
7	80.00	0.32	0.0	-100.0
8	80.00	0.32	4.000	-100.0
9	80.00	0.32	8.000	-100.0
10	80.00	0.32	12.000	-100.0
11	80.00	0.32	16.000	-100.0
12	80.00	0.32	20.000	-100.0
EQUATORIAL				
13	0.0	0.0	0.0	-20.0
14	0.0	0.0	0.0	-100.0
15	0.0	0.0	0.0	180.0

Figure 8.2 is a GDOP map for U1 at time t = 0. Note that GDOP is low, and relatively uniform across CONUS. The slight GDOP ridge along the 100° W longitude line is due to the fact that neither the easternmost nor the westernmost equatorial satellite is visible at this location. The four nearly circular GDOP depressions (GDOP = 1.25) are due to visibility of both a far equatorial satellite (almost on the eastern or western horizon) and a satellite near perigee (i.e., number 2 or 6).

Tables 8.4 to 8.6 summarize the GDOP statistics for all (approximately) uniform constellations. Examination of the U1 row of Table 8.4 shows that U1 provides 10.64 visible satellites on the average. This number is somewhat smaller than that for Hybrid (10.82). Nonetheless, U1 improves on the GDOP of Hybrid by 23%.

Figures 8.3 to 8.5 depict the projections of the unit mass configuration at time t = 0. Comparison of Figs. 8.4 with Fig. 6.13 immediately shows the reason for the improved GDOP's. Retrograde satellites numbers 2 and 6 (near perigee) and 4 (near apogee) eliminate the near planarity characteristic of posigrade orbits.

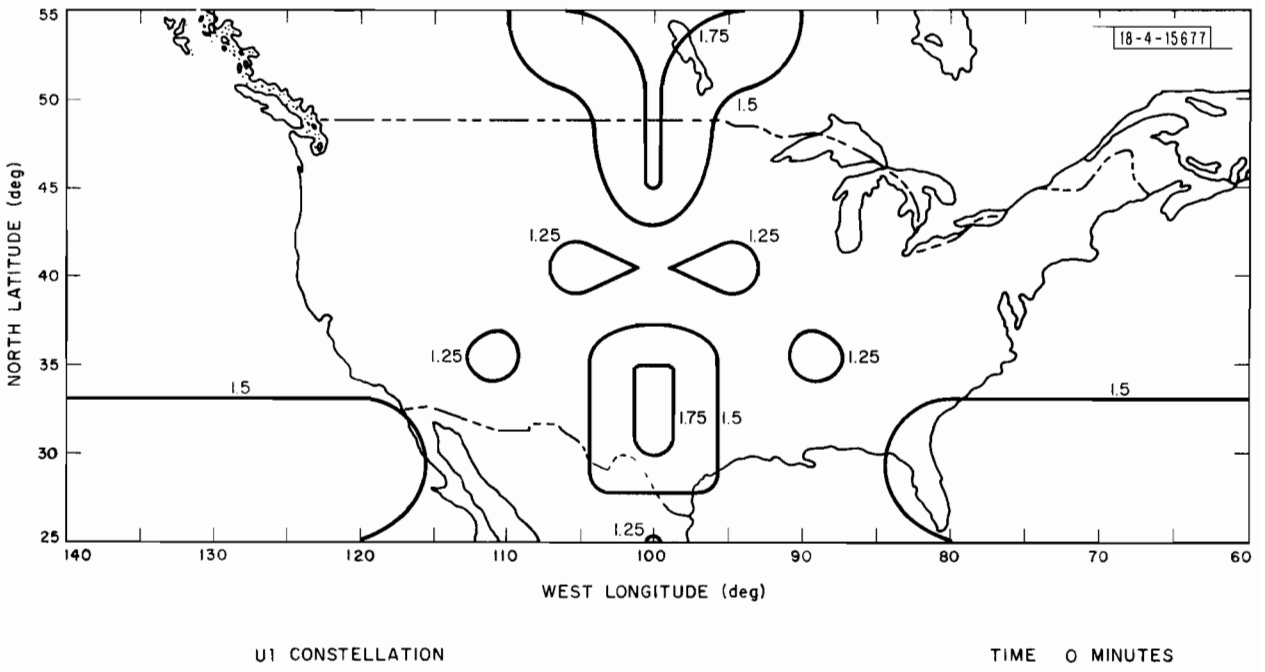

Fig. 8.2. GDOP map for U1 constellation.

Table 8.4. Nominal results.

Constellation	Average Number Visible	Average GDOP	rms Deviation	Excess
U1	10.64	1.465	0.167	1.753
U2	12.45	1.354	0.107	1.621
U3	12.22	1.356	0.136	1.623
U4	11.93	1.356	0.153	1.623
U5	12.47	1.356	0.121	1.623
U6	12.54	1.376	0.119	1.647
U7	10.43	1.383	0.136	1.656

Table 8.5. Dropout results.

Constellation	Average Number Visible	Average GDOP	Percent GDOP > 5	Sensitivity	Failed Satellite
U1	9.95	1.827	0%	3.81	4
U2	11.45	1.387	0%	0.30	14
U3	11.28	1.517	0%	1.54	15
U4	11.17	1.413	0%	0.66	6
U5	11.71	1.397	0%	0.49	7
U6	11.77	1.530	0%	1.83	4
U7	9.47	1.469	0%	0.68	4

Table 8.6. 30° bank results.

Constellation	Average Number Visible	Average GDOP	Percent. GDOP > 5
U1	9.27	1.912	0%
U2	9.92	1.687	0%
U3	10.48	1.709	0%
U4	10.09	1.791	0%
U5	10.86	1.816	0%
U6	10.75	1.824	0%
U7	8.74	1.939	0%

Projections of the Unit Masses for
the U1 Constellation

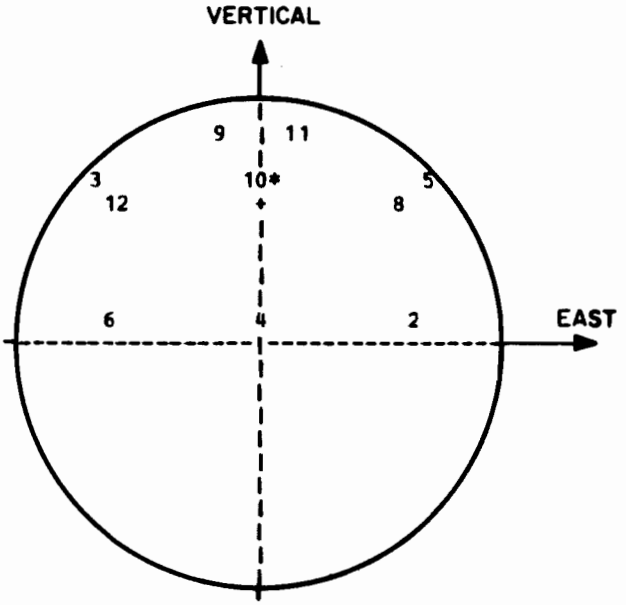

Fig. 8.3. Vertical-East projection.

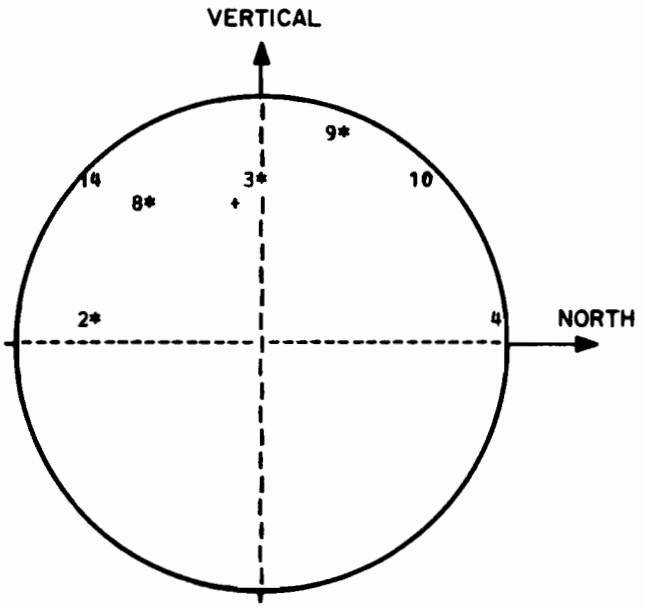

Fig. 8.4. Vertical-North projection.

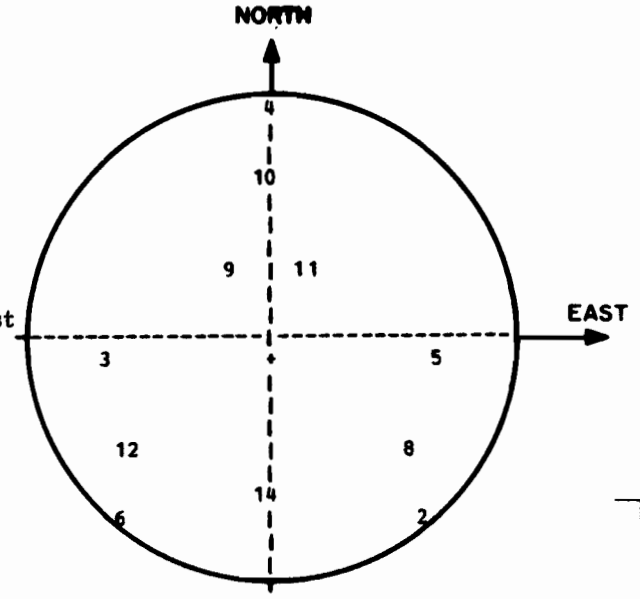

Fig. 8.5. North-East projection.

ATC-23(8.3-5)

THE VISIBLE SATELLITES ARE NUMBERS
2 3 4 5 6 8 9 10 11 12 14

8.5 APPROXIMATION METHOD II (Constellation U2)

The U2 constellation is the best of those produced by Method II. The U2 ground track is shown in Fig. 8.6. The constellation consists of twelve satellites in retrograde orbits of eccentricity 0.5 inclined at 116.6°, and three satellites in equatorial orbits. The orbital parameters are given in Table 8.7. Reference to the $\phi = 90^{\circ}$ dashed line shows that eleven of the twelve retrograde satellites are visible from Kansas at time t = 0 hours.

Figure 8.7 is the GDOP map for U2 at time t = 0. Clearly, GDOP is low and highly uniform throughout CONUS The slight hill in northern central CONUS is due to the fact that neither of the near-perigee satellites (Nos. 2 and 12) are visible there. The slight valley to the south is due to the fact that both of these satellites are visible there.

Examination of Tables 8.4 to 8.6 shows that U2 not only produces the smallest nominal GDOP of constellations U1- U7, but also produces the most uniform GDOP. In addition, the constellation U2 is the least sensitive to satellite failure and aircraft maneuvers.

Tables 8.8 to 8.10 contrast the performance of U2 with that of Hybrid. The improvement achieved through use of retrograde orbits is evident. The nominal GDOP is reduced by 33%. The sensitivity to satellite failure is reduced by more than an order of magnitude.

Figure 8.8 to 8.10 depict the unit mass plots for U2. The North-East projection clearly indicates the direction of movement of the retrograde satellites $2 \rightarrow 3 \rightarrow 4 \rightarrow 5 \rightarrow 6 \rightarrow 7 \rightarrow 8 \rightarrow 9 \rightarrow 10 \rightarrow 11 \rightarrow 12$ (no. 1 is at perigee and cannot be seen). Note the similarity between Fig. 8.10 and the "planetarium projection" of Fig. 7.7 for e = 0.5. The equatorial satellites (13, 14, and 15)

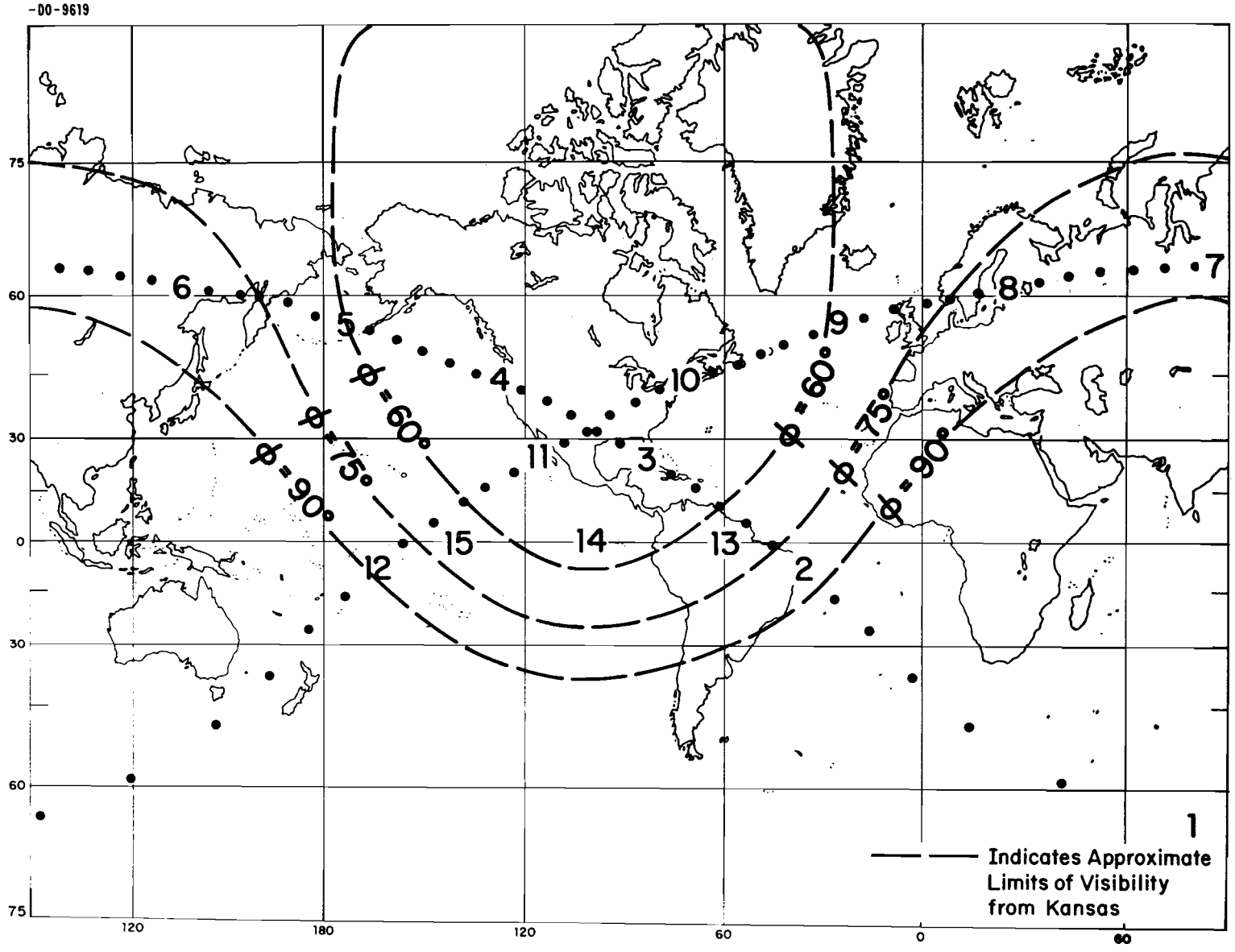

Fig. 8.6. Ground track for U2 constellation.

Table 8.7. The U2 constellation.

SATELLITE DEPLOYMENT

SATELLITE NO.	INC. (DEG)	ECC.	T(P) (HOURS)	LONG. (P) (DEG)
RETROGRADE				
1	116.6	0.50	0.0	-100.0
2	116.6	0.50	2.000	-100.0
3	116.6	0.50	4.000	-100.0
4	116.6	0.50	6.000	-100.0
5	116.6	0.50	8.000	-100.0
6	116.6	0.50	10.000	-100.0
7	116.6	0.50	12.000	-100.0
8	116.6	0.50	14.000	-100.0
9	116.6	0.50	16.000	-100.0
10	116.6	0.50	18.000	-100.0
11	116.6	0.50	20.000	-100.0
12	116.6	0.50	22.000	-100.0
EQUATORIAL				
13	0.0	0.0	0.0	-60.0
14	0.0	0.0	0.0	-100.0
15	0.0	0.0	0.0	-140.0

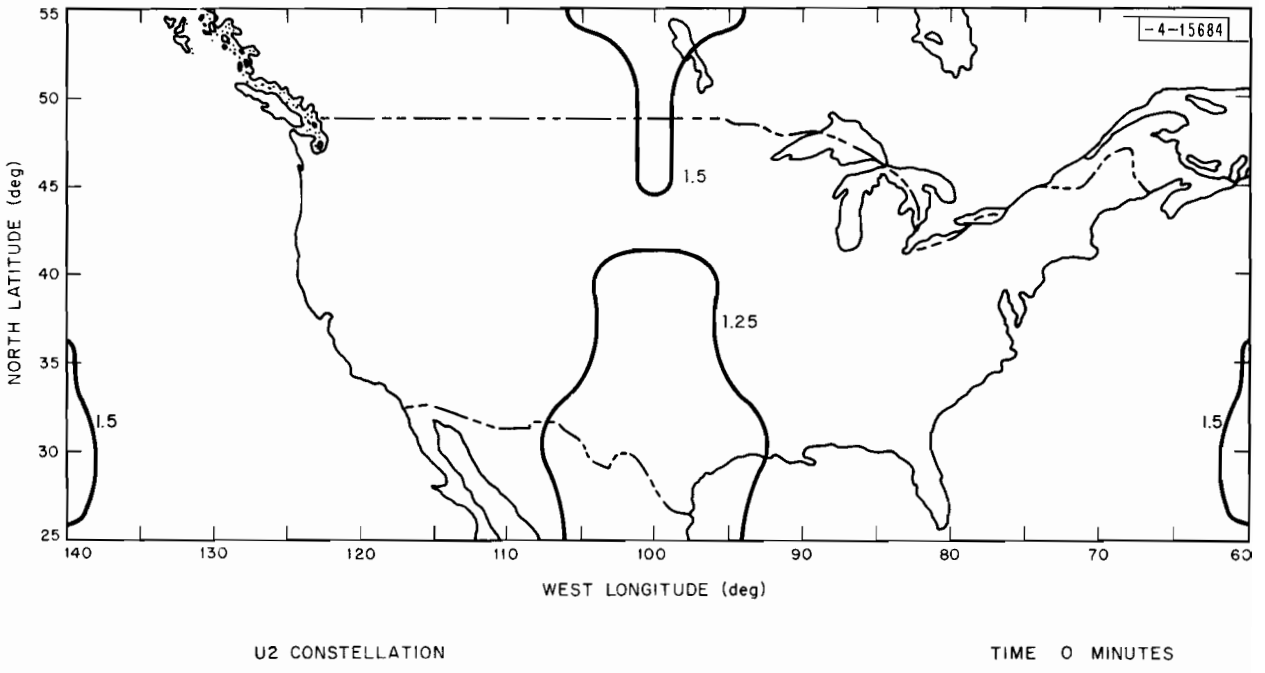

Fig. 8.7. GDOP map for U2 constellation.

Table 8.8. Nominal results.

	Average Number Visible	Average GDOP	rms Deviation	Excess
U2	12.454	1.354	0.10747	1.62064
Hybrid*	10.82	1.801	0.254	2.16

Table 8.9. Dropout results.

	Average Number Visible	Average GDOP	Sensitivity	Failed Satellite
U2	11.454	1.387	0.30353	14
Hybrid*	10.35	2.151	4.47	10

Table 8.10. 30^{o} bank results.

	Average Number Visible	Percent GDOP > 5	Average GDOP
U2	9.92	0%	1.687
Hybrid*	9.99	1.2%	2.329

*A viewing cone of 90^{o} half-angle is assumed for purposes of comparison.

Projections of the Unit Masses for
the U2 Constellation

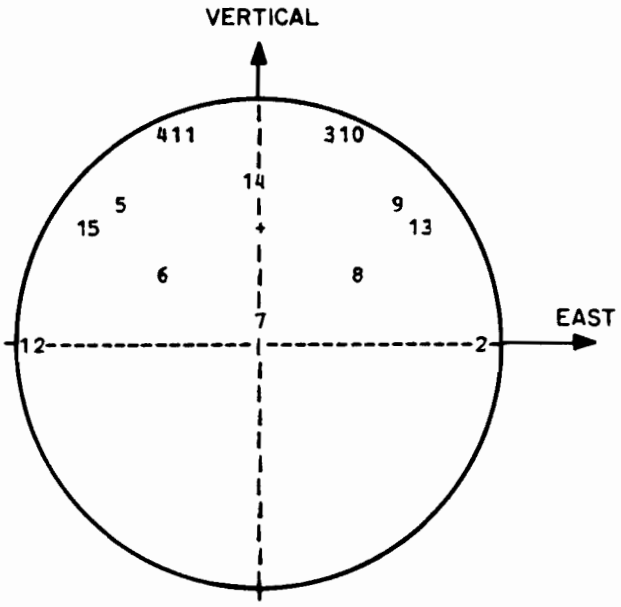

Fig. 8.8. Vertical-East projection.

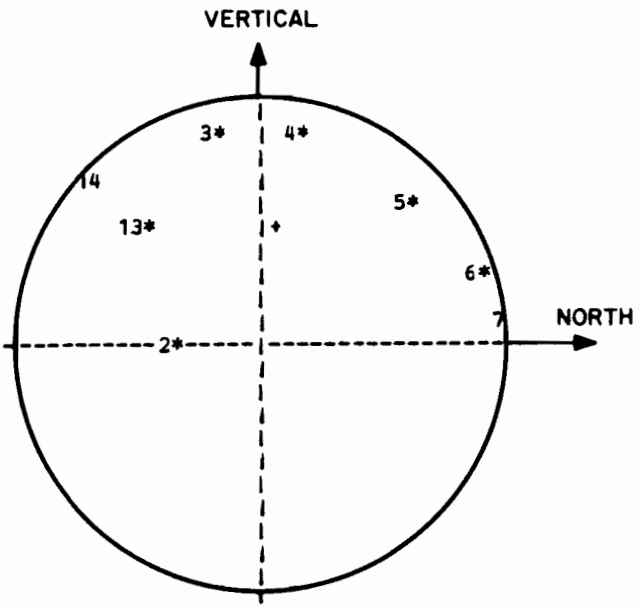

Fig. 8.9. Vertical-North projection.

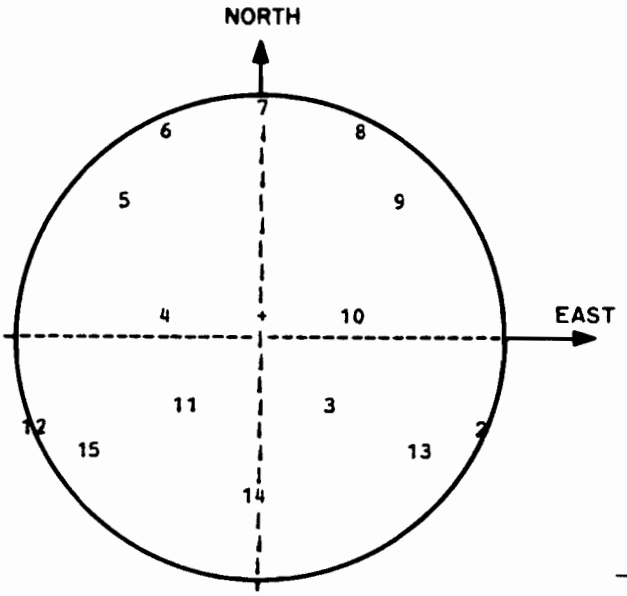

Fig. 8.10. North-East projection.

ATC-23(8.8-10)

THE VISIBLE SATELLITES ARE NUMBERS
2 3 4 5 6 7 8 9 10 11 12 13 14 15

"fill out" the southern horizon. The Vertical-North projection provides a good semi-circle of masses (compare with Fig. 6.13). The Vertical-East Projection, likewise, shows a good semicircle of masses with special assistance from Satellites 2 and 12 which are near perigee.

8.6 APPROXIMATION METHOD II (Constellations U3 to U6)

Constellations U3 to U6 are other constellations designed by Method II. The orbital parameters of U3 to U6 are given in Tables 8.11 to 8.14. The constellations are all variants of U2. Constellation U3 and U4 represent attempts to improve upon the allocation of satellites between retrograde and equatorial orbits. Constellation U5 and U6 represent attempts to improve upon the unit mass plots for U2. Specifically, the constellations aim at improving the distribution of mass in the east-west direction (see Fig. 8.10), and/or the distribution of mass in the due south direction (see Fig. 8.9)

The U3 constellation differs from U2 only in that thirteen satellites are placed in retrograde orbits, and two are placed in equatorial orbits. The primary effect of this re-allocation of satellites is to increase the constellation sensitivity to failure of an equatorial satellite (see Table 8.5).

The constellation U4 differs from U2 in that fewer satellites (ten) are placed in retrograde orbits, and more satellites (five) are placed in equatorial orbits. Again, the effect of the reallocation is negative. The nominal GDOP increases, as does the GDOP sensitivity to satellite failure and aircraft banking.

Table 8.11. The U3 constellation.

SATELLITE DEPLOYMENT

SATELLITE NO.	INC. (DEG)	ECC.	T(P) (HOURS)	LONG.(P) (DEG)
RETROGRADE				
1	116.6	0.50	0.0	-100.0
2	116.6	0.50	1.846	-100.0
3	116.6	0.50	3.692	-100.0
4	116.6	0.50	5.538	-100.0
5	116.6	0.50	7.404	-100.0
6	116.6	0.50	9.250	-100.0
7	116.6	0.50	11.096	-100.0
8	116.6	0.50	12.924	-100.0
9	116.6	0.50	14.770	-100.0
10	116.6	0.50	16.616	-100.0
11	116.6	0.50	18.462	-100.0
12	116.6	0.50	20.308	-100.0
13	116.6	0.50	22.154	-100.0
EQUATORIAL				
14	0.0	0.0	0.0	-60.0
15	0.0	0.0	0.0	-140.0

Table 8.12. The U4 constellation.

SATELLITE DEPLOYMENT

SATELLITE NO.	INC. (DEG)	ECC.	T(P) (HOURS)	LONG.(P) (DEG)
RETROGRADE				
1	116.6	0.50	0.0	-100.0
2	116.6	0.50	2.400	-100.0
3	116.6	0.50	4.800	-100.0
4	116.6	0.50	7.200	-100.0
5	116.6	0.50	9.600	-100.0
6	116.6	0.50	12.000	-100.0
7	116.6	0.50	14.400	-100.0
8	116.6	0.50	16.800	-100.0
9	116.6	0.50	19.200	-100.0
10	116.6	0.50	21.600	-100.0
EQUATORIAL				
11	0.0	0.0	0.0	-20.0
12	0.0	0.0	0.0	-60.0
13	0.0	0.0	0.0	-100.0
14	0.0	0.0	0.0	-140.0
15	0.0	0.0	0.0	180.0

Table 8.13. The U5 constellation.

SATELLITE DEPLOYMENT

SATELLITE NO.	INC. (DEG)	ECC.	T(P) (HOURS)	LONG.(P) (DEG)
RETROGRADE				
1	116.6	0.50	0.0	-100.0
2	116.6	0.50	2.000	-100.0
3	116.6	0.50	4.000	-100.0
4	116.6	0.50	6.000	-100.0
5	116.6	0.50	8.000	-100.0
6	116.6	0.50	10.000	-100.0
7	116.6	0.50	12.000	-100.0
8	116.6	0.50	14.000	-100.0
9	116.6	0.50	16.000	-100.0
10	116.6	0.50	18.000	-100.0
11	116.6	0.50	20.000	-100.0
12	116.6	0.50	22.000	-100.0
POSIGRADE				
13	25.00	0.0	0.0	-100.0
14	25.00	0.0	8.000	-100.0
15	25.00	0.0	16.000	-100.0

Table 8.14. The U6 constellation.

SATELLITE DEPLOYMENT

SATELLITE NO.	INC. (DEG)	ECC.	T(P) (HOURS)	LONG.(P) (DEG)
RETROGRADE				
1	116.6	0.50	0.0	-100.0
2	116.6	0.50	4.000	-100.0
3	116.6	0.50	8.000	-100.0
4	116.6	0.50	12.000	-100.0
5	116.6	0.50	16.000	-100.0
6	116.6	0.50	20.000	-100.0
POSIGRADE				
7	25.00	0.0	0.0	-100.0
8	25.00	0.0	8.000	-100.0
9	25.00	0.0	16.000	-100.0
10	20.00	0.0	0.0	-50.0
11	20.00	0.0	8.000	-50.0
12	20.00	0.0	16.000	-50.0
13	20.00	0.0	0.0	-150.0
14	20.00	0.0	8.000	-150.0
15	20.00	0.0	16.000	-150.0

The constellation U5 differs from U2 in that the equatorial satellites are perturbed into slightly inclined ($i = 25^{o}$) circular orbits. The intent here is to improve the due south distribution of mass in Fig. 8.9, possibly at the expense of the east-west distribution of mass. Once again, the perturbed constellation produces worse results than U2.

The constellation U6 represents a major perturbation of U2. Here the number of satellites in retrograde orbits is reduced to six. The remaining nine satellites are placed in circular orbits of low inclination ($i = 25^{o}$) so as to traverse three distinct ground tracks centered respectively at 50^{o}, 100^{o} and 150^{o} W longitude. The objective of the perturbation is to fill out the "empty" area of the unit mass plot in Fig. 8.9 corresponding to the southern horizon, and also to fill out the "empty" areas of Fig. 8.10 corresponding to the eastern and western horizons. Tables 8.4 to 8.6 show that this attempt to improve upon U2 also was unsuccessful.

8.7 APPROXIMATION METHOD III (Constellation U7)

The orbital parameters for constellation U7 are given in Table 8.15. The constellation consists of twelve satellites in retrograde orbits and three satellites in near-equatorial orbits. The retrograde satellites are arranged to traverse two identical ground tracks separated 140^{o} in longitude. The reason for offsetting the ground tracks is to provide improved coverage near the eastern and western horizons. The near-equatorial satellites are placed in slightly inclined circular orbits ($i = 35^{o}$) to provide improved coverage near the southern horizon.

Table 8.15. The U7 constellation.

SATELLITE DEPLOYMENT

SATELLITE NO.	INC. (DEG)	ECC.	T(P) (HOURS)	LONG.(P) (DEG)
RETROGRADE				
1	116.6	0.35	0.0	-30.0
2	116.6	0.35	4.000	-30.0
3	116.6	0.35	8.000	-30.0
4	116.6	0.35	12.000	-30.0
5	116.6	0.35	16.000	-30.0
6	116.6	0.35	20.000	-30.0
7	116.6	0.35	0.0	-170.0
8	116.6	0.35	4.000	-170.0
9	116.6	0.35	8.000	-170.0
10	116.6	0.35	12.000	-170.0
11	116.6	0.35	16.000	-170.0
12	116.6	0.35	20.000	-170.0
POSIGRADE				
13	35.00	0.0	0.0	-100.0
14	35.00	0.0	8.000	-100.0
15	35.00	0.0	16.000	-100.0

Figure 8.11 depicts the GDOP map for U7. Clearly, GDOP is low and highly uniform. The GDOP statistics of Tables 8.4 and 8.6 show that U7 provides fewer visible satellites than any of the other "uniform" constellations. Nonetheless, the average GDOP for U7 is almost as low as that for constellations U2 to U6.

Figures 8.12 to 8.14 depict the projections of the unit mass configuration for a grid point in Kansas. Note that the mass is distributed fairly evenly in all three projections. The wide spacing between Satellites 5 and 6 and between Satellites 8 and 9 in Fig. 8.14 suggests that the total number of satellites is too small to fully exploit the offset in the ground tracks.

8.8 TIME DEPENDENCE

Table 8.16 summarizes the time dependence of GDOP for constellation U2 over an entire period.

Note that the average GDOP is smallest at time t = 0 when Satellite 7 is at apogee, and Satellites 2 and 12 are far toward the southern horizon (see Fig. 8.6). The average GDOP is largest at time t = 60 min when Satellite 12 sinks below the horizon and Satellites 2 and 7 rise above the horizon (see Fig. 8.6).

The time dependence of GDOP was not determined for U3 to U7. Since the periods of U1, U3 to U7 are longer than that of U2, however, the GDOP's for these constellations can be expected to show larger time variations.

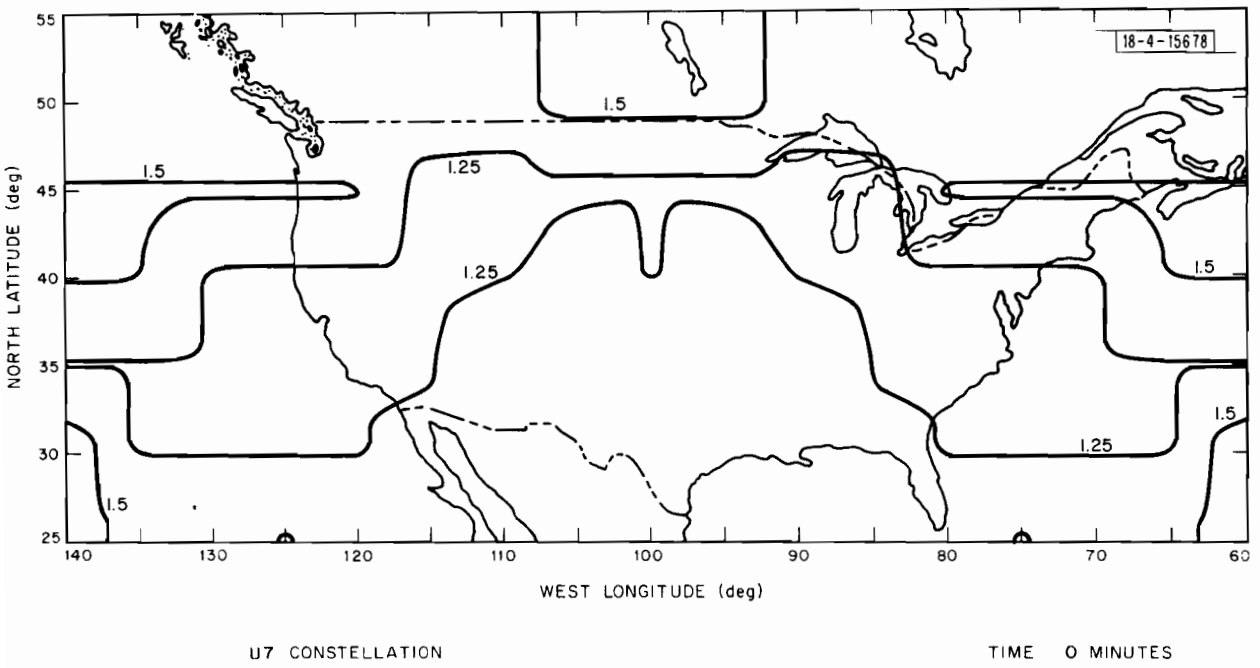

Fig. 8.11. GDOP map for U7 constellation.

Projections of the Unit Masses for
the U7 Constellation

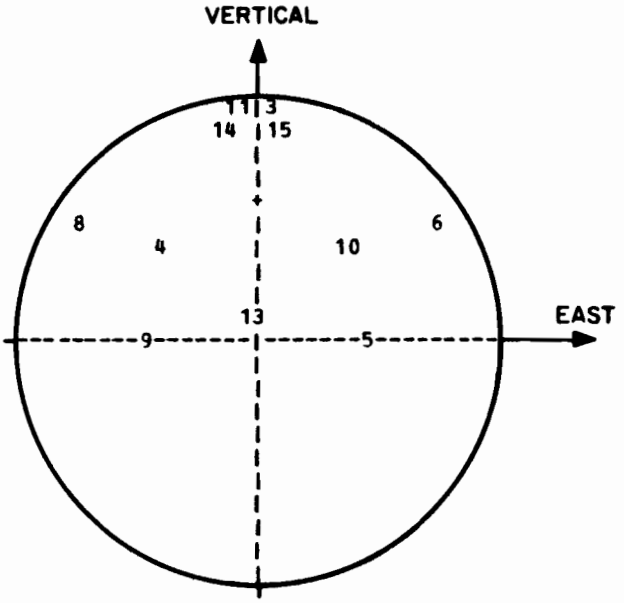

Fig. 8.12. Vertical-East projection.

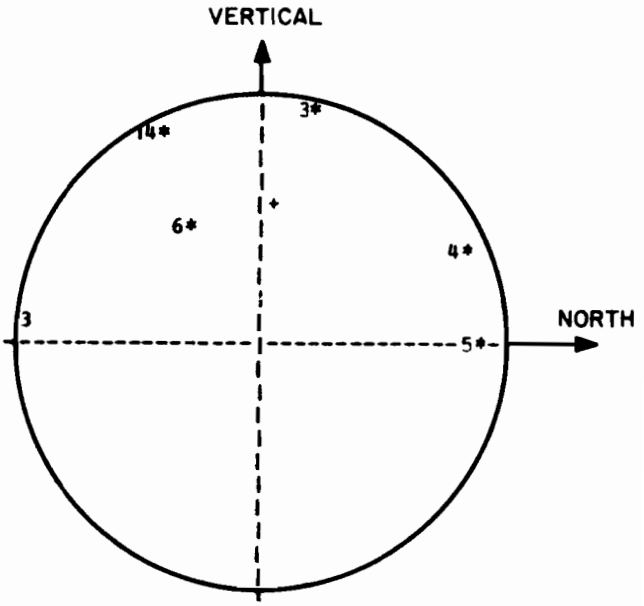

Fig. 8.13. Vertical-North projection.

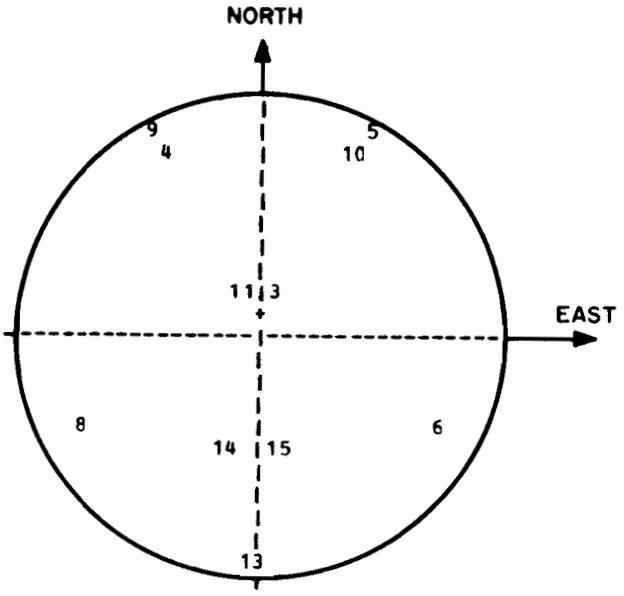

Fig. 8.14. North-East projection.

ATC-23(8.12-14)

THE VISIBLE SATELLITES ARE NUMBERS
3 4 5 6 8 9 10 11 13 14 15

Table 8.16. Time study of constellation U2.

Time (min)	Average Number Satellites Visible	Average GDOP	Excess
0	12.454	1.354	1.620
20	12.420	1.407	1.684
40	12.370	1.522	1.821
60	12.429	1.559	1.865
80	12.370	1.522	1.821
100	12.420	1.407	1.684

Average Number of Visible Satellites	Average GDOP	Average GDOP $\times \sqrt{N}$	Excess
12.41	1.462	5.150	1.749

8.9 THE BEST DESIGN PROCEDURE

The results of Sections 8.4 to 8.7 show that the best procedure (of those considered) is that implicit in the consstellation U2. The procedure can be summarized as follows:

Procedure

1. Place approximately 4/5 of the available satellites in retrograde orbits of modest eccentricity, such the the sub-satellite points are evenly spaced in time along a single ground track, and such that the apogee satellite is just above the northern rim of a viewing cone situated in Kansas.
2. Place the remaining satellites in circular equatorial orbits uniformly distributed between 20° and 180° W longitude.

SECTION 9

THE BEST LARGE CONSTELLATIONS

The procedure described in Section 8.9 was used to design "large," "medium," and "small" constellations for viewing cone half angles of $\phi = 90^{\circ}$, 75° and 60°. To facilitate comparison with the baseline constellations, the new constellations then were analyzed as described in Section 5.1.

Fifteen satellites were used in each large constellation. Ten satellites were used in each medium constellation, and seven satellites in each small constellation.

The resulting constellations were named according to the convention

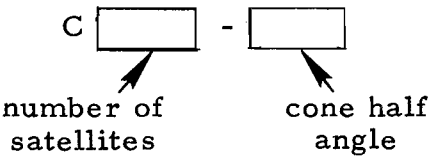

Thus, for example, C10-75 is the medium-sized constellation designed for a viewing cone half angle of $\phi = 75^{\circ}$.

This Section describes the resulting large constellations. Sections 10 and 11, respectively, describe the medium and small constellations.

9.1 DESIGN PROCEDURE

Each constellation was designed in two steps. First, a "ball park" constellation was designed using the procedure of Section 8.9. Then the constellation was "tuned" by varying

1. the relative numbers of satellites in retrograde and equatorial orbits,
2. the inclination of the retrograde orbits,
3. the eccentricity of the retrograde orbits, and
4. the longitudinal separation of the equatorial satellites.

The parameter values that produced the lowest average GDOP during level flight then were taken to be the final constellation parameters.

In each case, the initial inclination and eccentricity of the retrograde orbits were selected so that the satellite at apogee appeared to be resting on the northern rim of the viewing cone when observed from the grid point at 100° W longitude, 40° N latitude. The constellations also were made to be symmetrical about the central CONUS meridian at 100° W longitude.

The tuning step was greatly simplified by the discovery that the orbital parameters e and i have largely independent effects upon the average GDOP. This frequently made it possible to tune a constellation by finding the best value of i for a given value of e, and then finding the best value of e for the resulting i.

9.2 THE C15-90 CONSTELLATION

The U2 constellation of Section 8.5 is the best large constellation designed by the procedure of Section 8.9. Accordingly, U2 is the C15-90 constellation.

For convenient reference, the orbital parameters of the constellation are repeated in Table 9.1. The GDOP statistics are repeated in Tables 9.2 to 9.4.

Table 9.1. The C15-90 constellation.

SATELLITE DEPLOYMENT

SATELLITE NO.	INC. (DEG)	ECC.	T(P) (HOURS)	LONG.(P) (DEG)
RETROGRADE				
1	116.6	0.50	0.0	-100.0
2	116.6	0.50	2.000	-100.0
3	116.6	0.50	4.000	-100.0
4	116.6	0.50	6.000	-100.0
5	116.6	0.50	8.000	-100.0
6	116.6	0.50	10.000	-100.0
7	116.6	0.50	12.000	-100.0
8	116.6	0.50	14.000	-100.0
9	116.6	0.50	16.000	-100.0
10	116.6	0.50	18.000	-100.0
11	116.6	0.50	20.000	-100.0
12	116.6	0.50	22.000	-100.0
EQUATORIAL				
13	0.0	0.0	0.0	-60.0
14	0.0	0.0	0.0	-100.0
15	0.0	0.0	0.0	-140.0

Table 9.2. Nominal results.

Constellation	Average Number Visible	Average GDOP	rms Deviation	Excess
C15-90	12.45	1.354	0.107	1.621
C15-75	11.15	1.792	0.198	1.816
C15-60	9.08	2.938	0.665	2.250

Table 9.3. Dropout results.

Constellation	Average Number Visible	Average GDOP	Sensitivity	Failed Satellite
C15-90	11.45	1.387	0.30	14
C15-75	10.15	1.900	0.67	14
C15-60	8.34	3.181	1.02	14

Table 9.4. 30^{o} Bank results.

Constellation	Average Number Visible	Average GDOP < 10	Percent GDOP > 10
C15-90	9.92	1.687	0%
C15-75	9.75	2.338	0%
C15-60	7.96	4.008	1.8%

Reference to Table 2-17 in Appendix B shows that the remarkably low and uniform GDOP of C15-90 is due to visibility at almost every grid point of three equatorial satellites, and one or more near-perigee satellites (Nos. 2 and 12), in addition to the overhead satellites (Nos. 4, 5, 9, and 10).

The first rows of Tables 9.5 to 9.7 contrast the performance of C15-90 with that of Hybrid. Clearly GDOP for C15-90 is smaller in all categories.

9.3 THE C15-75 CONSTELLATION

The orbital parameters of C15-75 are given in Table 9.8. Comparison of Tables 9.8 and 9.1 shows that the parameters of C15-75 are identical to those of C15-90 except that the inclination of the retrograde orbits is reduced from 116.6° to 105°. This reduction is necessary for the retrograde satellites to remain visible over the nothern rim of the (smaller) viewing cone.

The GDOP map of C15-75 is shown in Fig. 9.1. At most grid points, two or more satellites near apogee, two or more satellites near perigee, and the three equatorial satellites are visible in addition to those overhead. Consequently, GDOP is well below two over most of CONUS. The two areas of very low GDOP (below 1.5) are regions where several key satellites are visible just above the rim of the viewing cone.

The GDOP statistics for C15-75 are given in Tables 9.2 to 9.4. Like C15-90, C15-75 is relatively insensitive to satellite dropout, and aircraft banking.

The second rows of Tables 9.5 to 9.7 contrast the GDOP's provided by C15-75 with those provided by the Hybrid constellation for a viewing cone with $\phi = 75^{\circ}$. Clearly, C15-75 produces smaller GDOP's in all cases.

Table 9.5. Nominal GDOP.

(a) Constellation	Average GDOP	(b) Constellation	Average GDOP
C15-90	1.354	Hybrid ($\phi = 90^{o}$)	1.801
C15-75	1.792	Hybrid ($\phi = 75^{o}$)	2.448
C15-60	2.938	Hybrid ($\phi = 60^{o}$)	3.793

Table 9.6. Dropout results.

(a) Constellation	Average GDOP	(b) Constellation	Average GDOP
C15-90	1.387	Hybrid ($\phi = 90^{o}$)	2.151
C15-75	1.900	Hybrid ($\phi = 75^{o}$)	2.784
C15-60	3.181	Hybrid ($\phi = 60^{o}$)	4.061

Table 9.7. 30^{o} Bank results.

(a) Constellation	Average GDOP < 10	(b) Constellation	Average GDOP < 10
C15-90	1.687	Hybrid ($\phi = 90^{o}$)	2.329
C15-75	2.338	Hybrid ($\phi = 75^{o}$)	3.151
C15-60	4.008*	Hybrid ($\phi = 60^{o}$)	4.554*

*Larger if GDOP's exceeding ten are included.

Table 9.8. The C15-75 constellation.

SATELLITE DEPLOYMENT

SATELLITE NO.	INC. (DEG)	ECC.	T(P) (HOURS)	LONG.(P) (DEG)
RETROGRADE				
1	105.0	0.50	0.0	-100.0
2	105.0	0.50	2.000	-100.0
3	105.0	0.50	4.000	-100.0
4	105.0	0.50	6.000	-100.0
5	105.0	0.50	8.000	-100.0
6	105.0	0.50	10.000	-100.0
7	105.0	0.50	12.000	-100.0
8	105.0	0.50	14.000	-100.0
9	105.0	0.50	16.000	-100.0
10	105.0	0.50	18.000	-100.0
11	105.0	0.50	20.000	-100.0
12	105.0	0.50	22.000	-100.0
EQUATORIAL				
13	0.0	0.0	0.0	-60.0
14	0.0	0.0	0.0	-100.0
15	0.0	0.0	0.0	-140.0

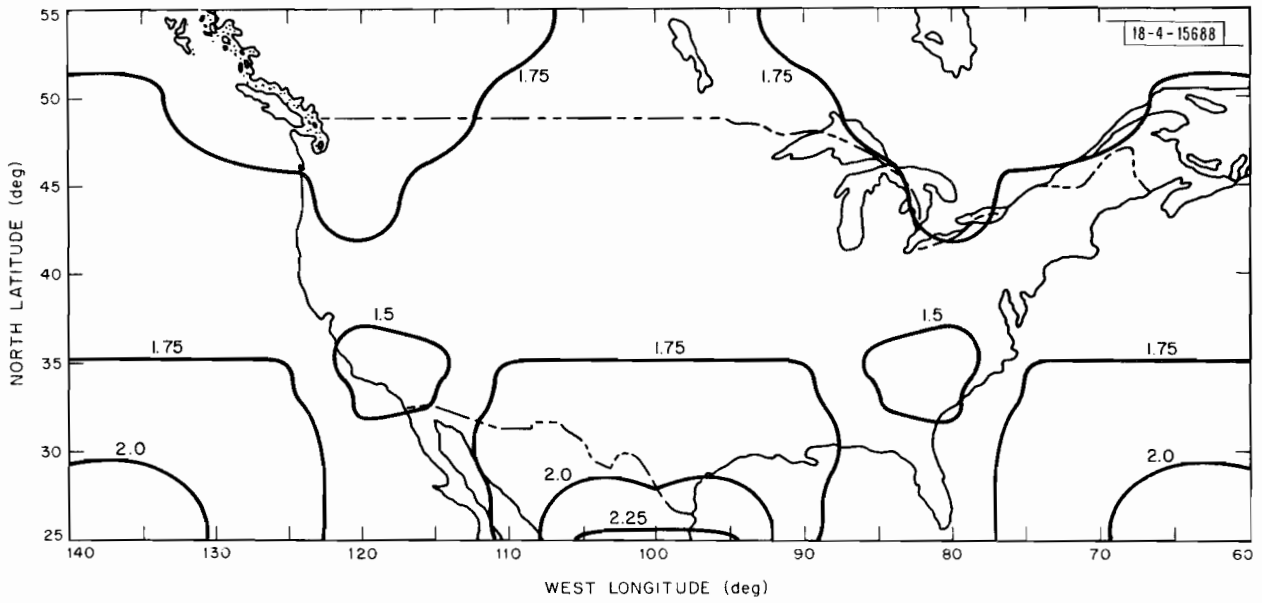

Fig. 9.1. C15-75 constellation. Time 0 minutes.

9.4 THE C15-60 CONSTELLATION

The parameters of C15-60 are given in Table 9.9. Comparison of Table 9.9 with Table 9.8 shows that the inclination of the retrograde orbits is reduced (six degrees) to 99°, and the longitudinal separation of the equatorial satellites is reduced (ten degrees) to 30°. Again, the changes are necessary to keep the majority of the satellites above the rim of the (still smaller) viewing cone.

The GDOP map of Fig. 9.2 shows that GDOP for C15-60 is less than three over most of CONUS and is quite uniform. The higher GDOP's in southern CONUS are due to the non-availability of the satellites near apogee (No. 6, 7, 8). The higher GDOP's in northern CONUS are due to the non-availability of equatorial satellites (Nos. 13, 14, 15). The best GDOP's occur in central CONUS where both the near-apogee satellites and the equatorial satellites are visible.

The GDOP statistics of C15-60 are given in Tables 9.2 to 9.4. Note that, on the average, C15-60 provides two fewer visible satellites than C15-75. This is due to the fact that either near-apogee satellites or equatorial satellites, but not both, are generally visible in C15-60. By contrast, both generally are visible in C15-75. Although GDOP's for C15-60 are well above those for C15-90 and C15-75 the GDOP's still are quite reasonable.

The third rows of Tables 9.5 to 9.7 contrast the GDOP's provided by C15-60 with those produced by Hybrid for a viewing cone with $\phi = 60^{\circ}$. Again, the "C" constellation produces the smallest GDOP's in all cases.

Table 9.9. The C15-60 constellation.

SATELLITE DEPLOYMENT				
SATELLITE NO.	INC. (DEG)	ECC.	T(P) (HOURS)	LONG.(P) (DEG)
RETROGRADE				
1	99.00	0.50	0.0	-100.0
2	99.00	0.50	2.000	-100.0
3	99.00	0.50	4.000	-100.0
4	99.00	0.50	6.000	-100.0
5	99.00	0.50	8.000	-100.0
6	99.00	0.50	10.000	-100.0
7	99.00	0.50	12.000	-100.0
8	99.00	0.50	14.000	-100.0
9	99.00	0.50	16.000	-100.0
10	99.00	0.50	18.000	-100.0
11	99.00	0.50	20.000	-100.0
12	99.00	0.50	22.000	-100.0
EQUATORIAL				
13	0.0	0.0	0.0	-70.0
14	0.0	0.0	0.0	-100.0
15	0.0	0.0	0.0	-130.0

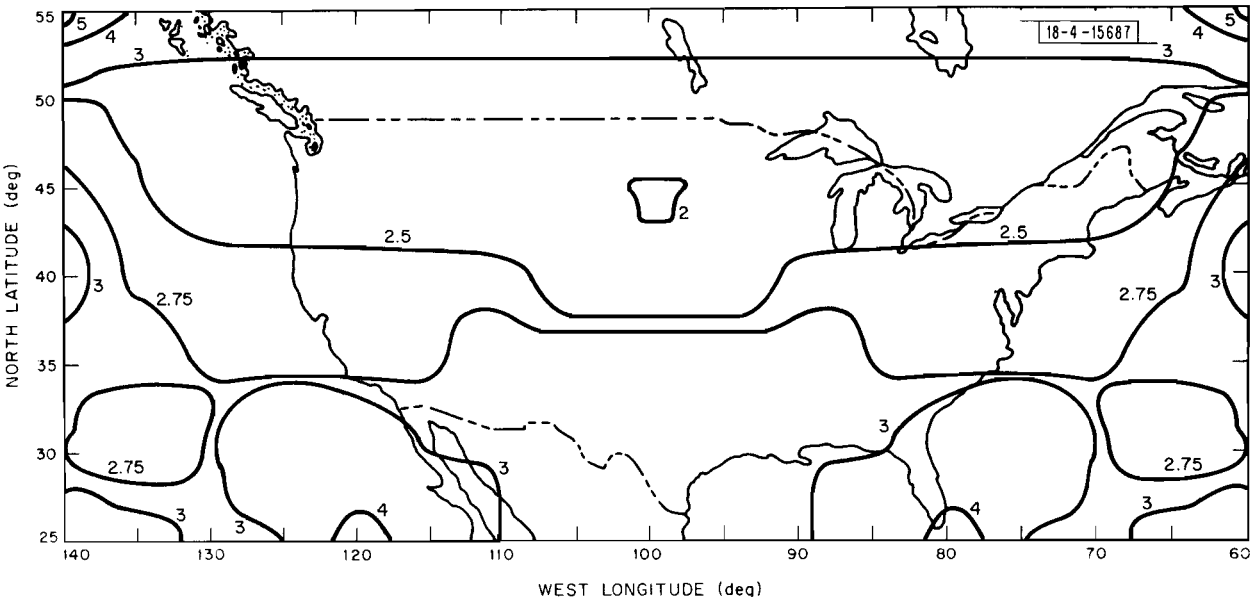

Fig. 9.2. C15-60. constellation. Time 0 minutes.

SECTION 10

THE BEST MEDIUM-SIZED CONSTELLATIONS

This section describes the best medium-sized (ten satellite) constellations designed by the method of Section 8.9. Except for minor deviations, the constellations are scaled-down versions of the large constellations described in Section 9. The resulting GDOP's are roughly $\sqrt{15/10}$ (= 1.23) times larger than those for the large constellations, as suggested by the scaling argument of Section 6.7. Also, the GDOP's are more sensitive to satellite failure and aircraft banking than those for the large constellations.

10.1 THE C10-90 CONSTELLATION

The orbital parameters for C10-90 are given in Table 10.1. The constellation consists of eight satellites in retrograde orbits of eccentricity 0.5 and inclination 110°, and two equatorial satellites separated by 150° longitude. A variety of tentative parameter values were examined as outlined in Section 9.1. Nonetheless, the final constellation is very nearly a scaled-down version of C15-90.

Figure 10.1 depicts the GDOP map for C10-90 at time t = 0. The GDOP's are low and highly uniform across CONUS. The valley of low GDOP (less than 1.5) in central CONUS is due to the visibility there of both equatorial satellites which rest almost on the horizon.

Table 10.1. The C10-90 constellation.

SATELLITE DEPLOYMENT

SATELLITE NO.	INC. (DEG)	ECC.	T(p) (HOURS)	LONG.(P) (DEG)
RETROGRADE				
1	110.0	0.50	0.0	-100.0
2	110.0	0.50	3.000	-100.0
3	110.0	0.50	6.000	-100.0
4	110.0	0.50	9.000	-100.0
5	110.0	0.50	12.000	-100.0
6	110.0	0.50	15.000	-100.0
7	110.0	0.50	18.000	-100.0
8	110.0	0.50	21.000	-100.0
EQUATORIAL				
9	0.0	0.0	0.0	-25.0
10	0.0	0.0	0.0	-175.0

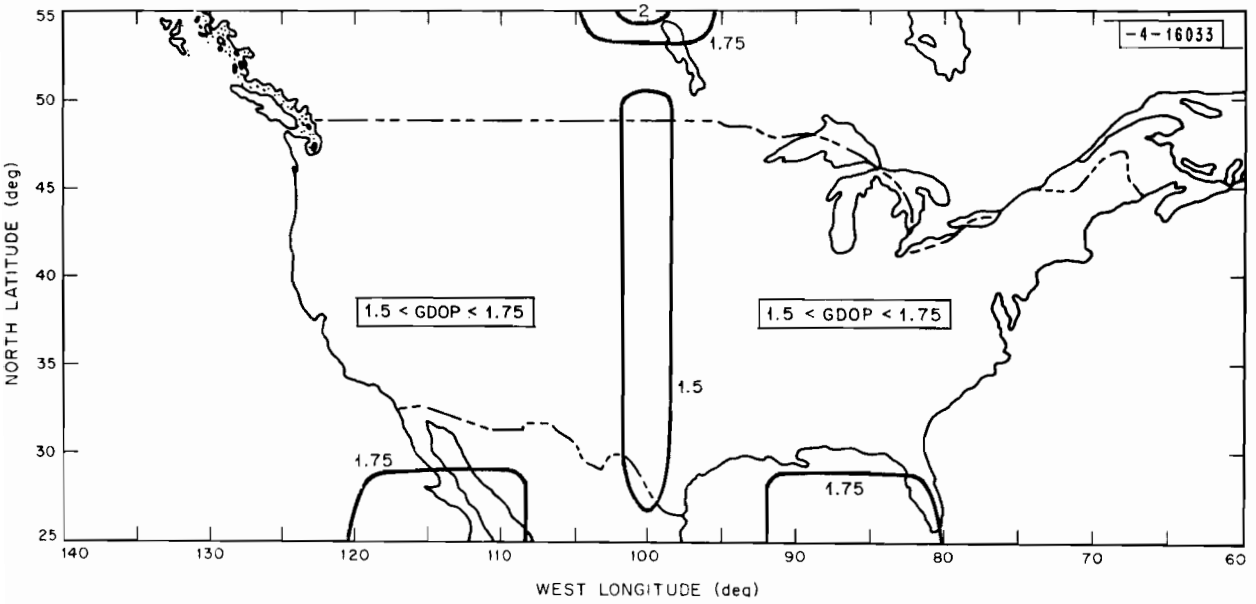

Fig. 10.1. C10-90 constellation. Time 0 minutes.

The GDOP statistics for all three medium constellations are given in Tables 10.2 to 10.4. It is evident from the C10-90 rows that C10-90 not only provides low GDOP's during level flight (Table 10.2), but also following a satellite failure (Table 10.3) or during aircraft banking (Table 10.4).

Figure 10.2 to 10.4 are the projections of the unit mass configuration for C10-90. Satellite 1 is not represented since it is at perigee and therefore not visible. The long moment arms of masses 9 and 10 reflect the highly favorable placement of the equatorial satellites. Figure 10.3 again illustrates how the combination of retrograde satellites (2 - 8) and equatorial satellites (9 - 10) effectively disrupts the planarity of the unit masses.

Tables 10.5 to 10.7 compare the GDOP's produced by all medium-sized constellations with those produced by the LL-I constellation (see Section 5.3). The first rows show that for a viewing cone half angle of $\phi = 90^{\circ}$, C10-90 produces the smaller GDOP in all cases.

Comparison of the first rows at Tables 10.5 to 10.7 and 9.5 to 9.7 reveals another interesting fact. Specifically, for a viewing cone angle of $\phi = 90^{\circ}$, C10-90 produces smaller GDOP's than the larger Hybrid constellation.

10.2 THE C10-75 CONSTELLATION

The orbital parameters of C10-75 are given in Table 10.8. The constellation consists of seven satellites in retrograde orbits of eccentricity 0.35 and inclination 100.0° and three satellites in circular equatorial orbits. The reduced inclination of the retrograde orbits is necessary to keep the satellites above the rim of the viewing cone at most grid points. Note that C10-75 has one more equatorial satellite, and one less retrograde satellite than C10-90. In addition, the retrograde orbits have reduced eccentricities (0.35 versus 0.5).

Projections of the Unit Masses for
the C10-90 Constellation

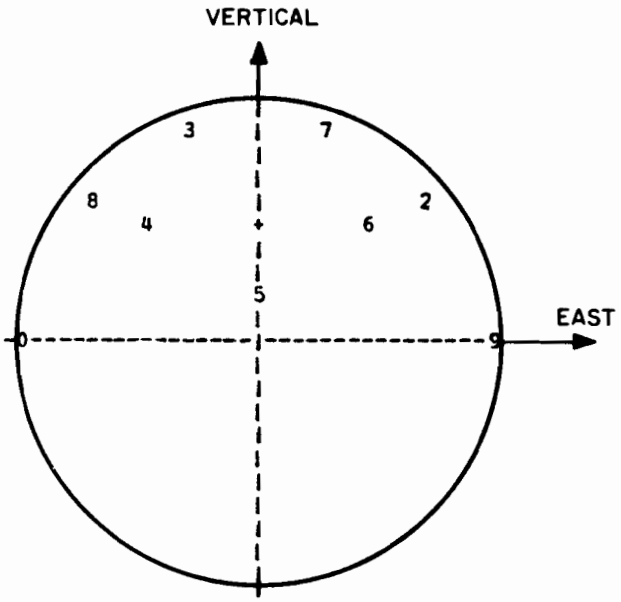

Fig. 10.2. Vertical-East projection.

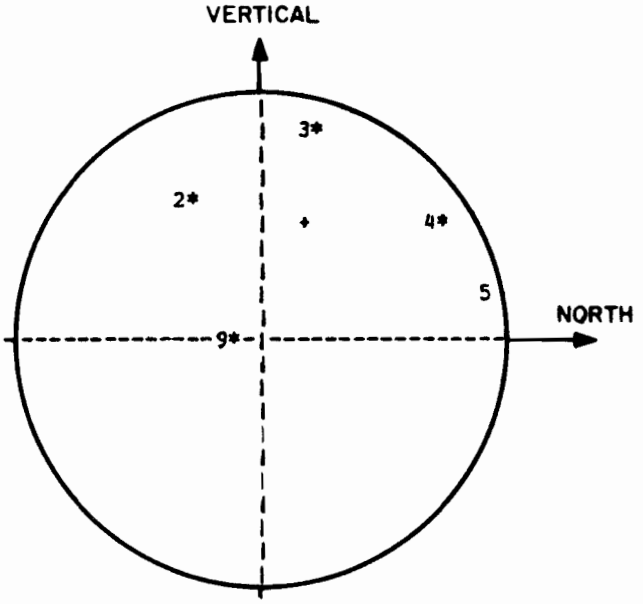

Fig. 10.3. Vertical-North projection.

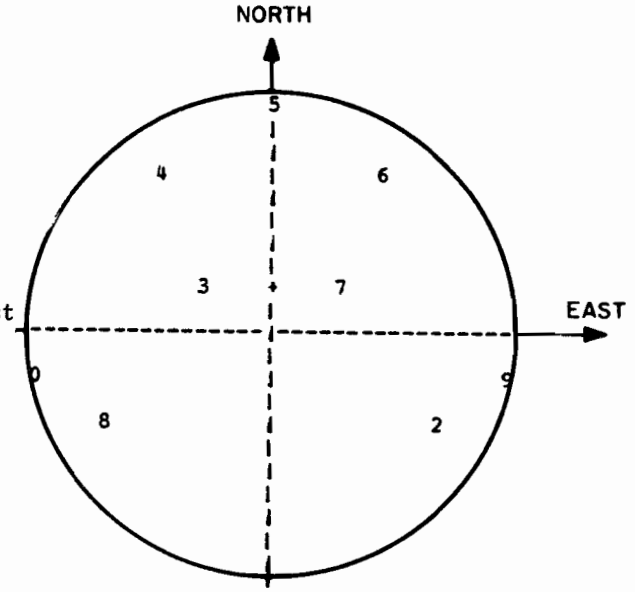

Fig. 10.4. North-East projection.

ATC-23(10.2-4)

THE VISIBLE SATELLITES ARE NUMBERS
2 3 4 5 6 7 8 9 10

Table 10.2. Nominal results.

Constellation	Average Number Visible	Average GDOP	rms Deviation	Excess
C10-90	8.00	1.717	0.095	1.678
C10-75	6.88	2.406	0.421	1.991
C10-60	6.63	3.713*+	0.928	2.323

*Larger if GDOP's greater than ten included.
+2.5% of GDOP's exceed ten.

Table 10.3. Dropout results.

Constellation	Average Number Visible	Average GDOP	Sensitivity	Failed Satellite
C10-90	7.47	2.002	2.51	9
C10-75	5.88	2.681*+	0.79*	9
C10-60	5.95	4.04*†	0.79*	9

*Larger if GDOP's greater than ten included.
+0.84% of GDOP's exceed ten.
†5.88 of GDOP's exceed ten.

Table 10.4. 30° bank results.

Constellation	Average Number Visible	Average GDOP (<10)	Percent GDOP > 10
C10-90	6.88	2.226*	0.05%
C10-75	5.87	3.007*	9.52%
C10-60	5.61	4.206*	36.51%

*Larger if GDOP's greater than ten included.

Table 10.5. Nominal results.

(a) Constellation	Average GDOP	(b) Constellation	Average GDOP
C10-90	1.717	LL-I ($\phi = 90^{\circ}$)	2.870
C10-75	2.406	LL-I ($\phi = 75^{\circ}$)	4.560
C10-60	3.713*	LL-1 ($\phi = 60^{\circ}$)	6.550

*Larger if GDOP's greater than ten are included.

Table 10.6. Dropout results.

(a) Constellation	Average GDOP	(b) Constellation	Average GDOP
C10-90	2.000	LL-I ($\phi = 90^{\circ}$)	3.70
C10-90	2.681	LL-I ($\phi = 75^{\circ}$)	6.55
C10-90	4.04*	LL-I ($\phi = 60^{\circ}$)	8.52*

*Larger if GDOP's greater than ten are included.

Table 10.7. 30° bank results.

(a) Constellation	Average GDOP (< 10)	(b) Constellation	Average GDOP
C10-90	2.226	LL-I ($\phi = 90^{\circ}$)	3.636
C10-75	3.007*	LL-I ($\phi = 75^{\circ}$)	4.696*
C10-60	4.206*	LL-I ($\phi = 60^{\circ}$)	6.210*

*Larger if GDOP's greater than ten are included.

Table 10.8. The C10-75 constellation.

SATELLITE DEPLOYMENT

SATELLITE NO.	INC. (DEG)	ECC.	T(P) (HOURS)	LONG.(P) (DEG)
RETROGRADE				
1	100.0	0.35	0.0	-100.0
2	100.0	0.35	3.429	-100.0
3	100.0	0.35	6.857	-100.0
4	100.0	0.35	10.286	-100.0
5	100.0	0.35	13.714	-100.0
6	100.0	0.35	17.143	-100.0
7	100.0	0.35	20.571	-100.0
EQUATORIAL				
8	0.0	0.0	0.0	-30.0
9	0.0	0.0	0.0	-100.0
10	0.0	0.0	0.0	-170.0

The GDOP map is given in Fig. 10.5. Observe that GDOP exhibits larger variation than the previous "C" constellations. This is due to the following factors:

1. Fewer satellites are available in favorable positions at any one time (due to the reduced total number of satellites).
2. The satellites in favorable positions influence GDOP over smaller geographical areas (due to the reduced size of the viewing cone).

The impact of the foregoing factors also is evident in the GDOP statistics of Tables 10.2 to 10.4. For example, comparison of the first two rows of Table 10.2 shows that the rms deviation of GDOP for C10-75 is more than four times that of C10-90. Similarly, the C10-75 entries of Tables 10.3 to 10.4 show that a small fraction of the GDOP's now exceed ten following a satellite failure or during aircraft banking.

Tables 10.5 to 10.7 and 9.5 to 9.7 show that C10-75 produces smaller GDOP's than either LL-I or Hybrid for a viewing cone with $\phi = 75^{\circ}$.

10.3 THE C10-60 CONSTELLATION

The constellation parameters for C10-60 are given in Table 10.9. The constellation consists of eight satellites in retrograde orbits of eccentricity 0.5 and inclination 95°, and two equatorial satellites. Again, the reduced inclination of the retrograde orbits, and the reduced separation of the equatorial satellites are necessary to ensure satellite visibility at a majority of CONUS grid points.

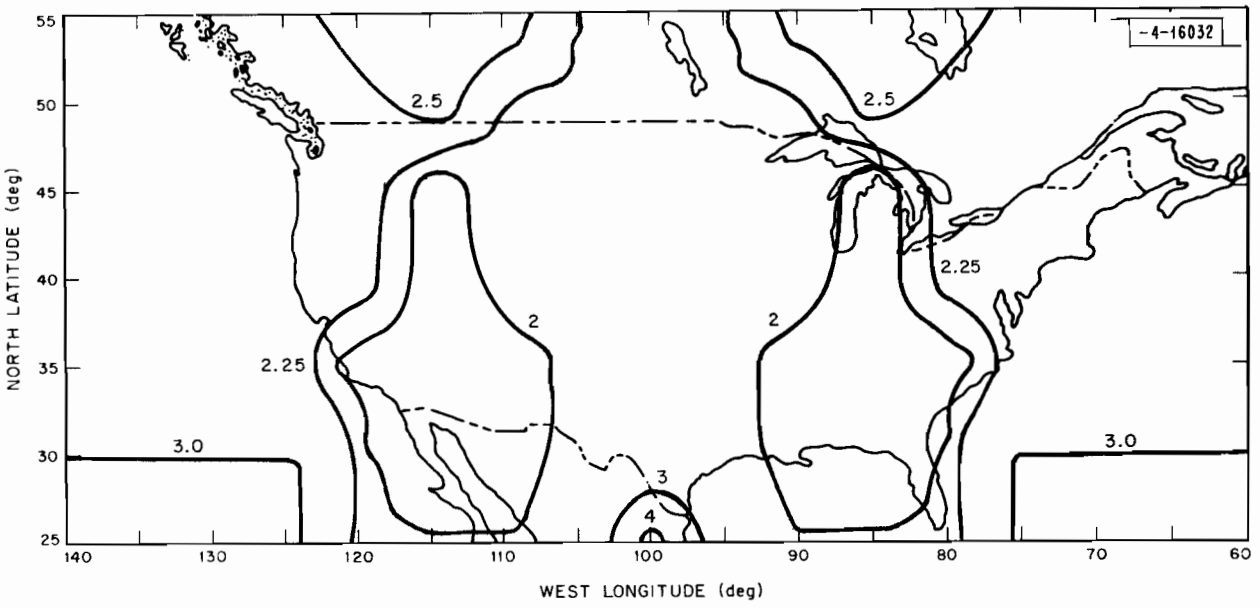

Fig. 10.5. C10-75 constellation. Time 0 minutes.

Table 10.9. The C10-60 constellation.

SATELLITE DEPLOYMENT

SATELLITE NO.	INC. (DEG)	ECC.	T(P) (HOURS)	LONG.(P) (DEG)
RETROGRADE				
1	95.00	0.50	0.0	-100.0
2	95.00	0.50	3.000	-100.0
3	95.00	0.50	6.000	-100.0
4	95.00	0.50	9.000	-100.0
5	95.00	0.50	12.000	-100.0
6	95.00	0.50	15.000	-100.0
7	95.00	0.50	18.000	-100.0
8	95.00	0.50	21.000	-100.0
EQUATORIAL				
9	0.0	0.0	0.0	-90.0
10	0.0	0.0	0.0	-110.0

The GDOP map for C10-60 is shown in Fig. 10.6. The effect of further reducing ϕ has been to increase GDOP and the fluctuations in GDOP. The low GDOP (less than 2.5) in north central CONUS results from the visibility there of all satellites except Satellite No. 1 at perigee. The higher GDOP's at points on the periphery of CONUS are due to the non-availability of satellites diametrically across CONUS. For example, the higher GDOP's over southern CONUS result from the non-availablity of two of the three satellites near apogee. (Nos. 4 to 6).

The third rows of Tables 10.2 to 10.4 underscore the increase both in GDOP, and the fluctuations in GDOP. The average GDOP is more than 50% greater than that for C10-75. In the case of failure of Satellite 9, an increased percentage (5.9%) of GDOP's exceed ten. In the case of banking, more than one third of the aircraft have GDOP's greater than ten.

Figures 10.7 to 10.9 depict the projections of the unit mass configuration. The effects of reducing ϕ is evident from Fig. 10.7 and 10.8. Designing the constellation for a 60° viewing cone begins to restore planarity to the unit masses. Consequently, GDOP increases for the reasons given in Section 7.3.

Although C10-60 exhibits higher GDOP's than the previous "C" constellations, it produces lower GDOP's than either LL-I or Hybrid for a 60° viewing cone (see Tables 10.5 to 10.7 and 9.5 to 9.7).

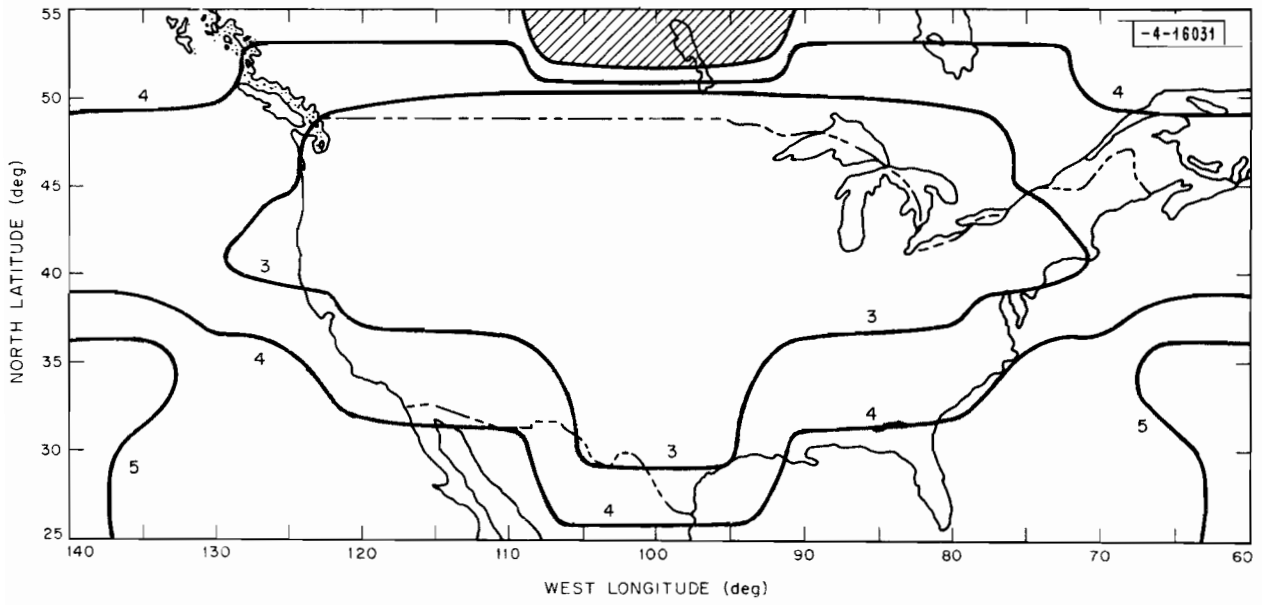

Fig. 10.6. C10-60 constellation. Time 0 minutes.

Projections of the Unit Masses for
the C10-60 Constellation

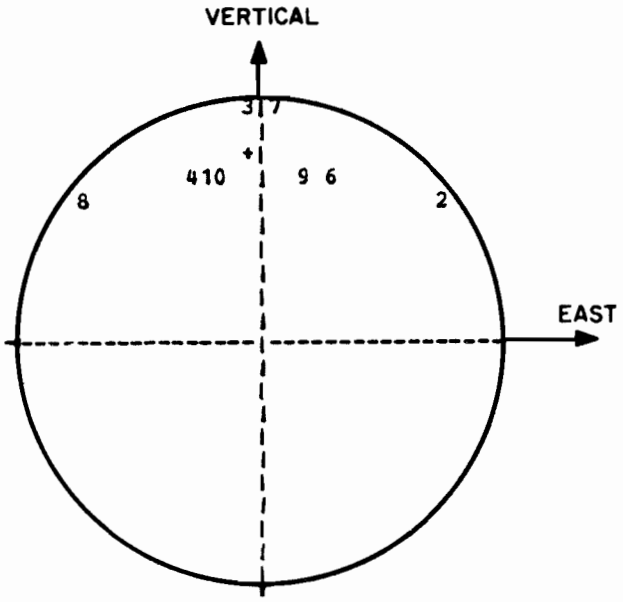

Fig. 10.7. Vertical-East projection.

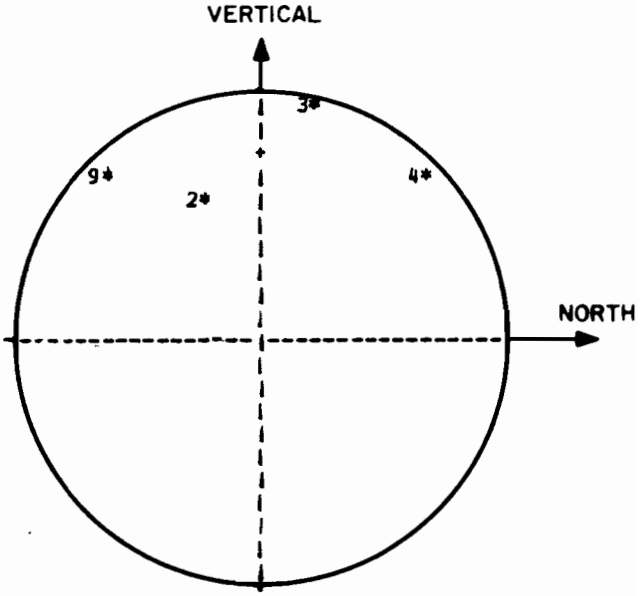

Fig. 10.8. Vertical-North projection.

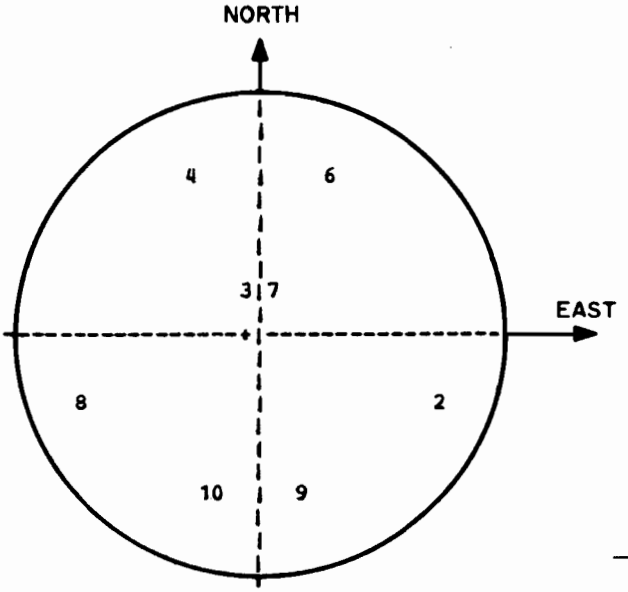

Fig. 10.9. North-East projection.

ATC-23(10.7-9)

THE VISIBLE SATELLITES ARE NUMBERS
2 3 4 6 7 8 9 10

SECTION 11

THE BEST SMALL CONSTELLATIONS

This section describes the best small (seven-satellite) constellations designed by the method of Section 8.9. Again, except for minor perturbations, the constellations are scaled-down versions of the large constellations described in Section 9. The average GDOP's for level flight are approximately $\sqrt{15/7}$ (= 1.46) times those for the large constellations, as suggested by Section 6.7. The GDOP's following satellite failure, or during banking are significantly higher than those predicted by the scaling argument of Section 6.7, however. This is due to the fact that average number of visible satellites closely approaches the minimum number (four).

11.1 THE C7-90 CONSTELLATION

The orbital parameters for C7-90 are given in Table 11.1. The constellation consists of five satellites in retrograde orbits of eccentricty 0.70 and inclination 116.6°, and two satellites in circular equatorial orbits. Like C10-90, C7-90 is very nearly a scaled-down version of C15-90.

The GDOP map is given in Fig. 11.1. The GDOP's generally are smaller than two and highly uniform.

The GDOP statistics for C7-90 are given in Tables 11.2 to 11.4 along with those for C7-75 and C7-60. On the average, 5.78 of the seven satellites

Table 11.1. The C7-90 constellation.

SATELLITE DEPLOYMENT

SATELLITE NO.	INC. (DEG)	ECC.	T(P) (HOURS)	LONG.(P) (DEG)
RETROGRADE				
1	116.6	0.70	0.0	-100.0
2	116.6	0.70	4.800	-100.0
3	116.6	0.70	9.600	-100.0
4	116.6	0.70	14.400	-100.0
5	116.6	0.70	19.200	-100.0
EQUATORIAL				
6	0.0	0.0	0.0	-62.0
7	0.0	0.0	0.0	-138.0

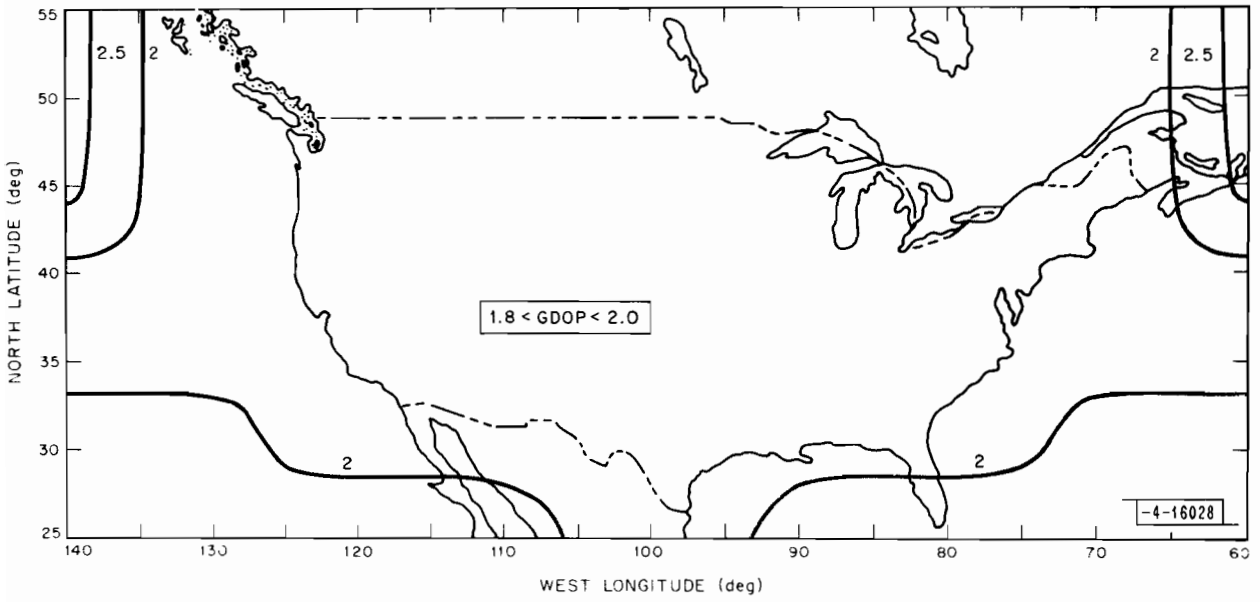

Fig. 11.1. C7-90 constellation. Time 0 minutes.

Table 11.2. Nominal results.

Constellation	Average Number Visible	Average GDOP (< 10)	rms Deviation	Excess
C7-90	5.78	1.983	0.189	1.622
C7-75	5.75	3.042	0.401	2.106
C7-60	5.08	4.136	0.380	2.165

Table 11.3. Dropout results.

Constellation	Average Number Visible	Average GDOP (< 10)	Sensitivity	Failed Satellite
C7-90	4.807	3.120*+	3.41*	7
C7-75	4.857	3.857*†	1.73*	7
C7-60	4.437	4.489*††	0.68*	7

*Larger if GDOP's greater than ten included.
+2.5% of GDOP's greater than ten.
†10.9% of GDOP's greater than ten.
††36% of GDOP's greater than ten.

Table 11.4. 30° bank results.

Constellation	Average Number Visible	Average GDOP (≤ 10)	Percent GDOP (> 10)
C7-90	4.96	2.689*	16.4%
C7-75	4.93	3.439*	28.0%
C7-60	3.71	4.464*	76.4%

*Larger if GDOP's greater than ten included.

are visible over CONUS. The only satellite not generally visible is that at perigee. Considering its small size, the constellation performs well following satellite failure. Table 11.3 shows that only 2.5% of the GDOP's exceed ten when Satellite 7 fails, and the remaining GDOP's average 3.12. Performance is more sensitive to aircraft banking. Table 11.4 shows that for 16.4% of the selected headings at CONUS grid points, GDOP exceeds ten, with the GDOP's averaging 2.699 on the remaing headings.

Tables 11.5 to 11.7 compare performance of the small constellations with that of RCA-8. It is evident that C7-90 provides lower GDOP's than (the larger) RCA-8 in all categories.

11.2 THE C7-75 CONSTELLATION

Table 11.8 contains the orbital parameters for C7-75. The constellation consists of five satellites in retrograde orbits of eccentricity 0.5 and inclination 95° and two satellites in circular equatorial orbits.

The GDOP map is given in Fig. 11.2. GDOP is close to three and reasonably uniform across CONUS.

The GDOP statistics for C7-75 are given in Tables 11.2 to 11.4. Note that while C7-75 and C7-90 provide approximately the same number of visible satellites, GDOP is significantly higher for C7-75. This is a direct consequence of the higher elevation angles of the C7-75 satellites. Table 11.3 indicates an increased sensitivity to satellite dropout. Specifically, failure of Satellite 7 causes GDOP to exceed ten at more than ten percent of the grid points. Table 11.4 indicates an increased sensitivity to aircraft banking, with GDOP exceeding ten at 28% of the test headings.

Table 11.5. Nominal results.

(a) Constellation	Average GDOP (< 10)	(b) Constellation	Average GDOP (< 10)
C7-90	1.983	RCA-8 ($\phi = 90^{\circ}$)	3.509
C7-75	3.042	RCA-8 ($\phi = 75^{\circ}$)	3.761
C7-60	4.136*	RCA-8 ($\phi = 60^{\circ}$)	4.700*

*Larger if GDOP's greater than ten are included.

Table 11.6. Dropout results.

(a) Constellation	Average GDOP (< 10)	(b) Constellation	Average GDOP (< 10)
C7-90	3.120*	RCA-8 ($\phi = 90^{\circ}$)	7.776
C7-75	3.857*	RCA-8 ($\phi = 75^{\circ}$)	7.621*
C7-60	4.489*	RCA-8 ($\phi = 60^{\circ}$)	7.417*

*Larger if GDOP's greater than ten are included.

Table 11.7. 30° bank results.

(a) Constellation	Average GDOP (< 10)	(b) Constellation	Average GDOP (< 10)
C7-90	2.689*	RCA-8 ($\phi = 90^{\circ}$)	3.846*
C7-75	3.439*	RCA-8 ($\phi = 75^{\circ}$)	4.554*
C7-60	4.464*	RCA-8 ($\phi = 60^{\circ}$)	5.534*

*Larger if GDOP's greater than ten are included.

Table 11.8. The C7-75 constellation.

SATELLITE DEPLOYMENT

SATELLITE NO.	INC. (DEG)	ECC.	T(P) (HOURS)	LONG.(P) (DEG)
RETROGRADE				
1	95.00	0.50	0.0	-100.0
2	95.00	0.50	4.800	-100.0
3	95.00	0.50	9.600	-100.0
4	95.00	0.50	14.400	-100.0
5	95.00	0.50	19.200	-100.0
EQUATORIAL				
6	0.0	0.0	0.0	-76.0
7	0.0	0.0	0.0	-124.0

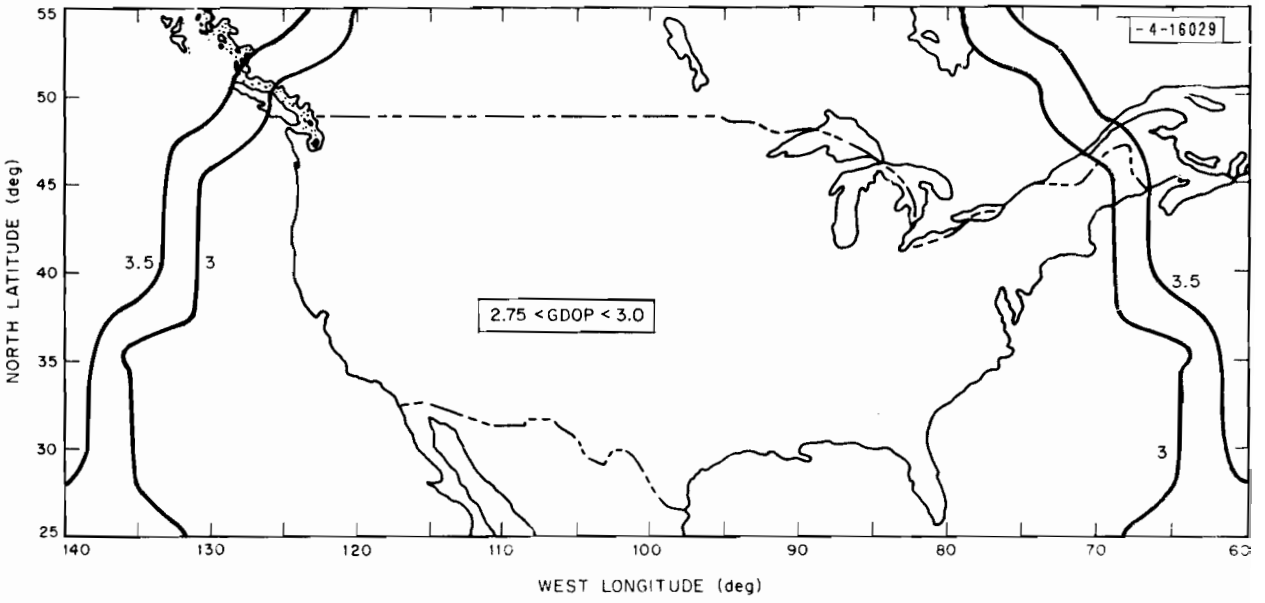

Fig. 11.2. C7-75 constellation. Time 0 minutes.

Reference to Table 11.5 to 11.7 shows that for a viewing cone with $\phi = 75^{\circ}$, C7-75 provides smaller GDOP's than RCA-8 in all categories.

11.3 THE C7-60 CONSTELLATION

The orbital parameters of C7-60 are given in Table 11.9. The constellation consists of five satellites in posigrade orbits of eccentricity 0.5 and inclination 87°, and two satellites in circular equatorial orbits. For the case of seven satellites and $\phi = 60^{\circ}$, the "tuning" step showed that retrograde orbits do not provide lower GDOP's than highly inclined posigrade orbits. Accordingly, posigrade orbits were used.

The GDOP map for C7-60 is given in Fig. 11.3. The GDOP's are higher and more variable than for the preceding constellations. The high GDOP's over extreme northern CONUS are due to the fact that only four satellites are visible there, and all at high elevation angles.

The GDOP statistics are given in Tables 11.2 to 11.4. Tables 11.3 and 11.4 show that performance is quite sensitive to satellite dropout and aircraft banking. For example, failure of Satellite 7 causes GDOP to exceed ten at over one third of the grid points. Table 11.4 shows that during aircraft banking, fewer than the minimum number of satellites are visible on the average. Consequently, GDOP exceeds ten over more than 75% of the test headings.

The projections of the unit mass configurations are given in Figs. 11.4 to 11.6. Figure 11.5 shows the reason for the high GDOP's. The near planarity of masses 2-7 produces high GDOP's as explained in Section 7.3. The short east-west moment arms in Fig. 11.6 further increase GDOP.

Table 11.9. The C7-60 constellation.

SATELLITE DEPLOYMENT

SATELLITE NO.	INC. (DEG)	ECC.	T(P) (HOURS)	LONG.(P) (DEG)
POSIGRADE				
1	87.00	0.50	0.0	-100.0
2	87.00	0.50	4.800	-100.0
3	87.00	0.50	9.600	-100.0
4	87.00	0.50	14.400	-100.0
5	87.00	0.50	19.200	-100.0
EQUATORIAL				
6	0.0	0.0	0.0	-85.0
7	0.0	0.0	0.0	-115.0

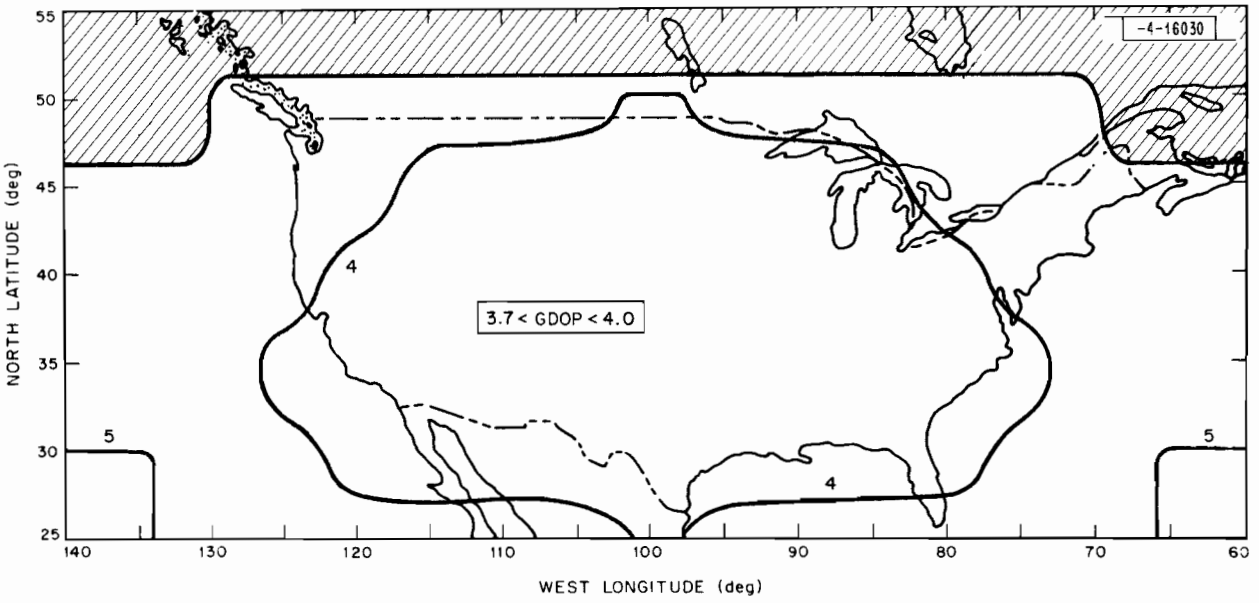

Fig. 11.3. C7-60 constellation. Time 0 minutes.

Projections of the Unit Masses for
the C7-60 Constellation

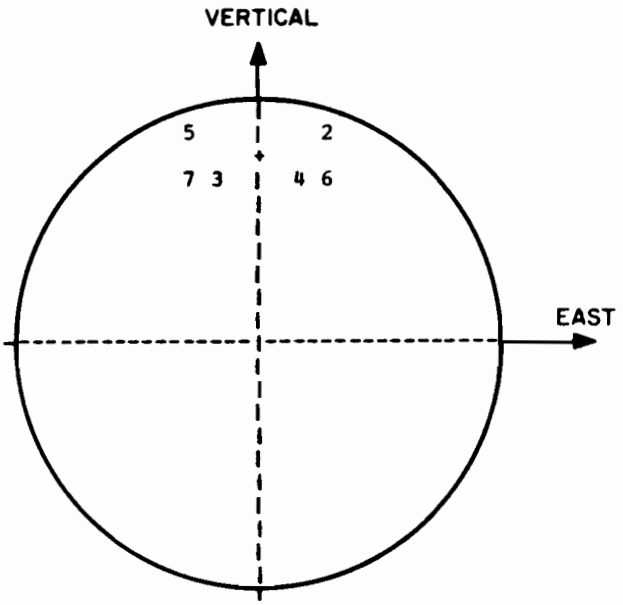

Fig. 11.4. Vertical-East projection.

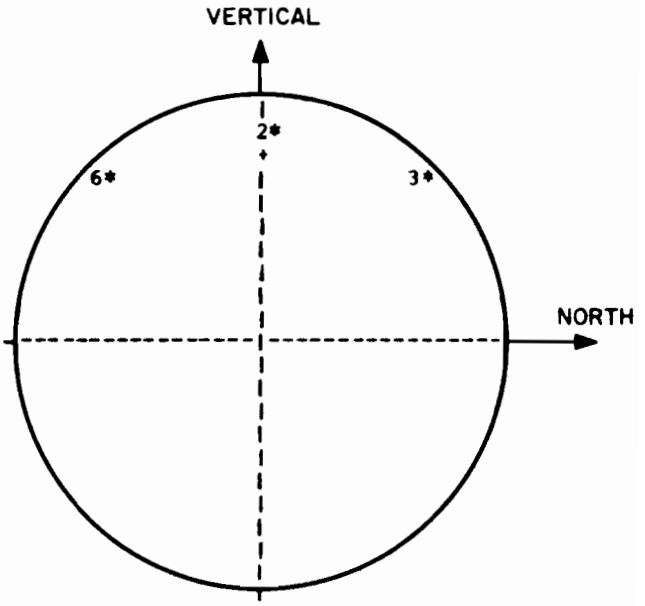

Fig. 11.5. Vertical-North projection.

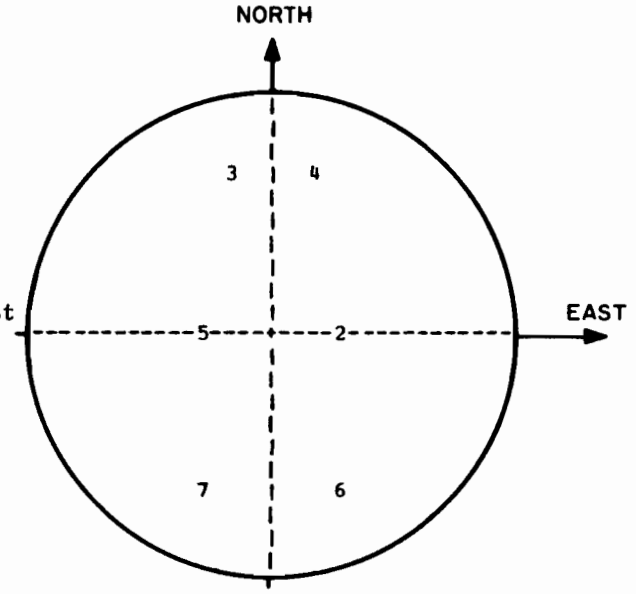

Fig. 11.6. North-East projection.

ATC-23(11.4-6)

THE VISIBLE SATELLITES ARE NUMBERS
2 3 4 5 6 7

The third rows of Tables 11.5 and 11.7 contrast the performance of C7-60 and RCA-8 for a viewing cone with $\phi = 60^{\circ}$. In spite of its shortcomings, C7-60 provides competitive GDOP's in all categories.

SECTION 12

CONCLUDING REMARKS

12.1 OTHER POSSIBLE ANALYSES

Almost all of the foregoing analyses are for time t = 0 hours. Thus, the results represent a sample of the performance of each constellation. Had additional resources been available, it would have been desirable to examine the time dependence of GDOP for each constellation over a complete period. Such analyses would have provided useful information on the time variation of GDOP for each constellation. Time averaging of the data also would have smoothed the sensitivity data.*

While additional analyses would have refined the results, it is doubtful that they would have altered any of the major conclusions. For example, the time study of Section 8.8 indicates that C15-90 exhibits its best performance at time t = 0. Thus, the comparison of Table 9.5 may not be entirely representative. Nonetheless, if a time-averaged GDOP, or even a worst-case GDOP, is used for C15-90, it is clear that C15-90 still produces improved GDOP's.

*Such as that presented in Table 5.15.

12.2 FURTHER GDOP IMPROVEMENTS

The constellations of Sections 9-11 are the best that we have devised. While the GDOP's improve upon those for the baseline constellations, they do not closely approximate the theoretical GDOP limit (3.1). Instead, the constellation Excesses are in the range

$$1.6 \leq \text{Excess} \leq 2.3 \tag{12.1}$$

so that the optimum GDOP's are 40% to 60% smaller than the acutal GDOPs. Therefore, it is relevant to ask whether further reductions in GDOP can be achieved.

It is our opinion, that although small (10%) reductions in GDOP may be possible, large reductions (30% or more) will be difficult in the context of the problem statement of Section 3. The reasons for this are as follows:

1. The satellites do not occupy fixed positions, but must traverse real physical orbits.
2. Low GDOP's are required not just at a single point, but throughout CONUS.
3. Low GDOP's are required not just at one instant, but at all times.

Certainly, satellites can be placed in orbits so that at a given time the optimum GDOP (3.1) is obtained at one location in CONUS. The optimum GDOP will not be obtained anywhere else in CONUS, however. Nor will the optimum value be obtained a short time later. Consequently, some departure from the

optimum value is unavoidable. Our experience suggest that the departure may be as great as 30%.

12.3 USEFUL TOOLS FOR RELATED WORK

In the course of the study, we have found three tools to be especially useful.

First, the moment of inertia viewpoint of Section 6.1 has provided considerable insight into constellation design. Moreover, when augmented by the unit mass plots, it has proven to be an effective troubleshooting tool (see Sections 6.6 and 8.6).

Second, the expression (3.1) for optimum GDOP has proven to be a convenient yardstick against which to measure the performance of candidate constellations.

Finally, the normalized GDOP of Section 6.7 has helped to resolve the "apples and oranges" problem of comparing the performance of constellations having different number of satellites.

Accordingly, we recommend these tools to others interested in the problem of designing constellations that provide low GDOP's.

ACKNOWLEDGEMENT

It is a pleasure to acknowledge several beneficial interchanges with Ron Loeliger of the Autonetics Division of Rockwell International Corp. early on in the work. The authors also wish to acknowledge the encouragement, support and stimulation of Irvin Stiglitz of M. I. T. Lincoln Laboratory.

REFERENCES

[1] D. D. Otten, "Study of a Navigation and Traffic Control Technique Employing Satellites," Vols. I-IV, Group Report 08710-6012-12000, TRW Systems, Redondo Beach, California (December 1967).

[2] I. G. Stiglitz, J. U. Beuch, A. Eckberg, and K. S. Schneider, "Concept Formulation Studies of the Surveillance Aspects of the Fourth Generation Air Traffic Control System," Project Report ATC-7, Lincoln Laboratory, M. I. T. (21 September 1971), DOT/TSC-241-1.

[3] "Final Report - Fourth Generation Air Traffic Control Study," Report C71-61/301, Rockwell International Corporation, Anaheim, California (November 1971).

[4] "Study and Concept Formulation of a Fourth Generation Air Traffic Control System," Vols. I-V, Report DOT-TSC-3601-1, Boeing Company, Renton, Washington (April 1972).

[5] P. M. Diamond, "The Potential of a System of Satellites as Part of an Air Traffic Control System," AGARD Conference Proceedings No. 105, pp. 20-1 (June 1972).

[6] L. Schuchman, "The ASTRO-DABS Concept," Technical Report MTR-6287, MITRE Corporation, McLean, Virginia (November 1972).

[7] K. D. McDonald, "A Survey of Satellite-Based Systems for Navigation, Position Surveillance, Traffic Control and Collision Avoidance," Addendum to Proceedings of ION National Aerospace Meeting, Institute of Navigation, Washington, D. C., (March 1973).

[8] "Final Report - Advanced Air Traffic Management System," Report C72-1206/210, Rockwell International Corporation, Anaheim, California (April 1973).

[9] "Advanced Air Traffic Management - System B Summary Report, MTR-6419 Series 1, MITRE Corporation, McLean, Virginia (June 1973), FAA-EM-73-10.

[10] F. N. David and J. Neyman, "Extension of the Markoff Theorem on Least Squares," Statistics Research Mem. 2, Dept. of Statistics, London (1938), pp. 105-116.

[11] H. B. Lee, "Accuracy Limitations of Hyperbolic Multilateration Systems," Technical Note 1973-11, Lincoln Laboratory, M. I. T. (22 March 1973) DOT/TSC-241-3.

APPENDIX A

DESCRIPTION OF COMPUTER PROGRAMS

A FORTRAN program to calculate the Geometric Dilution of Precision (GDOP) across an arbitrary grid on the earth's surface was made available by Autonetics (Ref. [8]). Several points in this program were changed to produce a program (GDOPN) more suitable for our purposes here. From GDOPN two more programs were developed for more specific uses. The first of these, MASS, calculates unit-mass plots and the moment of inertia matrix. The other, TRACK, calculates and plots sub-satellite points. A brief description of each of these programs follows:

GDOPN — Given a satellite constellation, the half angle of the viewing cone and various other parameters, GDOPN calculates each sub-satellite point, determines which satellites are visible across an input latitude-longitude grid, and computes the GDOP at each point on this grid. The output is in tabular as well as graphic form, the graph presenting contours of constant GDOP. It is also capable of "banking" the aircraft at an arbitrary angle, then rotating it in azimuth seeking a worst-case orientation. Although GDOPN has the ability to compare the power received at the satellite to an input reference power, this signal-to-noise comparison was not utilized in the report.

MASS Same input as GDOPN. This program calculates the unit vectors for an aircraft at the middle of the input grid and plots the unit masses in x-y, z-x, and z-y projections. Vectors are also presented in tabular form. Output may either be in the reference frame of the airplane, or in the frame of the earth, centered at the earth's center.

TRACK Same input as other two. Track calculates the sub-satellite points of the input satellites and plots them on a rectangular latitude-longitude grid. As in the above two programs, this may be done for any number of time intervals, with output presented for each time interval on the same graph.

APPENDIX B

TABLES OF GDOP FOR ALL CONSTELLATIONS

This appendix contains nominal GDOP values and lists of visible satellites at alternate grid points for RCA-8, LL-I, Hybrid, and the constellations described in Sections 8 to 12. These data should be useful to anyone wishing to verify or improve upon our results.

Table B-1. The RCA-8 constellation ($\phi = 90^{\circ}$).

GDOP OVER CONUS

LAT.	LONG.	GDOP	VISIBLE SATELLITES						
25.0	-140.0	3.64	2	3	4	5	6	7	8
25.0	-130.0	3.58	2	3	4	5	6	7	8
25.0	-120.0	3.54	2	3	4	5	6	7	8
25.0	-110.0	3.51	2	3	4	5	6	7	8
25.0	-100.0	3.50	2	3	4	5	6	7	8
25.0	-90.0	3.51	2	3	4	5	6	7	8
25.0	-80.0	3.54	2	3	4	5	6	7	8
25.0	-70.0	3.58	2	3	4	5	6	7	8
25.0	-60.0	3.64	2	3	4	5	6	7	8
35.0	-140.0	3.59	2	3	4	5	6	7	8
35.0	-130.0	3.53	2	3	4	5	6	7	8
35.0	-120.0	3.49	2	3	4	5	6	7	8
35.0	-110.0	3.47	2	3	4	5	6	7	8
35.0	-100.0	3.46	2	3	4	5	6	7	8
35.0	-90.0	3.47	2	3	4	5	6	7	8
35.0	-80.0	3.49	2	3	4	5	6	7	8
35.0	-70.0	3.53	2	3	4	5	6	7	8
35.0	-60.0	3.59	2	3	4	5	6	7	8
45.0	-140.0	3.55	2	3	4	5	6	7	8
45.0	-130.0	3.51	2	3	4	5	6	7	8
45.0	-120.0	3.48	2	3	4	5	6	7	8
45.0	-110.0	3.46	2	3	4	5	6	7	8
45.0	-100.0	3.45	2	3	4	5	6	7	8
45.0	-90.0	3.46	2	3	4	5	6	7	8
45.0	-80.0	3.48	2	3	4	5	6	7	8
45.0	-70.0	3.51	2	3	4	5	6	7	8
45.0	-60.0	3.55	2	3	4	5	6	7	8
55.0	-140.0	3.55	2	3	4	5	6	7	8
55.0	-130.0	3.51	2	3	4	5	6	7	8
55.0	-120.0	3.48	2	3	4	5	6	7	8
55.0	-110.0	3.47	2	3	4	5	6	7	8
55.0	-100.0	3.46	2	3	4	5	6	7	8
55.0	-90.0	3.47	2	3	4	5	6	7	8
55.0	-80.0	3.48	2	3	4	5	6	7	8
55.0	-70.0	3.51	2	3	4	5	6	7	8
55.0	-60.0	3.55	2	3	4	5	6	7	8

Table B-2. The RCA-8 constellation ($\phi = 75^{o}$).

GDOP OVER CONUS

LAT.	LONG.	GDOP	VISIBLE SATELLITES						
25.0	-140.0	4.14	3	4	5	6	7	8	
25.0	-130.0	3.58	2	3	4	5	6	7	8
25.0	-120.0	3.54	2	3	4	5	6	7	8
25.0	-110.0	3.51	2	3	4	5	6	7	8
25.0	-100.0	3.50	2	3	4	5	6	7	8
25.0	-90.0	3.51	2	3	4	5	6	7	8
25.0	-80.0	3.54	2	3	4	5	6	7	8
25.0	-70.0	3.58	2	3	4	5	6	7	8
25.0	-60.0	4.14	2	3	4	5	7	8	
35.0	-140.0	4.07	3	4	5	6	7	8	
35.0	-130.0	4.03	3	4	5	6	7	8	
35.0	-120.0	3.49	2	3	4	5	6	7	8
35.0	-110.0	3.47	2	3	4	5	6	7	8
35.0	-100.0	3.46	2	3	4	5	6	7	8
35.0	-90.0	3.47	2	3	4	5	6	7	8
35.0	-80.0	3.49	2	3	4	5	6	7	8
35.0	-70.0	4.03	2	3	4	5	7	8	
35.0	-60.0	4.07	2	3	4	5	7	8	
45.0	-140.0	4.03	3	4	5	6	7	8	
45.0	-130.0	3.99	3	4	5	6	7	8	
45.0	-120.0	3.48	2	3	4	5	6	7	8
45.0	-110.0	3.46	2	3	4	5	6	7	8
45.0	-100.0	3.45	2	3	4	5	6	7	8
45.0	-90.0	3.46	2	3	4	5	6	7	8
45.0	-80.0	3.48	2	3	4	5	6	7	8
45.0	-70.0	3.99	2	3	4	5	7	8	
45.0	-60.0	4.03	2	3	4	5	7	8	
55.0	-140.0	4.97	3	4	5	6	8		
55.0	-130.0	3.99	3	4	5	6	7	8	
55.0	-120.0	3.97	3	4	5	6	7	8	
55.0	-110.0	3.47	2	3	4	5	6	7	8
55.0	-100.0	3.46	2	3	4	5	6	7	8
55.0	-90.0	3.47	2	3	4	5	6	7	8
55.0	-80.0	3.97	2	3	4	5	7	8	
55.0	-70.0	3.99	2	3	4	5	7	8	
55.0	-60.0	4.97	2	3	4	5	7		

Table B-3. The RCA-8 constellation ($\phi = 60^{o}$).

GDOP OVER CONUS

LAT.	LONG.	GDOP	VISIBLE SATELLITES						
25.0	-140.0	13.33	3	5	6	8			
25.0	-130.0	12.42	3	5	6	7	8		
25.0	-120.0	12.14	3	5	6	7	8		
25.0	-110.0	7.38	2	3	5	6	7	8	
25.0	-100.0	7.34	2	3	5	6	7	8	
25.0	-90.0	7.38	2	3	5	6	7	8	
25.0	-80.0	12.14	2	3	5	7	8		
25.0	-70.0	12.42	2	3	5	7	8		
25.0	-60.0	13.33	2	3	5	7			
35.0	-140.0	5.03	3	4	5	6	8		
35.0	-130.0	5.00	3	4	5	6	8		
35.0	-120.0	4.00	3	4	5	6	7	8	
35.0	-110.0	3.98	3	4	5	6	7	8	
35.0	-100.0	3.46	2	3	4	5	6	7	8
35.0	-90.0	3.98	2	3	4	5	7	8	
35.0	-80.0	4.00	2	3	4	5	7	8	
35.0	-70.0	5.00	2	3	4	5	7		
35.0	-60.0	5.03	2	3	4	5	7		
45.0	-140.0	4.98	3	4	5	6	8		
45.0	-130.0	4.95	3	4	5	6	8		
45.0	-120.0	4.94	3	4	5	6	8		
45.0	-110.0	3.96	3	4	5	6	7	8	
45.0	-100.0	4.39	3	4	5	7	8		
45.0	-90.0	3.96	2	3	4	5	7	8	
45.0	-80.0	4.94	2	3	4	5	7		
45.0	-70.0	4.95	2	3	4	5	7		
45.0	-60.0	4.98	2	3	4	5	7		
55.0	-140.0			3	4	5			
55.0	-130.0			3	4	5			
55.0	-120.0			3	4	5			
55.0	-110.0			3	4	5			
55.0	-100.0			3	4	5			
55.0	-90.0			3	4	5			
55.0	-80.0			3	4	5			
55.0	-70.0			3	4	5			
55.0	-60.0			3	4	5			

Table B-4. The LL-I constellation ($\phi = 90^{o}$).

GDOP OVER CONUS

LAT.	LONG.	GDOP	VISIBLE SATELLITES										
25.0	-140.0	3.23	3	4	5	6	7	8	9	10	11	12	
25.0	-130.0	3.17	3	4	5	6	7	8	9	10	11	12	
25.0	-120.0	3.11	3	4	5	6	7	8	9	10	11	12	
25.0	-110.0	3.07	3	4	5	6	7	8	9	10	11	12	
25.0	-100.0	3.05	3	4	5	6	7	8	9	10	11	12	
25.0	-90.0	1.83	2	3	4	5	6	7	8	9	10	11	12
25.0	-80.0	1.83	2	3	4	5	6	7	8	9	10	11	12
25.0	-70.0	1.84	2	3	4	5	6	7	8	9	10	11	12
25.0	-60.0	2.60	2	3	4	5	6	7	8	9	10		
35.0	-140.0	3.19	3	4	5	6	7	8	9	10	11	12	
35.0	-130.0	3.13	3	4	5	6	7	8	9	10	11	12	
35.0	-120.0	3.08	3	4	5	6	7	8	9	10	11	12	
35.0	-110.0	3.05	3	4	5	6	7	8	9	10	11	12	
35.0	-100.0	3.03	3	4	5	6	7	8	9	10	11	12	
35.0	-90.0	3.03	3	4	5	6	7	8	9	10	11	12	
35.0	-80.0	1.84	2	3	4	5	6	7	8	9	10	11	12
35.0	-70.0	1.99	2	3	4	5	6	7	8	9	10	11	
35.0	-60.0	2.59	2	3	4	5	6	7	8	9	10		
45.0	-140.0	3.17	3	4	5	6	7	8	9	10	11	12	
45.0	-130.0	3.12	3	4	5	6	7	8	9	10	11	12	
45.0	-120.0	3.08	3	4	5	6	7	8	9	10	11	12	
45.0	-110.0	3.05	3	4	5	6	7	8	9	10	11	12	
45.0	-100.0	3.04	3	4	5	6	7	8	9	10	11	12	
45.0	-90.0	3.04	3	4	5	6	7	8	9	10	11	12	
45.0	-80.0	3.55	3	4	5	6	7	8	9	10	11		
45.0	-70.0	2.00	2	3	4	5	6	7	8	9	10	11	
45.0	-60.0	2.59	2	3	4	5	6	7	8	9	10		
55.0	-140.0	3.18	3	4	5	6	7	8	9	10	11	12	
55.0	-130.0	3.13	3	4	5	6	7	8	9	10	11	12	
55.0	-120.0	3.10	3	4	5	6	7	8	9	10	11	12	
55.0	-110.0	3.08	3	4	5	6	7	8	9	10	11	12	
55.0	-100.0	3.55	3	4	5	6	7	8	9	10	11		
55.0	-90.0	3.55	3	4	5	6	7	8	9	10	11		
55.0	-80.0	3.57	3	4	5	6	7	8	9	10	11		
55.0	-70.0	3.61	3	4	5	6	7	8	9	10	11		
55.0	-60.0	3.65	3	4	5	6	7	8	9	10	11		

Table B-5. The LL-I constellation ($\phi = 75^{\circ}$).

GDOP OVER CONUS

LAT.	LONG.	GDOP	VISIBLE SATELLITES
25.0	-140.0	3.58	3 5 6 7 8 9 10 11 12
25.0	-130.0	3.17	3 4 5 6 7 8 9 10 11 12
25.0	-120.0	3.11	3 4 5 6 7 8 9 10 11 12
25.0	-110.0	3.07	3 4 5 6 7 8 9 10 11 12
25.0	-100.0	3.05	3 4 5 6 7 8 9 10 11 12
25.0	-90.0	3.05	3 4 5 6 7 8 9 10 11 12
25.0	-80.0	9.20	3 4 5 6 7 8 9 10
25.0	-70.0	2.59	2 3 4 5 6 7 8 9 10
25.0	-60.0	2.60	2 3 4 5 6 7 8 9 10
35.0	-140.0	3.19	3 4 5 6 7 8 9 10 11 12
35.0	-130.0	3.13	3 4 5 6 7 8 9 10 11 12
35.0	-120.0	3.08	3 4 5 6 7 8 9 10 11 12
35.0	-110.0	3.05	3 4 5 6 7 8 9 10 11 12
35.0	-100.0	3.03	3 4 5 6 7 8 9 10 11 12
35.0	-90.0	3.52	3 4 5 6 7 8 9 10 11
35.0	-80.0	8.96	3 4 5 6 7 8 9 10
35.0	-70.0	9.11	3 4 5 6 7 8 9 10
35.0	-60.0	2.59	2 3 4 5 6 7 8 9 10
45.0	-140.0	3.64	3 4 5 6 7 8 9 10 11
45.0	-130.0	3.59	3 4 5 6 7 8 9 10 11
45.0	-120.0	3.55	3 4 5 6 7 8 9 10 11
45.0	-110.0	3.52	3 4 5 6 7 8 9 10 11
45.0	-100.0	3.51	3 4 5 6 7 8 9 10 11
45.0	-90.0	3.52	3 4 5 6 7 8 9 10 11
45.0	-80.0	8.81	3 4 5 6 7 8 9 10
45.0	-70.0	8.94	3 4 5 6 7 8 9 10
45.0	-60.0	9.09	3 4 5 6 7 8 9 10
55.0	-140.0	3.65	3 4 5 6 7 8 9 10 11
55.0	-130.0	3.61	3 4 5 6 7 8 9 10 11
55.0	-120.0	3.57	3 4 5 6 7 8 9 10 11
55.0	-110.0	3.55	3 4 5 6 7 8 9 10 11
55.0	-100.0	3.55	3 4 5 6 7 8 9 10 11
55.0	-90.0	3.55	3 4 5 6 7 8 9 10 11
55.0	-80.0	8.75	3 4 5 6 7 8 9 10

Table B-6. The LL-I constellation ($\phi = 60^{\circ}$).

GDOP OVER CONUS

LAT.	LONG.	GDOP	VISIBLE SATELLITES
25.0	-140.0	3.82	5 6 7 8 9 10 11 12
25.0	-130.0	3.52	3 5 6 7 8 9 10 11 12
25.0	-120.0	3.48	3 5 6 7 8 9 10 11 12
25.0	-110.0	3.07	3 4 5 6 7 8 9 10 11
25.0	-100.0	3.53	3 4 5 6 7 8 9 10 11
25.0	-90.0	9.07	3 4 5 6 7 8 9 10
25.0	-80.0	9.20	3 4 5 6 7 8 9 10
25.0	-70.0	9.38	3 4 5 6 7 8 9 10
25.0	-60.0	9.58	3 4 5 6 7 8 9 10
35.0	-140.0	5.58	5 6 7 8 9 10 11
35.0	-130.0	4.15	3 5 6 7 8 9 10 11
35.0	-120.0	3.55	3 4 5 6 7 8 9 10 11
35.0	-110.0	3.52	3 4 5 6 7 8 9 10 11
35.0	-100.0	3.51	3 4 5 6 7 8 9 10 11
35.0	-90.0	8.85	3 4 5 6 7 8 9 10
35.0	-80.0	8.96	3 4 5 6 7 8 9 10
35.0	-70.0	9.11	3 4 5 6 7 8 9 10
35.0	-60.0	9.29	3 4 5 6 7 8 9 10
45.0	-140.0	5.51	5 6 7 8 9 10 11
45.0	-130.0	3.86	4 5 6 7 8 9 10 11
45.0	-120.0	3.55	3 4 5 6 7 8 9 10 11
45.0	-110.0	3.52	3 4 5 6 7 8 9 10 11
45.0	-100.0	8.66	3 4 5 6 7 8 9 10
45.0	-90.0	8.72	3 4 5 6 7 8 9 10
45.0	-80.0	8.81	3 4 5 6 7 8 9 10
45.0	-70.0	8.94	3 4 5 6 7 8 9 10
45.0	-60.0	9.09	3 4 5 6 7 8 9 10
55.0	-140.0	5.47	5 6 7 8 9 10 11
55.0	-130.0	3.87	4 5 6 7 8 9 10 11
55.0	-120.0	3.57	3 4 5 6 7 8 9 10 11
55.0	-110.0	3.55	3 4 5 6 7 8 9 10 11
55.0	-100.0	8.64	3 4 5 6 7 8 9 10
55.0	-90.0	8.68	3 4 5 6 7 8 9 10
55.0	-80.0	8.75	3 4 5 6 7 8 9 10

Table B-7. The HYBRID constellation ($\phi = 90^{o}$).

GDOP OVER CONUS

LAT.	LONG.	GDOP	VISIBLE SATELLITES
25.0	-140.0	1.69	3 4 5 6 7 8 10 11 12 13 14
25.0	-130.0	1.68	3 4 5 6 7 8 10 11 12 13 14
25.0	-120.0	1.67	3 4 5 6 7 8 10 11 12 13 14
25.0	-110.0	1.67	3 4 5 6 7 8 10 11 12 13 14
25.0	-100.0	1.23	3 4 5 6 7 8 10 11 12 13 14 15
25.0	-90.0	1.67	3 4 5 6 7 8 11 12 13 14 15
25.0	-80.0	1.67	3 4 5 6 7 8 11 12 13 14 15
25.0	-70.0	1.68	3 4 5 6 7 8 11 12 13 14 15
25.0	-60.0	1.69	3 4 5 6 7 8 11 12 13 14 15
35.0	-140.0	2.26	3 4 5 6 7 8 10 11 12 13
35.0	-130.0	1.68	3 4 5 6 7 8 10 11 12 13 14
35.0	-120.0	1.67	3 4 5 6 7 8 10 11 12 13 14
35.0	-110.0	1.67	3 4 5 6 7 8 10 11 12 13 14
35.0	-100.0	2.38	3 4 5 6 7 8 11 12 13 14
35.0	-90.0	1.67	3 4 5 6 7 8 11 12 13 14 15
35.0	-80.0	1.67	3 4 5 6 7 8 11 12 13 14 15
35.0	-70.0	1.68	3 4 5 6 7 8 11 12 13 14 15
35.0	-60.0	2.26	3 4 5 6 7 8 12 13 14 15
45.0	-140.0	2.28	3 4 5 6 7 8 10 11 12 13
45.0	-130.0	1.70	3 4 5 6 7 8 10 11 12 13 14
45.0	-120.0	1.69	3 4 5 6 7 8 10 11 12 13 14
45.0	-110.0	1.69	3 4 5 6 7 8 10 11 12 13 14
45.0	-100.0	2.39	3 4 5 6 7 8 11 12 13 14
45.0	-90.0	1.69	3 4 5 6 7 8 11 12 13 14 15
45.0	-80.0	1.69	3 4 5 6 7 8 11 12 13 14 15
45.0	-70.0	1.70	3 4 5 6 7 8 11 12 13 14 15
45.0	-60.0	2.28	3 4 5 6 7 8 12 13 14 15
55.0	-140.0	2.30	3 4 5 6 7 8 10 11 12 13
55.0	-130.0	1.72	3 4 5 6 7 8 10 11 12 13 14
55.0	-120.0	1.71	3 4 5 6 7 8 10 11 12 13 14
55.0	-110.0	1.71	3 4 5 6 7 8 10 11 12 13 14
55.0	-100.0	2.43	3 4 5 6 7 8 11 12 13 14
55.0	-90.0	1.71	3 4 5 6 7 8 11 12 13 14 15
55.0	-80.0	1.71	3 4 5 6 7 8 11 12 13 14 15
55.0	-70.0	1.72	3 4 5 6 7 8 11 12 13 14 15
55.0	-60.0	2.30	3 4 5 6 7 8 12 13 14 15

Table B-8. The HYBRID constellation ($\phi = 75^{o}$).

GDOP OVER CONUS

LAT.	LONG.	GDOP	VISIBLE SATELLITES
25.0	-140.0	2.26	3 4 5 6 7 8 10 11 12 13
25.0	-130.0	2.24	3 4 5 6 7 8 10 11 12 13
25.0	-120.0	1.67	3 4 5 6 7 8 10 11 12 13 14
25.0	-110.0	2.39	3 4 5 6 7 8 11 12 13 14
25.0	-100.0	2.38	3 4 5 6 7 8 11 12 13 14
25.0	-90.0	2.39	3 4 5 6 7 8 11 12 13 14
25.0	-80.0	1.67	3 4 5 6 7 8 11 12 13 14 15
25.0	-70.0	2.24	3 4 5 6 7 8 12 13 14 15
25.0	-60.0	2.26	3 4 5 6 7 8 12 13 14 15
35.0	-140.0	2.26	3 4 5 6 7 8 10 11 12 13
35.0	-130.0	2.25	3 4 5 6 7 8 10 11 12 13
35.0	-120.0	1.67	3 4 5 6 7 8 10 11 12 13 14
35.0	-110.0	2.38	3 4 5 6 7 8 11 12 13 14
35.0	-100.0	2.38	3 4 5 6 7 8 11 12 13 14
35.0	-90.0	2.38	3 4 5 6 7 8 11 12 13 14
35.0	-80.0	1.67	3 4 5 6 7 8 11 12 13 14 15
35.0	-70.0	2.25	3 4 5 6 7 8 12 13 14 15
35.0	-60.0	2.26	3 4 5 6 7 8 12 13 14 15
45.0	-140.0	2.28	3 4 5 6 7 8 10 11 12 13
45.0	-130.0	2.26	3 4 5 6 7 8 10 11 12 13
45.0	-120.0	3.08	3 4 5 6 7 8 11 12 13
45.0	-110.0	2.40	3 4 5 6 7 8 11 12 13 14
45.0	-100.0	2.39	3 4 5 6 7 8 11 12 13 14
45.0	-90.0	2.40	3 4 5 6 7 8 11 12 13 14
45.0	-80.0	3.08	3 4 5 6 7 8 12 13 14
45.0	-70.0	2.26	3 4 5 6 7 8 12 13 14 15
45.0	-60.0	2.28	3 4 5 6 7 8 12 13 14 15
55.0	-140.0	2.87	3 4 5 6 7 8 10 11 12
55.0	-130.0	3.12	3 4 5 6 7 8 11 12 13
55.0	-120.0	3.11	3 4 5 6 7 8 11 12 13
55.0	-110.0	3.10	3 4 5 6 7 8 11 12 13
55.0	-100.0	2.43	3 4 5 6 7 8 11 12 13 14
55.0	-90.0	3.10	3 4 5 6 7 8 12 13 14
55.0	-80.0	3.11	3 4 5 6 7 8 12 13 14
55.0	-70.0	3.12	3 4 5 6 7 8 12 13 14
55.0	-60.0	2.87	3 4 5 6 7 8 13 14 15

Table B-9. The HYBRID constellation ($\phi = 60^{\circ}$).

GDOP OVER CONUS

LAT.	LONG.	GDOP	VISIBLE SATELLITES
25.0	-140.0	3.13	3 4 5 7 8 10 11 12
25.0	-130.0	3.53	3 4 5 7 8 11 12 13
25.0	-120.0	3.51	3 4 5 7 8 11 12 13
25.0	-110.0	3.08	3 4 5 6 7 8 11 12 13
25.0	-100.0	2.38	3 4 5 6 7 8 11 12 13 14
25.0	-90.0	3.08	3 4 5 6 7 8 12 13 14
25.0	-80.0	3.51	3 4 6 7 8 12 13 14
25.0	-70.0	3.53	3 4 6 7 8 12 13 14
25.0	-60.0	3.13	3 4 6 7 8 13 14 15
35.0	-140.0	2.84	3 4 5 6 7 8 10 11 12
35.0	-130.0	3.69	3 4 5 6 7 8 11 12
35.0	-120.0	3.07	3 4 5 6 7 8 11 12 13
35.0	-110.0	3.06	3 4 5 6 7 8 11 12 13
35.0	-100.0	2.38	3 4 5 6 7 8 11 12 13 14
35.0	-90.0	3.06	3 4 5 6 7 8 12 13 14
35.0	-80.0	3.07	3 4 5 6 7 8 12 13 14
35.0	-70.0	3.69	3 4 5 6 7 8 13 14
35.0	-60.0	2.84	3 4 5 6 7 8 13 14 15
45.0	-140.0	3.71	3 4 5 6 7 8 11 12
45.0	-130.0	3.68	3 4 5 6 7 8 11 12
45.0	-120.0	3.67	3 4 5 6 7 8 11 12
45.0	-110.0	3.07	3 4 5 6 7 8 11 12 13
45.0	-100.0	3.65	3 4 5 6 7 8 12 13
45.0	-90.0	3.07	3 4 5 6 7 8 12 13 14
45.0	-80.0	3.67	3 4 5 6 7 8 13 14
45.0	-70.0	3.68	3 4 5 6 7 8 13 14
45.0	-60.0	3.71	3 4 5 6 7 8 13 14
55.0	-140.0	7.04	4 5 6 7 8
55.0	-130.0	6.20	3 4 5 6 7 8
55.0	-120.0	6.16	3 4 5 6 7 8
55.0	-110.0	6.13	3 4 5 6 7 8
55.0	-100.0	6.12	3 4 5 6 7 8
55.0	-90.0	6.13	3 4 5 6 7 8
55.0	-80.0	6.16	3 4 5 6 7 8
55.0	-70.0	6.20	3 4 5 6 7 8
55.0	-60.0	7.04	3 4 5 6 7

Table B-10. The U1 constellation.

GDOP OVER CONUS

LAT.	LONG.	GDOP	VISIBLE SATELLITES
25.0	-140.0	1.74	3 5 6 8 9 10 11 12 14 15
25.0	-130.0	1.74	3 5 6 8 9 10 11 12 14 15
25.0	-120.0	1.48	2 3 5 6 8 9 10 11 12 14 15
25.0	-110.0	1.48	2 3 5 6 8 9 10 11 12 14 15
25.0	-100.0	1.25	2 3 5 6 8 9 10 11 12 13 14 15
25.0	-90.0	1.48	2 3 5 6 8 9 10 11 12 13 14
25.0	-80.0	1.48	2 3 5 6 8 9 10 11 12 13 14
25.0	-70.0	1.74	2 3 5 8 9 10 11 12 13 14
25.0	-60.0	1.74	2 3 5 8 9 10 11 12 13 14
35.0	-140.0	1.35	3 4 5 6 8 9 10 11 12 14 15
35.0	-130.0	1.35	3 4 5 6 8 9 10 11 12 14 15
35.0	-120.0	1.35	3 4 5 6 8 9 10 11 12 14 15
35.0	-110.0	1.16	2 3 4 5 6 8 9 10 11 12 14 15
35.0	-100.0	1.83	2 3 5 6 8 9 10 11 12 14
35.0	-90.0	1.16	2 3 4 5 6 8 9 10 11 12 13 14
35.0	-80.0	1.35	2 3 4 5 8 9 10 11 12 13 14
35.0	-70.0	1.35	2 3 4 5 8 9 10 11 12 13 14
35.0	-60.0	1.35	2 3 4 5 8 9 10 11 12 13 14
45.0	-140.0	1.35	3 4 5 6 8 9 10 11 12 14 15
45.0	-130.0	1.35	3 4 5 6 8 9 10 11 12 14 15
45.0	-120.0	1.35	3 4 5 6 8 9 10 11 12 14 15
45.0	-110.0	1.35	3 4 5 6 8 9 10 11 12 14 15
45.0	-100.0	1.79	3 4 5 8 9 10 11 12 14
45.0	-90.0	1.35	2 3 4 5 8 9 10 11 12 13 14
45.0	-80.0	1.35	2 3 4 5 8 9 10 11 12 13 14
45.0	-70.0	1.35	2 3 4 5 8 9 10 11 12 13 14
45.0	-60.0	1.35	2 3 4 5 8 9 10 11 12 13 14
55.0	-140.0	1.47	3 4 5 8 9 10 11 12 14 15
55.0	-130.0	1.47	3 4 5 8 9 10 11 12 14 15
55.0	-120.0	1.47	3 4 5 8 9 10 11 12 14 15
55.0	-110.0	1.47	3 4 5 8 9 10 11 12 14 15
55.0	-100.0	1.79	3 4 5 8 9 10 11 12 14
55.0	-90.0	1.47	3 4 5 8 9 10 11 12 13 14
55.0	-80.0	1.47	3 4 5 8 9 10 11 12 13 14
55.0	-70.0	1.47	3 4 5 8 9 10 11 12 13 14
55.0	-60.0	1.47	3 4 5 8 9 10 11 12 13 14

Table B-11. The U2 constellation.

GDOP OVER CONUS

LAT.	LONG.	GDOP	VISIBLE SATELLITES
25.0	-140.0	1.49	3 4 5 6 9 10 11 12 13 14 15
25.0	-130.0	1.48	3 4 5 6 9 10 11 12 13 14 15
25.0	-120.0	1.47	3 4 5 6 9 10 11 12 13 14 15
25.0	-110.0	1.47	3 4 5 6 9 10 11 12 13 14 15
25.0	-100.0	1.15	2 3 4 5 6 8 9 10 11 12 13 14 15
25.0	-90.0	1.47	2 3 4 5 8 9 10 11 13 14 15
25.0	-80.0	1.47	2 3 4 5 8 9 10 11 13 14 15
25.0	-70.0	1.48	2 3 4 5 8 9 10 11 13 14 15
25.0	-60.0	1.49	2 3 4 5 8 9 10 11 13 14 15
35.0	-140.0	1.50	3 4 5 6 7 8 9 10 11 12 14 15
35.0	-130.0	1.30	3 4 5 6 7 8 9 10 11 12 13 14 15
35.0	-120.0	1.30	3 4 5 6 7 8 9 10 11 12 13 14 15
35.0	-110.0	1.30	3 4 5 6 7 8 9 10 11 12 13 14 15
35.0	-100.0	1.10	2 3 4 5 6 7 8 9 10 11 12 13 14 15
35.0	-90.0	1.30	2 3 4 5 6 7 8 9 10 11 13 14 15
35.0	-80.0	1.30	2 3 4 5 6 7 8 9 10 11 13 14 15
35.0	-70.0	1.30	2 3 4 5 6 7 8 9 10 11 13 14 15
35.0	-60.0	1.50	2 3 4 5 6 7 8 9 10 11 13 14
45.0	-140.0	1.49	3 4 5 6 7 8 9 10 11 12 14 15
45.0	-130.0	1.30	3 4 5 6 7 8 9 10 11 12 13 14 15
45.0	-120.0	1.30	3 4 5 6 7 8 9 10 11 12 13 14 15
45.0	-110.0	1.29	3 4 5 6 7 8 9 10 11 12 13 14 15
45.0	-100.0	1.55	3 4 5 6 7 8 9 10 11 13 14 15
45.0	-90.0	1.29	2 3 4 5 6 7 8 9 10 11 13 14 15
45.0	-80.0	1.30	2 3 4 5 6 7 8 9 10 11 13 14 15
45.0	-70.0	1.30	2 3 4 5 6 7 8 9 10 11 13 14 15
45.0	-60.0	1.49	2 3 4 5 6 7 8 9 10 11 13 14
55.0	-140.0	1.49	3 4 5 6 7 8 9 10 11 12 14 15
55.0	-130.0	1.30	3 4 5 6 7 8 9 10 11 12 13 14 15
55.0	-120.0	1.30	3 4 5 6 7 8 9 10 11 12 13 14 15
55.0	-110.0	1.30	3 4 5 6 7 8 9 10 11 12 13 14 15
55.0	-100.0	1.56	3 4 5 6 7 8 9 10 11 13 14 15
55.0	-90.0	1.30	2 3 4 5 6 7 8 9 10 11 13 14 15
55.0	-80.0	1.30	2 3 4 5 6 7 8 9 10 11 13 14 15
55.0	-70.0	1.30	2 3 4 5 6 7 8 9 10 11 13 14 15
55.0	-60.0	1.49	2 3 4 5 6 7 8 9 10 11 13 14

Table B-12. The U3 constellation.

GDOP OVER CONUS

LAT.	LONG.	GDOP	VISIBLE SATELLITES
25.0	-140.0	1.37	3 4 5 6 7 10 11 12 13 14 15
25.0	-130.0	1.37	3 4 5 6 7 10 11 12 13 14 15
25.0	-120.0	1.52	3 4 5 6 10 11 12 13 14 15
25.0	-110.0	1.37	3 4 5 6 9 10 11 12 13 14 15
25.0	-100.0	1.16	2 3 4 5 6 9 10 11 12 13 14 15
25.0	-90.0	1.37	2 3 4 5 6 9 10 11 12 14 15
25.0	-80.0	1.52	2 3 4 5 9 10 11 12 14 15
25.0	-70.0	1.37	2 3 4 5 8 9 10 11 12 14 15
25.0	-60.0	1.37	2 3 4 5 8 9 10 11 12 14 15
35.0	-140.0	1.44	3 4 5 6 7 8 9 10 11 12 13 15
35.0	-130.0	1.24	3 4 5 6 7 8 9 10 11 12 13 14 15
35.0	-120.0	1.24	3 4 5 6 7 8 9 10 11 12 13 14 15
35.0	-110.0	1.24	3 4 5 6 7 8 9 10 11 12 13 14 15
35.0	-100.0	1.57	3 4 5 6 7 8 9 10 11 12 14 15
35.0	-90.0	1.24	2 3 4 5 6 7 8 9 10 11 12 14 15
35.0	-80.0	1.24	2 3 4 5 6 7 8 9 10 11 12 14 15
35.0	-70.0	1.24	2 3 4 5 6 7 8 9 10 11 12 14 15
35.0	-60.0	1.44	2 3 4 5 6 7 8 9 10 11 12 14
45.0	-140.0	1.43	3 4 5 6 7 8 9 10 11 12 13 15
45.0	-130.0	1.24	3 4 5 6 7 8 9 10 11 12 13 14 15
45.0	-120.0	1.24	3 4 5 6 7 8 9 10 11 12 13 14 15
45.0	-110.0	1.24	3 4 5 6 7 8 9 10 11 12 13 14 15
45.0	-100.0	1.57	3 4 5 6 7 8 9 10 11 12 14 15
45.0	-90.0	1.24	2 3 4 5 6 7 8 9 10 11 12 14 15
45.0	-80.0	1.24	2 3 4 5 6 7 8 9 10 11 12 14 15
45.0	-70.0	1.24	2 3 4 5 6 7 8 9 10 11 12 14 15
45.0	-60.0	1.43	2 3 4 5 6 7 8 9 10 11 12 14
55.0	-140.0	1.43	3 4 5 6 7 8 9 10 11 12 13 15
55.0	-130.0	1.24	3 4 5 6 7 8 9 10 11 12 13 14 15
55.0	-120.0	1.58	3 4 5 6 7 8 9 10 11 12 14 15
55.0	-110.0	1.57	3 4 5 6 7 8 9 10 11 12 14 15
55.0	-100.0	1.57	3 4 5 6 7 8 9 10 11 12 14 15
55.0	-90.0	1.57	3 4 5 6 7 8 9 10 11 12 14 15
55.0	-80.0	1.58	3 4 5 6 7 8 9 10 11 12 14 15
55.0	-70.0	1.24	2 3 4 5 6 7 8 9 10 11 12 14 15
55.0	-60.0	1.43	2 3 4 5 6 7 8 9 10 11 12 14

Table B-13. The U4 constellation.

GDOP OVER CONUS

LAT.	LONG.	GDOP	VISIBLE SATELLITES
25.0	-140.0	1.60	3 4 5 8 9 10 12 13 14 15
25.0	-130.0	1.59	3 4 5 8 9 10 12 13 14 15
25.0	-120.0	1.37	2 3 4 5 8 9 10 12 13 14 15
25.0	-110.0	1.27	2 3 4 5 7 8 9 10 12 13 14 15
25.0	-100.0	1.13	2 3 4 5 7 8 9 10 11 12 13 14 15
25.0	-90.0	1.27	2 3 4 5 7 8 9 10 11 12 13 14
25.0	-80.0	1.37	2 3 4 7 8 9 10 11 12 13 14
25.0	-70.0	1.59	2 3 4 7 8 9 11 12 13 14
25.0	-60.0	1.60	2 3 4 7 8 9 11 12 13 14
35.0	-140.0	1.65	3 4 5 6 7 8 9 10 13 14 15
35.0	-130.0	1.36	3 4 5 6 7 8 9 10 12 13 14 15
35.0	-120.0	1.21	2 3 4 5 6 7 8 9 10 12 13 14 15
35.0	-110.0	1.20	2 3 4 5 6 7 8 9 10 12 13 14 15
35.0	-100.0	1.34	2 3 4 5 6 7 8 9 10 12 13 14
35.0	-90.0	1.20	2 3 4 5 6 7 8 9 10 11 12 13 14
35.0	-80.0	1.21	2 3 4 5 6 7 8 9 10 11 12 13 14
35.0	-70.0	1.36	2 3 4 5 6 7 8 9 11 12 13 14
35.0	-60.0	1.65	2 3 4 5 6 7 8 9 11 12 13
45.0	-140.0	1.63	3 4 5 6 7 8 9 10 13 14 15
45.0	-130.0	1.35	3 4 5 6 7 8 9 10 12 13 14 15
45.0	-120.0	1.20	2 3 4 5 6 7 8 9 10 12 13 14 15
45.0	-110.0	1.20	2 3 4 5 6 7 8 9 10 12 13 14 15
45.0	-100.0	1.33	2 3 4 5 6 7 8 9 10 12 13 14
45.0	-90.0	1.20	2 3 4 5 6 7 8 9 10 11 12 13 14
45.0	-80.0	1.20	2 3 4 5 6 7 8 9 10 11 12 13 14
45.0	-70.0	1.35	2 3 4 5 6 7 8 9 11 12 13 14
45.0	-60.0	1.63	2 3 4 5 6 7 8 9 11 12 13
55.0	-140.0	1.63	3 4 5 6 7 8 9 10 13 14 15
55.0	-130.0	1.36	3 4 5 6 7 8 9 10 12 13 14 15
55.0	-120.0	1.35	3 4 5 6 7 8 9 10 12 13 14 15
55.0	-110.0	1.20	2 3 4 5 6 7 8 9 10 12 13 14 15
55.0	-100.0	1.34	2 3 4 5 6 7 8 9 10 12 13 14
55.0	-90.0	1.20	2 3 4 5 6 7 8 9 10 11 12 13 14
55.0	-80.0	1.35	2 3 4 5 6 7 8 9 11 12 13 14
55.0	-70.0	1.36	2 3 4 5 6 7 8 9 11 12 13 14
55.0	-60.0	1.63	2 3 4 5 6 7 8 9 11 12 13

Table B-14. The U5 constellation.

GDOP OVER CONUS

LAT.	LONG.	GDOP	VISIBLE SATELLITES
25.0	-140.0	1.51	3 4 5 6 9 10 11 12 13 14 15
25.0	-130.0	1.50	3 4 5 6 9 10 11 12 13 14 15
25.0	-120.0	1.50	3 4 5 6 9 10 11 12 13 14 15
25.0	-110.0	1.50	3 4 5 6 9 10 11 12 13 14 15
25.0	-100.0	1.11	2 3 4 5 6 8 9 10 11 12 13 14 15
25.0	-90.0	1.50	2 3 4 5 8 9 10 11 13 14 15
25.0	-80.0	1.50	2 3 4 5 8 9 10 11 13 14 15
25.0	-70.0	1.50	2 3 4 5 8 9 10 11 13 14 15
25.0	-60.0	1.51	2 3 4 5 8 9 10 11 13 14 15
35.0	-140.0	1.30	3 4 5 6 7 8 9 10 11 12 13 14 15
35.0	-130.0	1.29	3 4 5 6 7 8 9 10 11 12 13 14 15
35.0	-120.0	1.29	3 4 5 6 7 8 9 10 11 12 13 14 15
35.0	-110.0	1.29	3 4 5 6 7 8 9 10 11 12 13 14 15
35.0	-100.0	1.07	2 3 4 5 6 7 8 9 10 11 12 13 14 15
35.0	-90.0	1.29	2 3 4 5 6 7 8 9 10 11 13 14 15
35.0	-80.0	1.29	2 3 4 5 6 7 8 9 10 11 13 14 15
35.0	-70.0	1.29	2 3 4 5 6 7 8 9 10 11 13 14 15
35.0	-60.0	1.30	2 3 4 5 6 7 8 9 10 11 13 14 15
45.0	-140.0	1.30	3 4 5 6 7 8 9 10 11 12 13 14 15
45.0	-130.0	1.29	3 4 5 6 7 8 9 10 11 12 13 14 15
45.0	-120.0	1.29	3 4 5 6 7 8 9 10 11 12 13 14 15
45.0	-110.0	1.29	3 4 5 6 7 8 9 10 11 12 13 14 15
45.0	-100.0	1.50	3 4 5 6 7 8 9 10 11 13 14 15
45.0	-90.0	1.29	2 3 4 5 6 7 8 9 10 11 13 14 15
45.0	-80.0	1.29	2 3 4 5 6 7 8 9 10 11 13 14 15
45.0	-70.0	1.29	2 3 4 5 6 7 8 9 10 11 13 14 15
45.0	-60.0	1.30	2 3 4 5 6 7 8 9 10 11 13 14 15
55.0	-140.0	1.56	3 4 5 6 7 8 9 10 11 12 14 15
55.0	-130.0	1.56	3 4 5 6 7 8 9 10 11 12 14 15
55.0	-120.0	1.57	3 4 5 6 7 8 9 10 11 12 14 15
55.0	-110.0	1.30	3 4 5 6 7 8 9 10 11 12 13 14 15
55.0	-100.0	1.51	3 4 5 6 7 8 9 10 11 13 14 15
55.0	-90.0	1.30	2 3 4 5 6 7 8 9 10 11 13 14 15
55.0	-80.0	1.57	2 3 4 5 6 7 8 9 10 11 14 15
55.0	-70.0	1.56	2 3 4 5 6 7 8 9 10 11 14 15
55.0	-60.0	1.56	2 3 4 5 6 7 8 9 10 11 14 15

Table B-15. The U6 constellation.

GDOP OVER CONUS

LAT.	LONG.	GDOP	VISIBLE SATELLITES
25.0	-140.0	1.72	2 3 5 6 7 8 9 13 14 15
25.0	-130.0	1.50	2 3 5 6 7 8 9 11 12 13 14 15
25.0	-120.0	1.49	2 3 5 6 7 8 9 11 12 13 14 15
25.0	-110.0	1.35	2 3 5 6 7 8 9 10 11 12 13 14 15
25.0	-100.0	1.34	2 3 5 6 7 8 9 10 11 12 13 14 15
25.0	-90.0	1.35	2 3 5 6 7 8 9 10 11 12 13 14 15
25.0	-80.0	1.49	2 3 5 6 7 8 9 10 11 12 14 15
25.0	-70.0	1.50	2 3 5 6 7 8 9 10 11 12 14 15
25.0	-60.0	1.72	2 3 5 6 7 8 9 10 11 12
35.0	-140.0	1.47	2 3 4 5 6 7 8 9 13 14 15
35.0	-130.0	1.31	2 3 4 5 6 7 8 9 11 12 13 14 15
35.0	-120.0	1.30	2 3 4 5 6 7 8 9 11 12 13 14 15
35.0	-110.0	1.17	2 3 4 5 6 7 8 9 10 11 12 13 14 15
35.0	-100.0	1.17	2 3 4 5 6 7 8 9 10 11 12 13 14 15
35.0	-90.0	1.17	2 3 4 5 6 7 8 9 10 11 12 13 14 15
35.0	-80.0	1.30	2 3 4 5 6 7 8 9 10 11 12 14 15
35.0	-70.0	1.31	2 3 4 5 6 7 8 9 10 11 12 14 15
35.0	-60.0	1.47	2 3 4 5 6 7 8 9 10 11 12
45.0	-140.0	1.48	2 3 4 5 6 7 8 9 13 14 15
45.0	-130.0	1.32	2 3 4 5 6 7 8 9 11 12 13 14 15
45.0	-120.0	1.31	2 3 4 5 6 7 8 9 11 12 13 14 15
45.0	-110.0	1.31	2 3 4 5 6 7 8 9 11 12 13 14 15
45.0	-100.0	1.18	2 3 4 5 6 7 8 9 10 11 12 13 14 15
45.0	-90.0	1.31	2 3 4 5 6 7 8 9 10 11 12 14 15
45.0	-80.0	1.31	2 3 4 5 6 7 8 9 10 11 12 14 15
45.0	-70.0	1.32	2 3 4 5 6 7 8 9 10 11 12 14 15
45.0	-60.0	1.48	2 3 4 5 6 7 8 9 10 11 12
55.0	-140.0	1.55	2 3 4 5 6 8 9 11 13 14 15
55.0	-130.0	1.45	2 3 4 5 6 8 9 11 12 13 14 15
55.0	-120.0	1.44	2 3 4 5 6 8 9 11 12 13 14 15
55.0	-110.0	1.52	2 3 4 5 6 7 8 9 11 12 14 15
55.0	-100.0	1.52	2 3 4 5 6 7 8 9 11 12 14 15
55.0	-90.0	1.52	2 3 4 5 6 7 8 9 11 12 14 15
55.0	-80.0	1.44	2 3 4 5 6 8 9 10 11 12 14 15
55.0	-70.0	1.45	2 3 4 5 6 8 9 10 11 12 14 15
55.0	-60.0	1.55	2 3 4 5 6 8 9 10 11 12 15

Table B-16. The U7 constellation.

GDOP OVER CONUS

LAT.	LONG	GDOP	VISIBLE SATELLITES
25.0	-140.0	1.71	3 4 8 9 11 12 13 14 15
25.0	-130.0	1.37	3 4 6 8 9 11 12 13 14 15
25.0	-120.0	1.30	3 4 6 8 10 11 12 13 14 15
25.0	-110.0	1.48	3 4 6 8 10 11 13 14 15
25.0	-100.0	1.48	3 4 6 8 10 11 13 14 15
25.0	-90.0	1.48	3 4 6 8 10 11 13 14 15
25.0	-80.0	1.30	2 3 4 6 8 10 11 13 14 15
25.0	-70.0	1.37	2 3 5 6 8 10 11 13 14 15
25.0	-60.0	1.71	2 3 5 6 10 11 13 14 15
35.0	-140.0	1.25	3 4 6 8 9 10 11 12 13 14 15
35.0	-130.0	1.24	3 4 6 8 9 10 11 12 13 14 15
35.0	-120.0	1.24	3 4 6 8 9 10 11 12 13 14 15
35.0	-110.0	1.34	3 4 6 8 9 10 11 13 14 15
35.0	-100.0	1.48	3 4 6 8 10 11 13 14 15
35.0	-90.0	1.34	3 4 5 6 8 10 11 13 14 15
35.0	-80.0	1.24	2 3 4 5 6 8 10 11 13 14 15
35.0	-70.0	1.24	2 3 4 5 6 8 10 11 13 14 15
35.0	-60.0	1.25	2 3 4 5 6 8 10 11 13 14 15
45.0	-140.0	1.52	3 4 6 8 9 10 11 12 14 15
45.0	-130.0	1.52	3 4 6 8 9 10 11 12 14 15
45.0	-120.0	1.51	3 4 6 8 9 10 11 12 14 15
45.0	-110.0	1.13	3 4 5 6 8 9 10 11 12 13 14 15
45.0	-100.0	1.25	3 4 5 6 8 9 10 11 13 14 15
45.0	-90.0	1.13	2 3 4 5 6 8 9 10 11 13 14 15
45.0	-80.0	1.51	2 3 4 5 6 8 10 11 14 15
45.0	-70.0	1.52	2 3 4 5 6 8 10 11 14 15
45.0	-60.0	1.52	2 3 4 5 6 8 10 11 14 15
55.0	-140.0	1.40	3 4 5 6 8 9 10 11 12 14 15
55.0	-130.0	1.39	3 4 5 6 8 9 10 11 12 14 15
55.0	-120.0	1.39	3 4 5 6 8 9 10 11 12 14 15
55.0	-110.0	1.39	3 4 5 6 8 9 10 11 12 14 15
55.0	-100.0	1.63	3 4 5 6 8 9 10 11 14 15
55.0	-90.0	1.39	2 3 4 5 6 8 9 10 11 14 15
55.0	-80.0	1.39	2 3 4 5 6 8 9 10 11 14 15
55.0	-70.0	1.39	2 3 4 5 6 8 9 10 11 14 15
55.0	-60.0	1.40	2 3 4 5 6 8 9 10 11 14 15

Table B-17. The C15-90 constellation.

GDOP CVER CONUS

LAT.	LONG.	GDOP	VISIBLE SATELLITES
25.0	-140.0	1.49	3 4 5 6 9 10 11 12 13 14 15
25.0	-130.0	1.48	3 4 5 6 9 10 11 12 13 14 15
25.0	-120.0	1.47	3 4 5 6 9 10 11 12 13 14 15
25.0	-110.0	1.47	3 4 5 6 9 10 11 12 13 14 15
25.0	-100.0	1.15	2 3 4 5 6 8 9 10 11 12 13 14 15
25.0	-90.0	1.47	2 3 4 5 8 9 10 11 13 14 15
25.0	-80.0	1.47	2 3 4 5 8 9 10 11 13 14 15
25.0	-70.0	1.48	2 3 4 5 8 9 10 11 13 14 15
25.0	-60.0	1.49	2 3 4 5 8 9 10 11 13 14 15
35.0	-140.0	1.50	3 4 5 6 7 8 9 10 11 12 14 15
35.0	-130.0	1.30	3 4 5 6 7 8 9 10 11 12 13 14 15
35.0	-120.0	1.30	3 4 5 6 7 8 9 10 11 12 13 14 15
35.0	-110.0	1.30	3 4 5 6 7 8 9 10 11 12 13 14 15
35.0	-100.0	1.10	2 3 4 5 6 7 8 9 10 11 12 13 14 15
35.0	-90.0	1.30	2 3 4 5 6 7 8 9 10 11 13 14 15
35.0	-80.0	1.30	2 3 4 5 6 7 8 9 10 11 13 14 15
35.0	-70.0	1.30	2 3 4 5 6 7 8 9 10 11 13 14 15
35.0	-60.0	1.50	2 3 4 5 6 7 8 9 10 11 13 14
45.0	-140.0	1.49	3 4 5 6 7 8 9 10 11 12 14 15
45.0	-130.0	1.30	3 4 5 6 7 8 9 10 11 12 13 14 15
45.0	-120.0	1.30	3 4 5 6 7 8 9 10 11 12 13 14 15
45.0	-110.0	1.29	3 4 5 6 7 8 9 10 11 12 13 14 15
45.0	-100.0	1.55	3 4 5 6 7 8 9 10 11 13 14 15
45.0	-90.0	1.29	2 3 4 5 6 7 8 9 10 11 13 14 15
45.0	-80.0	1.30	2 3 4 5 6 7 8 9 10 11 13 14 15
45.0	-70.0	1.30	2 3 4 5 6 7 8 9 10 11 13 14 15
45.0	-60.0	1.49	2 3 4 5 6 7 8 9 10 11 13 14
55.0	-140.0	1.49	3 4 5 6 7 8 9 10 11 12 14 15
55.0	-130.0	1.30	3 4 5 6 7 8 9 10 11 12 13 14 15
55.0	-120.0	1.30	3 4 5 6 7 8 9 10 11 12 13 14 15
55.0	-110.0	1.30	3 4 5 6 7 8 9 10 11 12 13 14 15
55.0	-100.0	1.56	3 4 5 6 7 8 9 10 11 13 14 15
55.0	-90.0	1.30	2 3 4 5 6 7 8 9 10 11 13 14 15
55.0	-80.0	1.30	2 3 4 5 6 7 8 9 10 11 13 14 15
55.0	-70.0	1.30	2 3 4 5 6 7 8 9 10 11 13 14 15
55.0	-60.0	1.49	2 3 4 5 6 7 8 9 10 11 13 14

Table B-18. The C15-75 constellation

GDOP OVER CONUS

LAT.	LONG	GDOP	VISIBLE SATELLITES
25.0	-140.0	2.29	3 4 5 6 10 11 12 14 15
25.0	-130.0	1.97	3 4 5 6 9 10 11 12 14 15
25.0	-120.0	1.58	3 4 5 6 9 10 11 12 13 14 15
25.0	-110.0	1.76	3 4 5 9 10 11 12 13 14 15
25.0	-100.0	2.30	3 4 5 9 10 11 13 14 15
25.0	-90.0	1.76	2 3 4 5 9 10 11 13 14 15
25.0	-80.0	1.58	2 3 4 5 8 9 10 11 13 14 15
25.0	-70.0	1.97	2 3 4 5 8 9 10 11 13 14
25.0	-60.0	2.29	2 3 4 8 9 10 11 13 14
35.0	-140.0	1.77	3 4 5 6 7 9 10 11 12 14 15
35.0	-130.0	1.77	3 4 5 6 7 9 10 11 12 14 15
35.0	-120.0	1.38	3 4 5 6 7 8 9 10 11 12 13 14 15
35.0	-110.0	1.76	3 4 5 6 8 9 10 11 13 14 15
35.0	-100.0	1.76	3 4 5 6 8 9 10 11 13 14 15
35.0	-90.0	1.76	3 4 5 6 8 9 10 11 13 14 15
35.0	-80.0	1.38	2 3 4 5 6 7 8 9 10 11 13 14 15
35.0	-70.0	1.77	2 3 4 5 7 8 9 10 11 13 14
35.0	-60.0	1.77	2 3 4 5 7 8 9 10 11 13 14
45.0	-140.0	1.65	3 4 5 6 7 8 9 10 11 12 14 15
45.0	-130.0	1.64	3 4 5 6 7 8 9 10 11 12 14 15
45.0	-120.0	1.96	3 4 5 6 7 8 9 10 11 14 15
45.0	-110.0	1.65	3 4 5 6 7 8 9 10 11 13 14 15
45.0	-100.0	1.65	3 4 5 6 7 8 9 10 11 13 14 15
45.0	-90.0	1.65	3 4 5 6 7 8 9 10 11 13 14 15
45.0	-80.0	1.96	3 4 5 6 7 8 9 10 11 13 14
45.0	-70.0	1.64	2 3 4 5 6 7 8 9 10 11 13 14
45.0	-60.0	1.65	2 3 4 5 6 7 8 9 10 11 13 14
55.0	-140.0	1.97	3 4 5 6 7 8 9 10 11 14 15
55.0	-130.0	1.96	3 4 5 6 7 8 9 10 11 14 15
55.0	-120.0	1.96	3 4 5 6 7 8 9 10 11 14 15
55.0	-110.0	1.96	3 4 5 6 7 8 9 10 11 14 15
55.0	-100.0	1.65	3 4 5 6 7 8 9 10 11 13 14 15
55.0	-90.0	1.96	3 4 5 6 7 8 9 10 11 13 14
55.0	-80.0	1.96	3 4 5 6 7 8 9 10 11 13 14
55.0	-70.0	1.96	3 4 5 6 7 8 9 10 11 13 14
55.0	-60.0	1.97	3 4 5 6 7 8 9 10 11 13 14

Table B-19. The C15-60 constellation.

GDOP OVER CONUS

LAT.	LONG.	GDOP	VISIBLE SATELLITES
25.0	-140.0	3.40	4 5 10 11 12 14 15
25.0	-130.0	2.78	3 4 5 10 11 12 14 15
25.0	-120.0	4.50	3 4 5 10 11 14 15
25.0	-110.0	2.99	3 4 5 9 10 11 13 14 15
25.0	-100.0	2.99	3 4 5 9 10 11 13 14 15
25.0	-90.0	2.99	3 4 5 9 10 11 13 14 15
25.0	-80.0	4.50	3 4 9 10 11 13 14
25.0	-70.0	2.78	2 3 4 9 10 11 13 14
25.0	-60.0	3.40	2 3 4 9 10 13 14
35.0	-140.0	2.80	4 5 6 10 11 12 14 15
35.0	-130.0	2.70	3 4 5 6 9 10 11 14 15
35.0	-120.0	2.69	3 4 5 6 9 10 11 14 15
35.0	-110.0	2.96	3 4 5 9 10 11 13 14 15
35.0	-100.0	2.96	3 4 5 9 10 11 13 14 15
35.0	-90.0	2.96	3 4 5 9 10 11 13 14 15
35.0	-80.0	2.69	3 4 5 8 9 10 11 13 14
35.0	-70.0	2.70	3 4 5 8 9 10 11 13 14
35.0	-60.0	2.80	2 3 4 8 9 10 13 14
45.0	-140.0	2.85	4 5 6 7 9 10 11 15
45.0	-130.0	2.18	3 4 5 6 7 8 9 10 11 14 15
45.0	-120.0	2.17	3 4 5 6 7 8 9 10 11 14 15
45.0	-110.0	2.17	3 4 5 6 7 8 9 10 11 14 15
45.0	-100.0	1.91	3 4 5 6 7 8 9 10 11 13 14 15
45.0	-90.0	2.17	3 4 5 6 7 8 9 10 11 13 14
45.0	-80.0	2.17	3 4 5 6 7 8 9 10 11 13 14
45.0	-70.0	2.18	3 4 5 6 7 8 9 10 11 13 14
45.0	-60.0	2.85	3 4 5 7 8 9 10 13
55.0	-140.0	5.04	4 5 6 7 8 9 10 11
55.0	-130.0	3.95	3 4 5 6 7 8 9 10 11
55.0	-120.0	3.93	3 4 5 6 7 8 9 10 11
55.0	-110.0	3.92	3 4 5 6 7 8 9 10 11
55.0	-100.0	3.91	3 4 5 6 7 8 9 10 11
55.0	-90.0	3.92	3 4 5 6 7 8 9 10 11
55.0	-80.0	3.93	3 4 5 6 7 8 9 10 11
55.0	-70.0	3.95	3 4 5 6 7 8 9 10 11
55.0	-60.0	5.04	3 4 5 6 7 8 9 10

Table B-20. The C10-90 constellation.

GDOP OVER CONUS

LAT.	LONG	GDOP	VISIBLE SATELLITES
25.0	-140.0	1.75	2 3 4 5 6 7 8 10
25.0	-130.0	1.75	2 3 4 5 6 7 8 10
25.0	-120.0	1.75	2 3 4 5 6 7 8 10
25.0	-110.0	1.90	2 3 4 6 7 8 10
25.0	-100.0	1.53	2 3 4 6 7 8 9 10
25.0	-90.0	1.90	2 3 4 6 7 8 9
25.0	-80.0	1.75	2 3 4 5 6 7 8 9
25.0	-70.0	1.75	2 3 4 5 6 7 8 9
25.0	-60.0	1.75	2 3 4 5 6 7 8 9
35.0	-140.0	1.73	2 3 4 5 6 7 8 10
35.0	-130.0	1.73	2 3 4 5 6 7 8 10
35.0	-120.0	1.73	2 3 4 5 6 7 8 10
35.0	-110.0	1.73	2 3 4 5 6 7 8 10
35.0	-100.0	1.38	2 3 4 5 6 7 8 9 10
35.0	-90.0	1.73	2 3 4 5 6 7 8 9
35.0	-80.0	1.73	2 3 4 5 6 7 8 9
35.0	-70.0	1.73	2 3 4 5 6 7 8 9
35.0	-60.0	1.73	2 3 4 5 6 7 8 9
45.0	-140.0	1.72	2 3 4 5 6 7 8 10
45.0	-130.0	1.72	2 3 4 5 6 7 8 10
45.0	-120.0	1.72	2 3 4 5 6 7 8 10
45.0	-110.0	1.72	2 3 4 5 6 7 8 10
45.0	-100.0	1.38	2 3 4 5 6 7 8 9 10
45.0	-90.0	1.72	2 3 4 5 6 7 8 9
45.0	-80.0	1.72	2 3 4 5 6 7 8 9
45.0	-70.0	1.72	2 3 4 5 6 7 8 9
45.0	-60.0	1.72	2 3 4 5 6 7 8 9
55.0	-140.0	1.72	2 3 4 5 6 7 8 10
55.0	-130.0	1.72	2 3 4 5 6 7 8 10
55.0	-120.0	1.72	2 3 4 5 6 7 8 10
55.0	-110.0	1.72	2 3 4 5 6 7 8 10
55.0	-100.0	2.23	2 3 4 5 6 7 8
55.0	-90.0	1.72	2 3 4 5 6 7 8 9
55.0	-80.0	1.72	2 3 4 5 6 7 8 9
55.0	-70.0	1.72	2 3 4 5 6 7 8 9
55.0	-60.0	1.72	2 3 4 5 6 7 8 9

Table B-21. The C10-75 constellation.

GDOP OVER CONUS

LAT.	LONG.	GDOP	VISIBLE SATELLITES
25.0	-140.0	3.14	3 4 6 7 9 10
25.0	-130.0	3.13	3 4 6 7 9 10
25.0	-120.0	2.03	2 3 4 6 7 9 10
25.0	-110.0	2.03	2 3 4 6 7 9 10
25.0	-100.0	4.66	2 3 6 7 9
25.0	-90.0	2.03	2 3 5 6 7 8 9
25.0	-80.0	2.03	2 3 5 6 7 8 9
25.0	-70.0	3.13	2 3 5 6 8 9
25.0	-60.0	3.14	2 3 5 6 8 9
35.0	-140.0	2.42	3 4 5 6 7 9 10
35.0	-130.0	2.41	3 4 5 6 7 9 10
35.0	-120.0	1.82	2 3 4 5 6 7 9 10
35.0	-110.0	1.82	2 3 4 5 6 7 9 10
35.0	-100.0	2.21	2 3 4 5 6 7 9
35.0	-90.0	1.82	2 3 4 5 6 7 8 9
35.0	-80.0	1.82	2 3 4 5 6 7 8 9
35.0	-70.0	2.41	2 3 4 5 6 8 9
35.0	-60.0	2.42	2 3 4 5 6 8 9
45.0	-140.0	2.40	3 4 5 6 7 9 10
45.0	-130.0	2.39	3 4 5 6 7 9 10
45.0	-120.0	2.39	3 4 5 6 7 9 10
45.0	-110.0	2.20	2 3 4 5 6 7 9
45.0	-100.0	2.20	2 3 4 5 6 7 9
45.0	-90.0	2.20	2 3 4 5 6 7 9
45.0	-80.0	2.39	2 3 4 5 6 8 9
45.0	-70.0	2.39	2 3 4 5 6 8 9
45.0	-60.0	2.40	2 3 4 5 6 8 9
55.0	-140.0	2.40	3 4 5 6 7 9 10
55.0	-130.0	2.39	3 4 5 6 7 9 10
55.0	-120.0	2.70	3 4 5 6 7 9
55.0	-110.0	2.70	3 4 5 6 7 9
55.0	-100.0	2.20	2 3 4 5 6 7 9
55.0	-90.0	2.70	2 3 4 5 6 9
55.0	-80.0	2.70	2 3 4 5 6 9
55.0	-70.0	2.39	2 3 4 5 6 8 9
55.0	-60.0	2.40	2 3 4 5 6 8 9

Table B-22. The C10-60 constellation.

GDOP OVER CONUS

LAT.	LONG.	GDOP	VISIBLE SATELLITES
25.0	-140.0	5.94	3 4 7 8 10
25.0	-130.0	4.36	3 4 7 8 9 10
25.0	-120.0	4.37	3 4 7 8 9 10
25.0	-110.0	4.40	3 4 7 8 9 10
25.0	-100.0	4.03	2 3 7 8 9 10
25.0	-90.0	4.40	2 3 6 7 9 10
25.0	-80.0	4.37	2 3 6 7 9 10
25.0	-70.0	4.36	2 3 6 7 9 10
25.0	-60.0	5.94	2 3 6 7 9
35.0	-140.0	5.90	3 4 7 8 10
35.0	-130.0	4.31	3 4 7 8 9 10
35.0	-120.0	3.19	3 4 6 7 8 9 10
35.0	-110.0	3.17	3 4 6 7 8 9 10
35.0	-100.0	2.70	2 3 4 6 7 8 9 10
35.0	-90.0	3.17	2 3 4 6 7 9 10
35.0	-80.0	3.19	2 3 4 6 7 9 10
35.0	-70.0	4.31	2 3 6 7 9 10
35.0	-60.0	5.90	2 3 6 7 9
45.0	-140.0	3.08	3 4 5 6 7 8 10
45.0	-130.0	3.07	3 4 5 6 7 8 10
45.0	-120.0	2.66	3 4 5 6 7 8 9 10
45.0	-110.0	2.65	3 4 5 6 7 8 9 10
45.0	-100.0	2.32	2 3 4 5 6 7 8 9 10
45.0	-90.0	2.65	2 3 4 5 6 7 9 10
45.0	-80.0	2.66	2 3 4 5 6 7 9 10
45.0	-70.0	3.07	2 3 4 5 6 7 9
45.0	-60.0	3.08	2 3 4 5 6 7 9
55.0	-140.0	4.26	3 4 5 6 7 8
55.0	-130.0	4.26	3 4 5 6 7 8
55.0	-120.0	4.26	3 4 5 6 7 8
55.0	-110.0	4.26	3 4 5 6 7 8
55.0	-100.0	0.16	3 4 5 6 7
55.0	-90.0	4.26	2 3 4 5 6 7
55.0	-80.0	4.26	2 3 4 5 6 7
55.0	-70.0	4.26	2 3 4 5 6 7
55.0	-60.0	4.26	2 3 4 5 6 7

Table B-23. The C7-90 constellation.

GDOP OVER CONUS

LAT.	LONG.	GDOP	VISIBLE SATELLITES
25.0	-140.0	2.18	2 3 5 6 7
25.0	-130.0	2.16	2 3 5 6 7
25.0	-120.0	2.16	2 3 5 6 7
25.0	-110.0	2.16	2 3 5 6 7
25.0	-100.0	1.91	2 3 4 5 6 7
25.0	-90.0	2.16	2 4 5 6 7
25.0	-80.0	2.16	2 4 5 6 7
25.0	-70.0	2.16	2 4 5 6 7
25.0	-60.0	2.18	2 4 5 6 7
35.0	-140.0	1.93	2 3 4 5 6 7
35.0	-130.0	1.92	2 3 4 5 6 7
35.0	-120.0	1.90	2 3 4 5 6 7
35.0	-110.0	1.90	2 3 4 5 6 7
35.0	-100.0	1.90	2 3 4 5 6 7
35.0	-90.0	1.90	2 3 4 5 6 7
35.0	-80.0	1.90	2 3 4 5 6 7
35.0	-70.0	1.92	2 3 4 5 6 7
35.0	-60.0	1.93	2 3 4 5 6 7
45.0	-140.0	2.70	2 3 4 5 7
45.0	-130.0	1.90	2 3 4 5 6 7
45.0	-120.0	1.89	2 3 4 5 6 7
45.0	-110.0	1.89	2 3 4 5 6 7
45.0	-100.0	1.88	2 3 4 5 6 7
45.0	-90.0	1.89	2 3 4 5 6 7
45.0	-80.0	1.89	2 3 4 5 6 7
45.0	-70.0	1.90	2 3 4 5 6 7
45.0	-60.0	2.70	2 3 4 5 6
55.0	-140.0	2.67	2 3 4 5 7
55.0	-130.0	1.90	2 3 4 5 6 7
55.0	-120.0	1.89	2 3 4 5 6 7
55.0	-110.0	1.89	2 3 4 5 6 7
55.0	-100.0	1.88	2 3 4 5 6 7
55.0	-90.0	1.89	2 3 4 5 6 7
55.0	-80.0	1.89	2 3 4 5 6 7
55.0	-70.0	1.90	2 3 4 5 6 7
55.0	-60.0	2.67	2 3 4 5 6

Table B-24. The C7-75 constellation.

GDOP OVER CONUS

LAT.	LONG.	GDOP	VISIBLE SATELLITES
25.0	-140.0	3.19	2 3 5 6 7
25.0	-130.0	2.87	2 3 4 5 6 7
25.0	-120.0	2.84	2 3 4 5 6 7
25.0	-110.0	2.83	2 3 4 5 6 7
25.0	-100.0	2.82	2 3 4 5 6 7
25.0	-90.0	2.83	2 3 4 5 6 7
25.0	-80.0	2.84	2 3 4 5 6 7
25.0	-70.0	2.87	2 3 4 5 6 7
25.0	-60.0	3.19	2 4 5 6 7
35.0	-140.0	3.83	2 3 4 5 7
35.0	-130.0	2.84	2 3 4 5 6 7
35.0	-120.0	2.82	2 3 4 5 6 7
35.0	-110.0	2.80	2 3 4 5 6 7
35.0	-100.0	2.79	2 3 4 5 6 7
35.0	-90.0	2.80	2 3 4 5 6 7
35.0	-80.0	2.82	2 3 4 5 6 7
35.0	-70.0	2.84	2 3 4 5 6 7
35.0	-60.0	3.83	2 3 4 5 6
45.0	-140.0	3.79	2 3 4 5 7
45.0	-130.0	2.83	2 3 4 5 6 7
45.0	-120.0	2.81	2 3 4 5 6 7
45.0	-110.0	2.79	2 3 4 5 6 7
45.0	-100.0	2.79	2 3 4 5 6 7
45.0	-90.0	2.79	2 3 4 5 6 7
45.0	-80.0	2.81	2 3 4 5 6 7
45.0	-70.0	2.83	2 3 4 5 6 7
45.0	-60.0	3.79	2 3 4 5 6
55.0	-140.0	3.78	2 3 4 5 7
55.0	-130.0	3.76	2 3 4 5 7
55.0	-120.0	2.82	2 3 4 5 6 7
55.0	-110.0	2.80	2 3 4 5 6 7
55.0	-100.0	2.80	2 3 4 5 6 7
55.0	-90.0	2.80	2 3 4 5 6 7
55.0	-80.0	2.82	2 3 4 5 6 7
55.0	-70.0	3.76	2 3 4 5 6
55.0	-60.0	3.78	2 3 4 5 6

Table B-25. The C7-60 constellation.

GDOP OVER CONUS

LAT.	LONG.	GDOP	VISIBLE SATELLITES
25.0	-140.0	5.09	2 3 5 7
25.0	-130.0	4.21	2 3 5 6 7
25.0	-120.0	4.19	2 3 5 6 7
25.0	-110.0	4.18	2 3 5 6 7
25.0	-100.0	3.79	2 3 4 5 6 7
25.0	-90.0	4.18	2 4 5 6 7
25.0	-80.0	4.19	2 4 5 6 7
25.0	-70.0	4.21	2 4 5 6 7
25.0	-60.0	5.09	2 4 5 6
35.0	-140.0	4.39	2 3 4 5 7
35.0	-130.0	4.35	2 3 4 5 7
35.0	-120.0	3.76	2 3 4 5 6 7
35.0	-110.0	3.74	2 3 4 5 6 7
35.0	-100.0	3.73	2 3 4 5 6 7
35.0	-90.0	3.74	2 3 4 5 6 7
35.0	-80.0	3.76	2 3 4 5 6 7
35.0	-70.0	4.35	2 3 4 5 6
35.0	-60.0	4.39	2 3 4 5 6
45.0	-140.0	4.35	2 3 4 5 7
45.0	-130.0	4.32	2 3 4 5 7
45.0	-120.0	4.29	2 3 4 5 7
45.0	-110.0	3.72	2 3 4 5 6 7
45.0	-100.0	3.71	2 3 4 5 6 7
45.0	-90.0	3.72	2 3 4 5 6 7
45.0	-80.0	4.29	2 3 4 5 6
45.0	-70.0	4.32	2 3 4 5 6
45.0	-60.0	4.35	2 3 4 5 6
55.0	-140.0	318.04	2 3 4 5
55.0	-130.0	398.38	2 3 4 5
55.0	-120.0	571.35	2 3 4 5
55.0	-110.0	1112.23	2 3 4 5
55.0	-100.0	*********	2 3 4 5
55.0	-90.0	1112.25	2 3 4 5
55.0	-80.0	571.36	2 3 4 5
55.0	-70.0	398.38	2 3 4 5
55.0	-60.0	318.04	2 3 4 5